

**Interactions between
iron oxidizing and reducing bacteria
in iron-rich pelagic aggregates (iron snow)**

Dissertation

To Fulfill the
Requirements for the Degree of
„doctor rerum naturalium“ (Dr. rer. nat.)

**Submitted to the Council of the Faculty of
Biological Sciences
of the Friedrich Schiller University Jena**

by M.Sc. Qianqian Li

born on 09.07.1990 in Jining, China

Reviewers:

1. Prof. Dr. Kirsten Küsel (Friedrich Schiller University Jena)
2. Prof. Dr. Erika Kothe (Friedrich Schiller University Jena)
3. Prof. Dr. Joel Kostka (Georgia Institute of Technology, USA)

Date of defense: 20.07.2021

Contents	I
Summary	II
Zusammenfassung	IV
1. Introduction	1
2. Draft genome sequences of <i>Acidithrix</i> sp. strain C25 and <i>Acidocella</i> sp. strain C78, acidophiles isolated from iron-rich pelagic aggregates (iron snow)	18
Published in Microbiology Resource Announcements	
3. Insights into autotrophic activities and carbon flow in iron-rich pelagic aggregates (iron snow)	22
Published in Microorganisms	
4. Molecular mechanisms underpinning aggregation in <i>Acidiphilium</i> sp. C61 isolated from iron-rich pelagic aggregates	46
Published in Microorganisms	
5. General Discussion	67
References	83
Declaration of authorship	VII
Acknowledgments	VIII
Published articles and Pending manuscripts	IX
Curriculum Vitae	XI

Summary

Fe-cycling bacteria are often found coexisting in nature and a variety of interactions occur between acidophilic Fe(II)-oxidizing bacteria (FeOB) and Fe(III)-reducing bacteria (FeRB). A perfect low-complexity environment to disentangle the mechanisms underlying these microbial interactions is within iron-rich pelagic aggregates (“iron snow”), which are dominated by acidophilic Fe-cycling microbes, best represented by the FeOB (*Acidithrix*, *Ferrovum*) and the FeRB (*Acidiphilium*). *Acidithrix* is known to facilitate Fe(III) mineral deposition and induces the co-colonization of *Acidiphilium* via a secondary signaling metabolite (2-phenethylamine, PEA). The subsequent colonization of *Ferrovum* contributes to the formation of the iron-cell aggregates. The overarching aim of this thesis was to elucidate the metabolic mechanisms between different FeOB and FeRB shaping iron snow formations.

First, to identify the potential metabolic capabilities of the dominant Fe-cycling microbes in iron snow, the whole genomes of representative FeOB (*Acidithrix* sp. C25) and FeRB (*Acidiphilium* sp. C61, *Acidocella* sp. C78) strains were sequenced. These genomes paired with a two-year metatranscriptome profiling monitored the activities of the iron snow microbiome, including the uncultivated *Ferrovum*. Both approaches revealed the presence and expression of genes involved in the synthesis of the infochemical PEA in FeOB, and the motility and polysaccharide hydrolysis enabling FeRB to join and colonize FeOB. *Ferrovum* showed high transcriptional activity for CO₂ fixation and exopolysaccharide biosynthesis, essential steps in providing necessary organic matter (e.g., extracellular polymeric substances, EPS) for establishing iron snow formation.

A follow-up experiment was designed to trace the autotrophic activities and follow the carbon flow within iron snow, a protein-based ^{13}C labeling approach profiled the ^{13}C incorporation into iron snow microbiome under oxic and anoxic conditions. Supporting our previous findings, ^{13}C quantification confirmed that chemolithoautotrophic *Ferrovum* fixed CO_2 to produce organic carbon under both conditions and FeRB *Acidiphilium* and *Acidocella* took up the carbon under oxic conditions. Taken together, these results demonstrate the importance of chemolithoautotrophic *Ferrovum* (FeOB) in feeding FeRB within iron snow, implying cooperative interactions between them.

Finally, the specificity and the detailed aggregation mechanism of PEA on the Fe(III)-reducing members was investigated as it represents one of the first steps in establishing iron snow. The morphologies of different FeRB strains and gene expression patterns of *Acidiphilium* sp. C61 in the presence of PEA were evaluated. The addition of PEA induced aggregation in all tested *Acidiphilium* spp., but not in the iron snow isolate *Acidocella* sp. C78. Comparative transcriptomics indicated the upregulated expression patterns of genes associated with flagellar motility in *Acidiphilium* sp. C61. The specific aggregation and motility induction effect of PEA on FeRB promotes rapid co-colonization onto the surface of the iron snow particles.

Collectively, these findings addressed that FeOB in iron snow create niches for the co-colonizing heterotrophic FeRB by providing chemolithoautotrophically-fixed organic carbon. Additionally, specific FeRB species rapidly find FeOB by recognizing the infochemicals. These specific inter-species relationships between FeOB and FeRB are advantageous to fulfill their metabolic dependencies through the formation and aggregates stability of iron snow.

Zusammenfassung

Bakterien des Fe-Kreislaufes koexistieren in der Natur häufig und eine Vielzahl von Interaktionen zwischen acidophilen Fe(II)-oxidierenden Bakterien (FeOB) und Fe(III)-reduzierenden Bakterien (FeRB) finden statt. Eine perfekte Umgebung mit geringer Komplexität, um die Mechanismen zu entschlüsseln, die diesen mikrobiellen Interaktionen zugrunde liegen, stellen eisenreiche pelagische Aggregate ("Eisenschnee") dar. Diese werden von acidophilen Mikroorganismen des Fe-Kreislaufes dominiert, am besten repräsentiert durch die FeOB (*Acidithrix*, *Ferrovum*) und die FeRB (*Acidiphilium*). Von *Acidithrix* ist bekannt, dass es die Fe(III)-Mineralablagerung fördert und die Co-Besiedlung von *Acidiphilium* über einen sekundären Signalstoff (2-Phenethylamin, PEA) induziert. Die anschließende Besiedlung von *Ferrovum* trägt zur Bildung der Eisenzellaggregate bei. Das übergeordnete Ziel dieser Arbeit war es, die metabolischen Mechanismen zwischen verschiedenen FeOB und FeRB aufzuklären, die die Eisenschneebildung beeinflussen.

Um die potentiellen metabolischen Fähigkeiten der dominanten Mikroorganismen des Fe-Kreislaufes im Eisenschnee zu identifizieren, wurden zunächst die kompletten Genome von repräsentativen FeOB (*Acidithrix* sp. C25) und FeRB (*Acidiphilium* sp. C61, *Acidocella* sp. C78) Stämmen sequenziert. Diese Genome, zusammen mit einem zweijährigen Profiling des Metatranskriptoms wurden genutzt, um die Aktivitäten des Eisenschnee-Mikrobioms, einschließlich des unkultivierten *Ferrovum*, zu verfolgen. Beide Ansätze zeigten die Anwesenheit und die Expression von Genen, die an der Synthese der Signalchemikalie PEA in FeOB beteiligt sind, sowie die Motilität und Polysaccharidhydrolyse, die es FeRB ermöglicht, sich FeOB anzuschließen und zu kolonisieren. *Ferrovum* zeigte eine hohe transkriptionelle Aktivität für die CO₂-

Fixierung und die Exopolysaccharid-Biosynthese, wesentliche Schritte bei der Bereitstellung der notwendigen organischen Substanz (z.B. extrazelluläre polymere Substanzen, EPS) für die Etablierung der Eisenschneebildung.

Ein Folgeexperiment diente dazu, die autotrophen Aktivitäten nachzuvollziehen und den Kohlenstofffluss innerhalb des Eisenschnees zu verfolgen. Ein proteinbasierter ^{13}C -Markierungsansatz verfolgte den ^{13}C -Einbau in das Eisenschnee-Mikrobiom unter oxidischen und anoxischen Bedingungen. Die ^{13}C -Quantifizierung bestätigte unsere früheren Ergebnisse, dass das chemolithoautotrophe *Ferrovum* unter beiden Bedingungen CO_2 fixierte, um organischen Kohlenstoff zu produzieren, während FeRB *Acidiphilium* und *Acidocella* den Kohlenstoff unter oxidischen Bedingungen aufnahmen. Zusammengenommen zeigen diese Ergebnisse die Bedeutung des chemolithoautotrophen *Ferrovum* (FeOB) bei der Nährstoffzufuhr von FeRB innerhalb des Eisenschnees, was kooperative Interaktionen zwischen ihnen impliziert.

Schließlich wurden die Spezifität und der detaillierte Aggregationsmechanismus von PEA auf den Fe(III)-reduzierenden Mitgliedern untersucht, da dies einen der ersten Schritte bei der Etablierung von Eisenschnee darstellt. Die Morphologien verschiedener FeRB-Stämme und die Genexpressionsmuster von *Acidiphilium* sp. C61 in Gegenwart von PEA wurden ausgewertet. Die Zugabe von PEA induzierte die Aggregation in allen getesteten *Acidiphilium* spp., jedoch nicht in dem Eisenschnee-Isolat *Acidocella* sp. C78. Vergleichende Transkriptomik zeigte die hochregulierten Expressionsmuster von Genen, die mit der Flagellenbewegung in *Acidiphilium* sp. C61 assoziiert sind. Der spezifische Aggregations- und Motilitätsinduktionseffekt von PEA auf FeRB fördert die schnelle Co-Kolonisierung auf der Oberfläche der Eisenschneepartikel.

Zusammengefasst zeigen diese Ergebnisse, dass FeOB im Eisenschnee Nischen für die co-kolonisierenden heterotrophen FeRB schaffen, indem sie chemolithoautotroph fixierten organischen Kohlenstoff bereitstellen. Zusätzlich spüren spezifische FeRB-Arten FeOB schnell auf, indem sie deren Signalchemikalien erkennen. Diese besonderen Inter-Spezies-Beziehungen zwischen FeOB und FeRB sind vorteilhaft, um ihre metabolischen Abhängigkeiten durch die Bildung und Aggregatstabilität von Eisenschnee zu erfüllen.

1. Introduction

1.1 Pelagic aggregates

In the water column of deep stratified waters, amorphous pelagic aggregates are composed of microorganisms, phytoplankton, feces, detritus, and biominerals which are stabilized by extracellular polymeric matrix (Alldredge and Silver, 1988; Grossart and Simon, 1993; Thornton, 2002). These aggregates vary in size, ranging from micrometers to centimeters, depending on their residence time in the water column and the trophic state of the ecosystem (Riebesell, 1992; Lehours *et al.*, 2010; Passow *et al.*, 2012). They occur in oceans, tidally affected coastal areas, rivers, and lakes (Simon *et al.*, 2002).

1.1.1 Marine/Lake snow

Large (> 500 μm) pelagic aggregates, found in oceans and lakes, are termed marine snow (Suzuki and Kato, 1953) or lake snow (Grossart and Simon, 1993). Similar aggregates have also been identified in rivers (river snow) (Böckelmann, 2000; Neu, 2000). Physical coagulation leads to collisions between particles in the water column through Brownian motion, fluid shear, differential settlement, and animal feeding (McCave, 1984; Engel, 2000). Once brought together, two biologically-mediated pathways have been proposed to enhance macroaggregate formation via physical aggregation: (1) production of sticky mucus, exopolymers, or products of cell lysis, which increase the attachment probability of colliding particles, and (2) biological alteration of the effective size and surface characteristics of component particles, which potentially increase collision probabilities (Simon *et al.*, 2002).

The role of marine/lake snow in the transformation of particulate organic matter (POM) is essential for the transformation and cycling of elements in pelagic marine and

limnetic ecosystems (**Figure 1**) (Grossart and Simon, 1998b; Ploug *et al.*, 1999). They drive the biological carbon pump via sedimentation of organic matter from the surface ocean to the deep ocean, where carbon can be sequestered for years. During the sinking, organic matter in aggregates is decomposed as POM in the food web, thus providing energy to heterotrophic organisms in the surrounding waters and sediments (Grossart and Simon, 1998a; Herndl and Reinthaler, 2013; Turner, 2015).

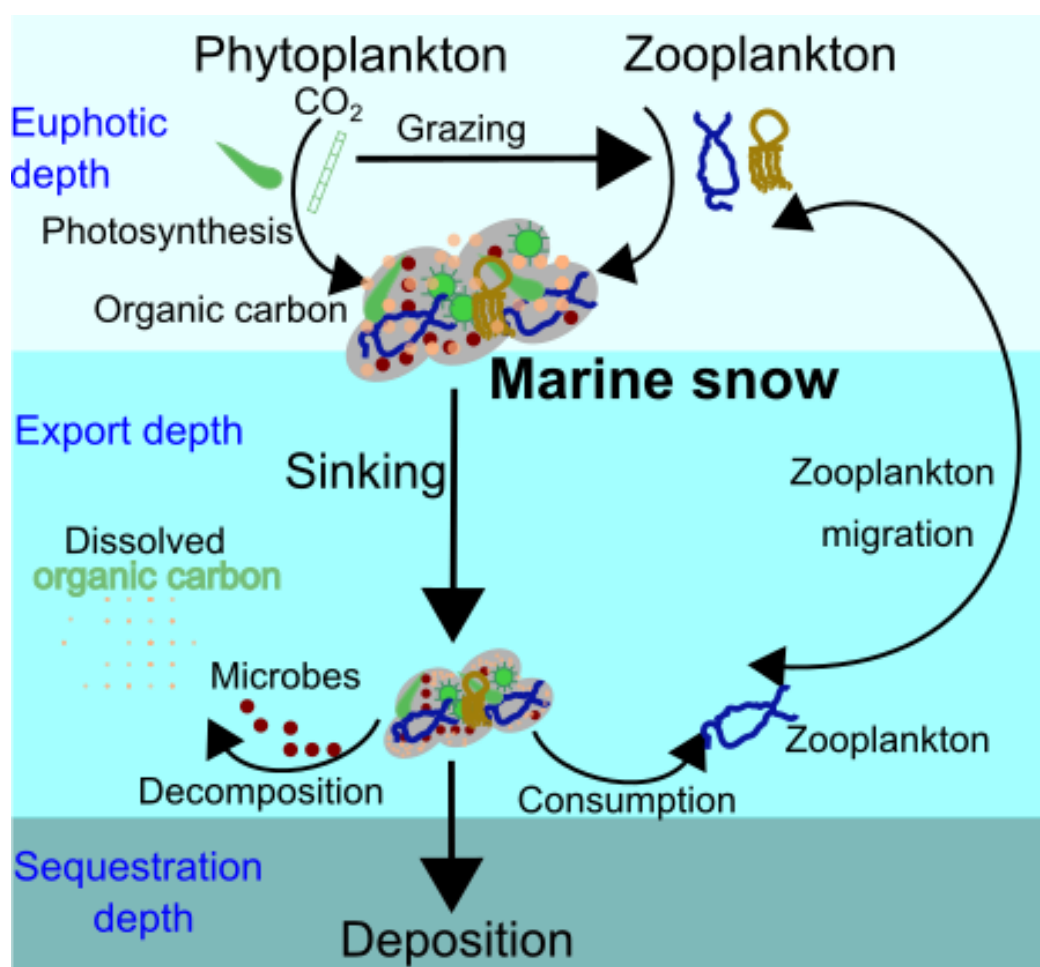


Figure 1. The biological pump of marine snow transforms dissolved inorganic carbon into organic biomass and pumps it in particulate or dissolved form into the deep ocean.

Phytoplankton incorporate carbon into biomass, which either sinks to the sediment or being grazed or decomposed (figure modified from Ducklow *et al.*, 2001).

1.1.2 Fe(III) mineral-cell aggregates in ferruginous lakes

Pelagic aggregates are also found in ferruginous meromictic lakes that provide geochemical analogs of the conditions that dominated the Earth's oceans during the Precambrian (Koeksoy *et al.*, 2016; Lambrecht *et al.*, 2018; Thompson *et al.*, 2019). These lakes are permanently stratified with a superficial O₂-rich layer and a deeper anoxic layer separated by a zone called the redoxcline that exhibits strong opposing gradients of oxygen and Fe(II) (Miracle *et al.*, 1992; Havig *et al.*, 2018). Redoxclines with neutral pH lead to the precipitation of Fe-minerals mediated by abiotic and biotic Fe oxidation in a range of ferruginous lakes, like, Lake Matano (Indonesia; Zegeye *et al.*, 2007), Lake La Cruz (Spain; Rodrigo *et al.*, 2001), Lake Pavin (France; Cosmidis *et al.*, 2014), and the ferruginous Kabuno Bay within Lake Kivu (Democratic Republic of Congo; Michiels *et al.*, 2017). These Fe(III) mineral-cell aggregates with a high specific surface area and their organic carbon component make them ideal sorbents for several solutes (Fortin *et al.*, 1993; Clarke *et al.*, 1997). Consequently, these aggregates produced in redoxclines will settle down to accumulate in the bottom sediment and transport and mobilize various ions, metal complexes in modern Fe-rich water columns (Posth *et al.*, 2010).

1.1.3 Iron-rich pelagic aggregates (iron snow) in acidic pit lake

As in the case of natural lakes, pit lakes are vertically stratified (Schultze, 2013). Compared to stratification mostly from variability in temperature, depending on the seasons in natural lakes, artificial mine pit lakes are chemically stratified, mainly resulting from mineralization (Boehrer and Schultze, 2008). They are found to be formed in former excavations of brown coal, sand mines, peat bogs for many centuries around the world (Sienkiewicz and Gasiorowski, 2016). Most pit lakes are acidic or extremely acidic (pH < 3), although some are neutral or even alkaline (Savage *et al.*,

1. Introduction

2009). The acidic pit lake water may be contaminated with elevated concentrations of heavy metals and/or acid mine drainage (AMD) (Banks *et al.*, 1997).

In the south-eastern part of Germany, acid mining lakes were formed from previous surface mining in the Lusatian district (Schultze and Geller, 1996; Geller *et al.*, 1998). When opencast mining of coal and metals terminated, the water drainage pumps were shut off and groundwater and rainfall accumulated, forming pit lakes. Acidic lake 77 is an acidic ferruginous post lignite mining lake (pH 2.5). The water quality is mainly influenced by the acidification caused by pyrite oxidation and the accompanying mobilization of acidity, iron, and sulfate (Schultze *et al.*, 2011). The lake is characterized by the formation of iron-rich pelagic aggregates at redoxcline with steeply opposing gradients of oxygen and Fe(II). These aggregates ($\leq 380 \mu\text{m}$) have a high sedimentation velocity ($\sim 2 \text{ m h}^{-1}$) and contain high amounts of Fe(III)-sulfate minerals ($\geq 35\%$), schwertmannite as the dominant minerals, and a low amount of organic matter ($< 11\%$) (Reiche *et al.*, 2011). The higher inorganic fractions in aggregates lead to a higher sinking velocity and limited light penetration in the water column. Given the pronounced differences compared to organic-rich “snows” from oceans, lakes, and rivers, these particles from Lake 77 were called “iron snow” (Reiche *et al.*, 2011; **Figure 2**).



Figure 2. Photos of Lake 77 and iron snow.

(A) Lignite mine Lake 77 in the Lusatian mining area in eastern Germany. (B) Iron snow precipitated from lake water collected below the redoxcline of the lake in 2015. Figures from Lu, 2012.

1.2 Diversity of bacteria in pelagic aggregates

Pelagic aggregates provide a niche for microbes that can exploit these physical structures and resources for growth. Thus, they are local hot spots for microbial activity in energy fluxing, biogeochemical cycling, and food web dynamics (Caron *et al.*, 1982; Alldredge and Gotschalk, 1990; Grossart and Ploug, 2000; Long and Azam, 2001). Due to different aggregates in different aquatic systems, the bacterial diversity and their relative abundances vary greatly.

1.2.1 Marine/Lake Snow-attached bacteria

Marine/Lake aggregates are colonized by phytoplankton and a rich and diverse detrital community of bacteria with densities from 10^6 cells to 10^9 cells per aggregate or ml, usually at concentrations many-fold higher than in the surrounding water (Alldredge *et al.*, 1986; Grossart and Simon, 1993; Schweitzer *et al.*, 2001). Phytoplankton (e.g., cyanobacteria, algae) represent a prominent group of primary producers in marine snow or lake snow (Simon *et al.*, 1990; Kaltenbock and Herndl, 1992; Grossart *et al.*, 1997). β -proteobacteria, α -proteobacteria, γ -proteobacteria, and Bacteroidetes (formerly known as the *Cytophaga-Flavobacteria-Bacteroides*) are the most abundant bacteria on these aggregates (Tang *et al.*, 2012). Aggregate-associated bacteria mainly degrade organic matter into the dissolved phase during sinking (Steinberg *et al.*, 2008). Besides, eukaryotes, such as copepods, hydrozoans, radiolarians, and dinoflagellates, are also detected from marine snow particles (Lundgreen *et al.*, 2019).

1.2.2 Fe(III) mineral-cell aggregates-attached bacteria in ferruginous lakes

Fe- and S-cycling microorganisms have been considered as significant players in Precambrian oceans (Farquhar *et al.*, 2000; Johnson *et al.*, 2008; Planavsky *et al.*, 2009). Similarly, modern meromictic lakes studied so far host large populations of

microbes at redoxclines, especially with metabolisms involved in Fe and S biogeochemical cycles. These metabolisms may contribute to primary production and mineral formation through biomineralization processes (Boyd and Ellwood, 2010; Brown *et al.*, 2011; Berg *et al.*, 2016; Miot *et al.*, 2016). In Lake Pavin, nitrate-dependent Fe(II)-oxidizing bacteria (FeOB) are present in the water column and promote Fe-oxyhydroxide and Fe-phosphate precipitation (Miot *et al.*, 2014). Lower light absorption in the ferruginous lakes would permit greater light penetration illuminating the Fe(II)-rich anoxic waters below. In Lake Matano, anoxygenic phototrophic sulfur bacteria may be responsible for forming carbonated green rust together with magnetite as abundant Fe minerals below the chemocline (Crowe, Jones, *et al.*, 2008; Zegeye *et al.*, 2012). In Lake La Cruz, a large community of anoxygenic phototrophic sulfur bacteria and photoferrotrophs establish the carbonate mineral particles below the chemocline (Rodrigo *et al.*, 1993). So far, only one study has targeted the eukaryotes in the water column of the ferruginous lake (Lake Pavin) and revealed a high genetic diversity of unicellular eukaryotes, e.g., Alveolata and Fungi in the permanent anoxic zone (Lepère *et al.*, 2016).

1.2.3 Iron-rich pelagic aggregates (iron snow)-attached bacteria in acidic pit Lake 77

Due to the low pH and enormously different biogeochemical conditions (high amount of Fe(III) fraction) from other ferruginous lakes (Kamjunke *et al.*, 2005; Boehrer *et al.*, 2009), neutrophiles (e.g., photoferrotrophs) are excluded in acidic mining lakes. Iron snow is colonized by acidophilic microbial communities ($\sim 10^{10}$ cells [g dry weight]⁻¹), and Fe-cycling microorganisms constitute nearly 60% of the total community (Lu *et al.*, 2013). One hundred thirty-three bacterial isolates were obtained from iron snow below the redoxcline, and these isolates belong to either acidophilic FeOB related to *Acidithrix* (Actinobacteria), *Ferrovum* (β -Proteobacteria), or FeRB related to

Acidiphilium, *Acidocella*, and *Acidisphaera* (α -Proteobacteria) (Mori *et al.*, 2017). The most dominant groups (*Acidithrix*, *Ferrovum*, *Acidiphilium*, *Acidocella*) comprise up to 50% of the total community (Lu *et al.*, 2013). Key players (*Acidithrix* sp. C25, *Ferrovum* sp. C4, *Acidiphilium* sp. C61, *Acidocella* sp. C78) from each group were isolated. But *Ferrovum* sp. C4 failed to grow due to multiple transfers. Only key players (*Acidithrix* sp. C25, *Acidiphilium* sp. C61, *Acidocella* sp. C78) are kept.

1.3 Fe-cycling bacteria under acidic conditions

Acidic pit lakes, due to anthropogenic activity, are often associated with the oxidation of sulfide minerals, many of which contain iron (pyrite, FeS_2) (Johnson and Aguilera, 2019). Abiotic and microbially mediated redox cycling of Fe plays an essential role in biogeochemistry (**Figure 3**). Ionic forms of (uncomplexed) iron are far more soluble (especially Fe(III)) at low pH than at circumneutral pH. Under neutral pH conditions, soluble Fe(II) reacts more quickly with oxygen into insoluble Fe(III) oxides, and the spontaneous chemical oxidation of Fe(II) outcompetes the biological oxidation of most bacteria (Emerson *et al.*, 2010). This limits neutrophilic FeOB to the microoxic (e.g., *Gallionella*) or anoxic environments (e.g., *Acidovorax* (nitrate-dependent FeOB), *Rhodobacter* (phototrophic FeOB)) (Kucera and Wolfe, 1957; Widdel *et al.*, 1993; Straub *et al.*, 1996). These neutrophilic FeOB use different strategies to evade cell encrustation due to the increased exposure to poorly soluble Fe(III) oxides (Chan *et al.*, 2009; Schädler *et al.*, 2009; Schmid *et al.*, 2014). The oxidized Fe(III) acts as an electron acceptor and neutrophilic Fe(III)-reducing bacteria (FeRB) (e.g., *Shewanella*, *Geobacter*) develop different strategies to cope with the difficulty of transferring electrons from the cell to the surface of a barely soluble electron acceptor at circumneutral pH (Ghiorse, 1984; Lovley *et al.*, 2004).

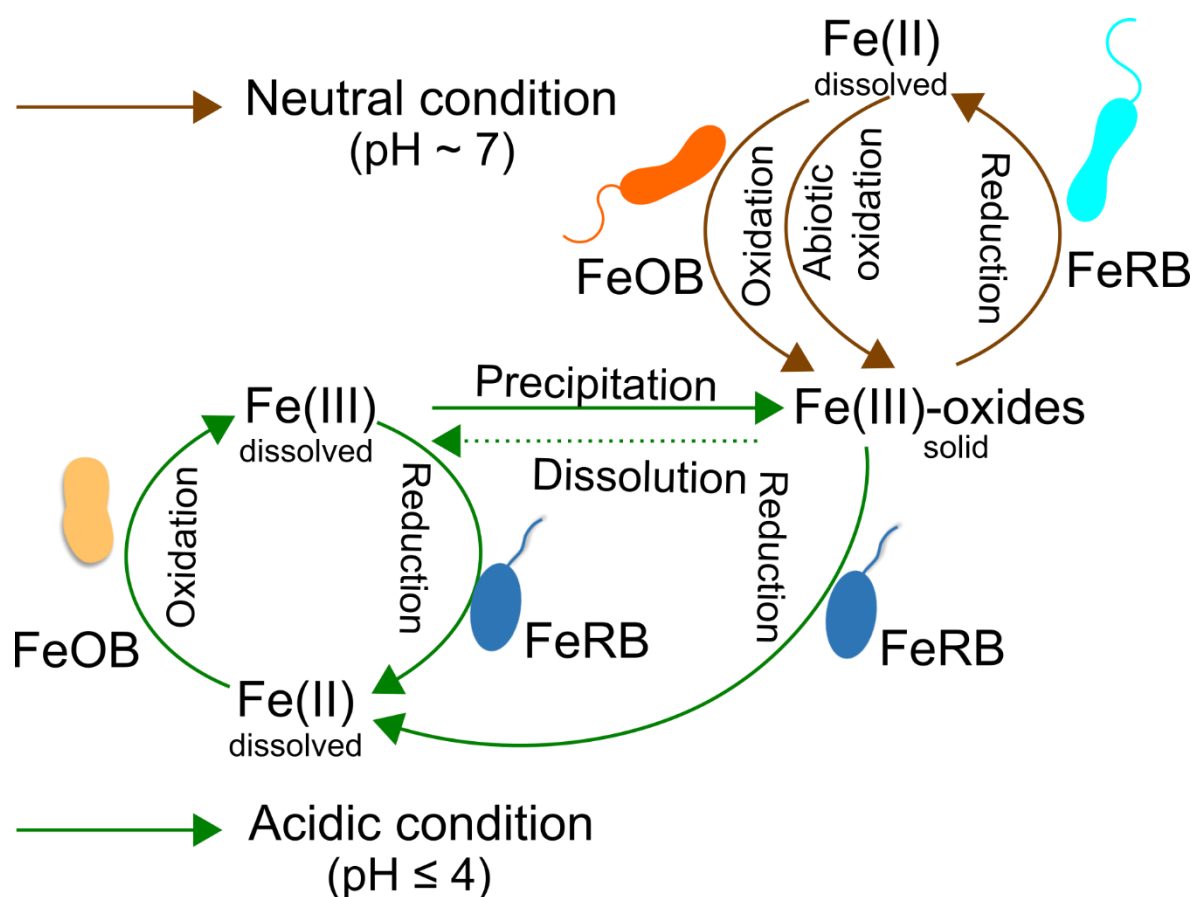


Figure 3. Microbial Fe cycling under acidic and circumneutral conditions.

Figure is modified from Kappler and Straub, 2005; Mori, 2016.

Microbial Fe cycling in acidic environments is different from neutral environments due to low rates of chemical Fe(II) oxidation in the presence of oxygen. A broad range of acidophilic Fe-cycling microorganisms from iron-rich systems such as bioleaching systems, AMD biofilms, mine pit lakes have been investigated (Tyson *et al.*, 2004; Acosta *et al.*, 2014; Falagán *et al.*, 2014). In phylogenetic terms, Fe-cycling acidophiles are distributed across the domain Bacteria within the phyla of Proteobacteria, Nitrospirae, Firmicutes, Actinobacteria, and Acidobacteria, and in the domain Archaea within the Crenarchaeota and Euryarchaeota phyla (Johnson and Hallberg, 2003; Johnson, 2012). Within the phylum β -Proteobacteria, Nitrospirae, Actinobacteria, the most relevant FeOB genus known to inhabit acidic mine environments are *Ferrovum*, *Leptospirillum*, *Acidimicrobium* separately, while

Acidiphilium, *Acidocella* within α -Proteobacteria are frequent FeRB in acidic mine environments (Nordstrom *et al.*, 2000; Wenderoth and Abraham, 2005).

1.3.1 Acidophilic Fe(II) oxidizing bacteria (FeOB)

Chemolithoautotrophic *Leptospirillum* is one of the most important acidophilic FeOB in acidic and metal-rich environments. *Leptospirillum* couples the fixation of inorganic carbon and nitrogen with the oxidation of Fe(II) as their primary energy source (Sand *et al.*, 1995; Goltsman *et al.*, 2009; Christel *et al.*, 2017). *Leptospirillum* has been identified to catalyze mineral dissolution (Acosta *et al.*, 2014) and produced extracellular polymeric substances (EPS) to mediate attachment of bacterial cells and biofilm formation on the surface of sulfide minerals (Vardanyan *et al.*, 2019). The novel proposed genus “*Ferrovum*” was discovered in the last decade in AMD habitats worldwide (Hallberg *et al.*, 2006; Heinzl *et al.*, 2009; Hua *et al.*, 2015). Despite the difficulties related to the isolation of *Ferrovum*, *Ferrovum myxofaciens* strain P3G was successfully isolated from an abandoned copper mine (Johnson *et al.*, 2014). Further *Ferrovum* strains were isolated from pit water (Ullrich, González, *et al.*, 2016; Ullrich, Poehlein, *et al.*, 2016). Chemolithoautotrophic *Ferrovum* is known for producing copious amounts of EPS and nitrogen fixation (Johnson *et al.*, 2014; Grettenberger *et al.*, 2020).

Acidimicrobium-related bacteria have also been detected in many acidic environments where they contribute to primary production and Fe(II) oxidization (Brown *et al.*, 2011; Tyson *et al.*, 2004). Heterotrophic *Acidithrix* is a novel genus within Acidimicrobiaceae (Kay *et al.*, 2013) and the isolate Py-F3 is the type strain of *Acidithrix ferroxidans* that was isolated from an abandoned mine (Jones and Johnson, 2015). *Acidithrix* sp. C25, isolated from iron snow, represents only the second isolated strain within the *Acidithrix* genus (Mori *et al.*, 2016). Two *Acidithrix* strains can oxidize Fe(II) under oxic conditions

and reduce Fe(III) under microoxic and anoxic conditions, which has never been shown in neutrophiles. Only the genome of *Acidithrix ferrooxidans* Py-F3 was sequenced. Genes encoding Rubisco and several enzymes required for carbon fixation via the Calvin-Benson-Bassham (CBB) cycle were found (Eisen *et al.*, 2015). However, the ability to fix CO₂ by strain Py-F3 has not yet been tested.

1.3.2 Acidophilic Fe(III) reducing bacteria (FeRB)

A variety of autotrophic and heterotrophic bacteria that thrive in acidic environments at low pH (< 3) can grow by Fe(III) reduction (Straub, 2011). All known acidophiles that use Fe(III) as an electron acceptor for their growth are facultative FeRB and reduce oxygen (Johnson *et al.*, 2012). Both organic and inorganic electron donors can be coupled with Fe(III) reduction by FeRB. Autotrophic FeRB (e.g., *Acidithiobacillus ferrooxidans*, *Thiobacillus ferrooxidans*) can grow by Fe(III) respiration using either sulfur or hydrogen as electron donors under anoxic conditions (Pronk *et al.*, 1991; Pronk and Johnson, 1992; Ohmura *et al.*, 2002).

Heterotrophic FeRB, such as *Acidiphilium* and *Acidocella*, use organic electron donors (e.g., glucose or glycerol) to reduce soluble Fe(III) as the terminal electron acceptor (Johnson and McGinness, 1991; Küsel *et al.*, 1999). This is widespread among heterotrophic FeRB under anoxic conditions (Coupland and Johnson, 2008). *Acidiphilium* strain SJH is capable of reducing a variety of Fe(III) minerals, with the highest reduction rates observed for dissolved Fe(III) (Bridge and Johnson, 2000). However, anoxic conditions are not required for Fe(III) reduction in acidophilic FeRB. *Acidiphilium cryptum* JF-5 reduced soluble Fe(III) and schwertmannite in sediment microcosms at pH 3 under oxic conditions (Küsel *et al.*, 2002). The enzymatic system related to Fe(III) reduction remains unknown, but evidence exists that this process may involve iron reductases (Schröder *et al.*, 2003; Bird *et al.*, 2011).

1.4 Microbial interactions in pelagic aggregates

Organisms that exploit interspecific interactions to increase ecological performance often co-aggregate. Microbial interactions are the effects that the organisms in a community have on one another, and they are a ubiquitous, diverse, critical component of any biological community. Microbial interactions are likely to drive population structure and dynamics at microscale diverse taxonomic cell aggregates (~100 μm) (Cordero and Datta, 2016). Marine/Lake snow aggregates with high microbial densities are found to act as local hot spots for microbial interaction (**Figure 4**), and these interactions include quorum sensing (Gram *et al.*, 2002; Hmelo *et al.*, 2011), antagonistic interactions via antibiotics (Long and Azam, 2001) and exploitation of public goods (Smith *et al.*, 1992; Cordero *et al.*, 2012).

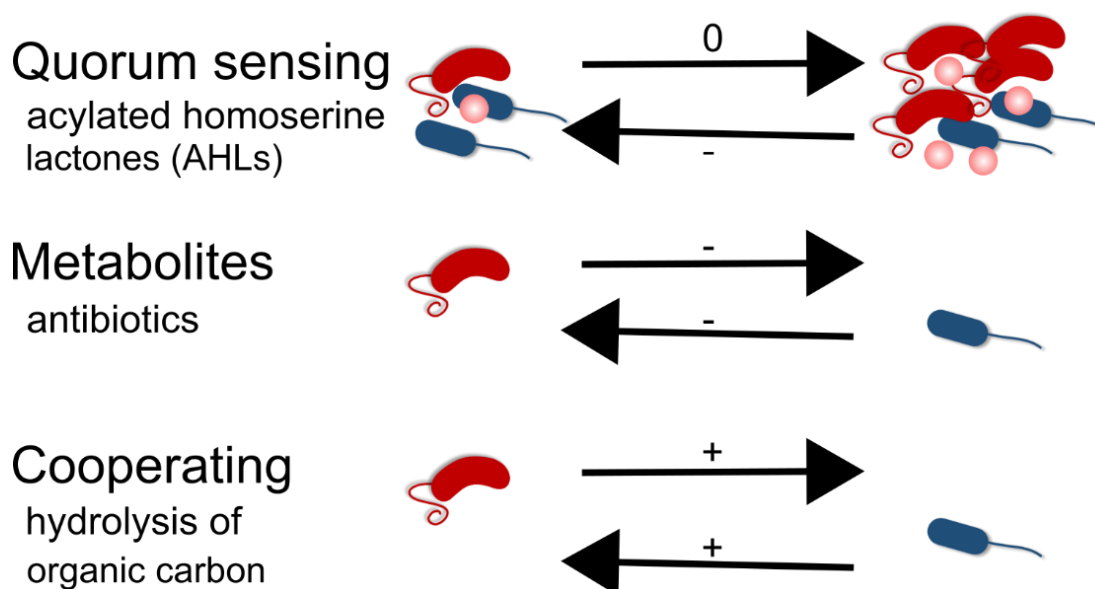


Figure 4. Different forms of microbial interactions between bacteria in marine snow.

+ indicates the positive benefit, whereas - depicts the negative constraint. 0 means no effect.

Iron snow is characterized by lower microbial and chemical complexity than marine and lake snow (Reiche *et al.*, 2011). Former studies have indicated that different acidophilic FeOB (*Acidithrix*, *Ferrovum*) coexist with FeRB (*Acidiphilium*) in iron snow

aggregates. A range of microbial interactions have been demonstrated to occur between acidophilic microorganisms (Johnson, 1998), including competition (Johnson, 1991; Schrenk *et al.*, 1998), predation (McGinness and Johnson, 1992; Johnson and Rang, 1993), mutualism (Hallmann *et al.*, 1992; Johnson and Roberto, 1997) and synergy (Norris, 1990; Clark and Norris, 1996). Thus, interspecies cell signaling between the acidophilic FeOB and FeRB may evolve through different mechanisms like marine/lake snow to adhere to and colonize in iron snow.

1.4.1 Quorum sensing (QS)

Particle-associated bacteria are metabolically more active than free-living bacteria (Smith *et al.*, 1995), and microbial colonization and coordinated group behavior are likely regulated by chemicals, including QS signaling molecules within pelagic aggregates (Gram *et al.*, 2002; Dang and Lovell, 2016). QS is a possible mechanism in marine snow bacteria that produce acylated homoserine lactones (AHLs) to govern phenotypic traits (biofilm formation, exoenzyme production, and antibiotic production) when the population reaches high densities (Gram *et al.*, 2002). QS system has also been identified in the acidophilic *Acidithiobacillus ferrooxidans* (Mamani *et al.*, 2016). It can produce AHL analog to modulate cell adhesion to solid Fe substrates and establish optimal niches within biofilms (Altermann, 2014).

1.4.2 Secondary metabolites-driven interactions

Within aggregates on the order of 100 μm , cell-cell distances are short enough for diffusible metabolites to reach neighboring cells (Datta *et al.*, 2016). Long and Azam (2001) showed that approximately 50% of particle-associated bacteria growing on marine snow produced inhibitory molecules and displayed antagonistic activities towards other bacteria. The excreted metabolites produced by one partner and

needed by the other can also drive mutualistic interactions that positively affect the growth of co-existing organisms. Two co-occurring bacteria (*Acidithrix*, *Acidiphilium*) that make up 29.8% of the community in iron snow showed the role of metabolite signaling, 2-phenethylamine (PEA) (Mori *et al.*, 2017). Increased rates of Fe(II) oxidation in FeOB *Acidithrix* sp. C25 and the induced bacterial aggregation in *Acidiphilium* sp. C61 were found when incubated with cell-free supernatants of each partner (Mori *et al.*, 2017), which may suggest the mutualistic interaction from metabolites released in the individual culture media.

1.4.3 Cooperation

Oligosaccharides hydrolyzed from complex insoluble organic materials by extracellular enzymes can act as common goods that promote cooperative growth in microbial populations, whereby aggregates increase both the per capita availability of resources and the per-cell growth rate (Ebrahimi *et al.*, 2019). As carbon sources are severely limited in acidic waters, obligate interactions between microbial members are probably critical in optimizing acidic microbial activity (Baker and Banfield, 2003). Notably, some typical acidophilic FeOB contain genes that enable them to fix CO₂ through different pathways. *At. ferrooxidans* (Valdés *et al.*, 2008), *Ferrovum myxofaciens* (Johnson *et al.*, 2014), and *Acidimicrobium ferrooxidans* (Caldwell *et al.*, 2007) may perform carbon fixation through the CBB cycle while several *Leptospirillum*-related members, such as *L. rubarum*, *L. ferrodiazotrophum* (Ram *et al.*, 2005; Goltsman *et al.*, 2009, 2013) may fix CO₂ through the reductive tricarboxylic acid (rTCA) cycle. On the other hand, obligate heterotrophic FeRB that belong to the *Alphaproteobacteria* (*Acidiphilium* except for *A. acidophilum*, *Acidocella*, *Acidisphaera*, and *Acidicaldus*) benefit from secreted metabolites and remnants of the biomass from FeOB by utilizing them as carbon and energy sources (Harrison, 1984; González-Toril

et al., 2011; Liu *et al.*, 2011). Hence as the heterotrophs also supply the autotrophs with CO₂ by oxidizing organic carbon compounds, which further boosts the growth of autotrophs (Kermer *et al.*, 2012), similar cooperative interactions between the autotrophic FeOB and heterotrophic FeRB may exist in iron snow.

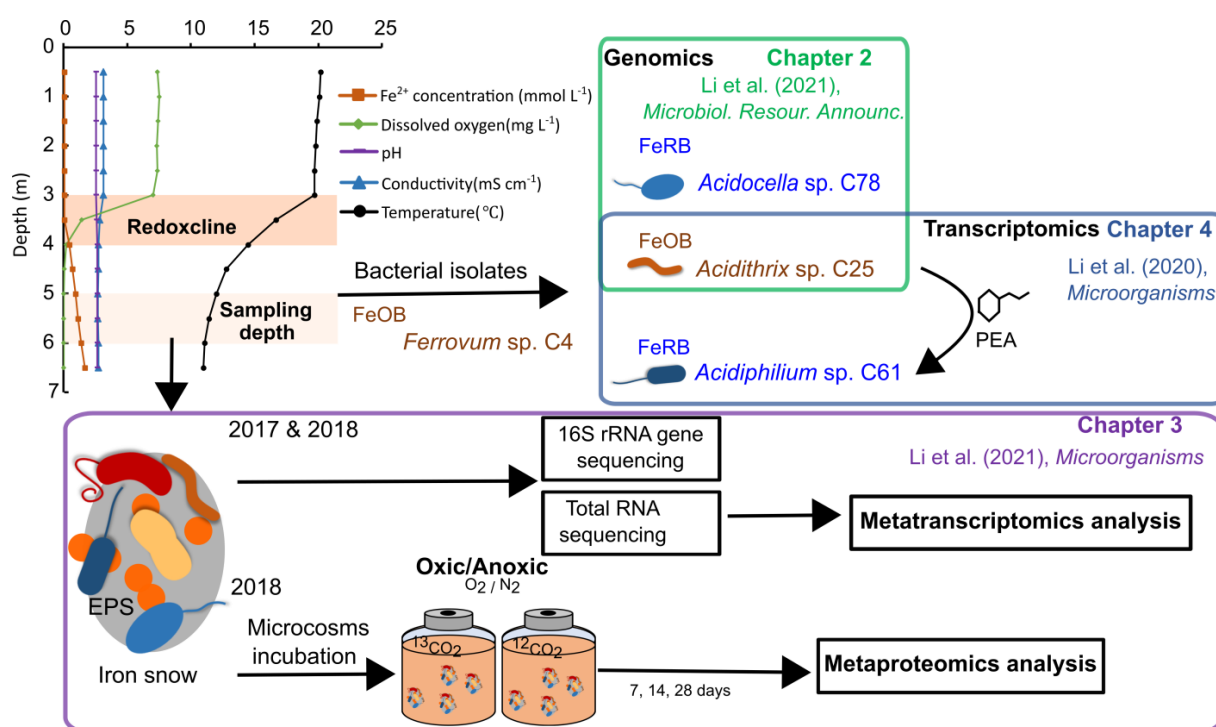
1.5 Project background and hypotheses

The acidic ferruginous lignite mine lake 77 in the Lusatian mining district (Brandenburg Germany) formed after lignite mining ceased in the 1960s. Lake 77 receives the acidic, Fe(II)-rich underground AMD inflow and is characterized by oxic-anoxic redoxclines. These redoxclines which occur in the water column of the lake lead to iron snow formation. Three dominant Fe-cycling groups (*Ferrovum*, *Acidithrix*, *Acidiphilium*) inhabit iron snow (Lu *et al.*, 2013). Using the available strains (*Acidithrix* sp. C25, *Acidiphilium* sp. C61), chemical signaling (2-phenethylamine, PEA) was characterized in the former studies (Mori *et al.*, 2017). However, the genome potentials of *Acidithrix* sp. C25, *Acidiphilium* sp. C61 involved in the above chemical interaction remain unknown. Further investigations are needed to clarify the specificity and aggregation mechanisms of PEA on *Acidiphilium*.

The co-occurrence of *Ferrovum* and *Acidiphilium* has long been known (Kipry *et al.*, 2013; Tischler *et al.*, 2013). Due to the lack of *Ferrovum* isolate from iron snow, the cultivation-independent method, metatranscriptomics, is used to reveal the diversity and metabolic activities within iron snow environmental samples, including the uncultivated FeOB (*Ferrovum*). We could examine the link between the taxonomies and functions, e.g., CO₂ fixation, EPS production, EPS degradation, motility, which are linked to iron snow formation and stability. Further methods based on stable isotope probing (SIP) allow relating taxonomic identification to the metabolic activity of that organism through the assimilation of an isotopically labeled substrate in complex

1. Introduction

communities (Radajewski *et al.*, 2000). Organisms that utilize the labeled substrate take up the isotopic label and incorporate it in their biomass, e.g., proteins. The proteins can be identified and analyzed by mass spectroscopy, and subsequently, their taxonomic affiliation is assigned using reference databases (Taubert *et al.*, 2011; Taubert, 2019). By applying genomics, transcriptomics, and protein-SIP to profile the genes involved in metabolic potentials, gene expression patterns, protein expression patterns, and ^{13}C incorporation in iron snow microbes, this study aims to elucidate the metabolic activities and microbial interactions mechanisms of dominant FeOB and FeRB shaping the iron snow formation and structure (**Figure 5**).



H1: Chemolithoautotrophy is the driving factor for building biomass. (Chapter 3)

H2: Organic carbon derived from the chemolithoautotrophic CO₂ fixation in FeOB acts as a carbon source for FeRB. (Chapter 2, Chapter 3)

H3: The secondary metabolite, 2-phenethylamine (PEA), produced by *Acidithrix* sp. C25, targets the Fe(III)-reducing members to induce aggregation. (Chapter 2, Chapter 4)

Figure 5. Project workflow to investigate the three hypotheses (H1-H3) in this dissertation.

Multi-omics in combination with experimental methods were used to address all three hypotheses in the following chapters of this thesis.

Hypothesis I Chemolithoautotrophy is the driving factor for building biomass.

Hypothesis II Organic carbon derived from the chemolithoautotrophic CO₂ fixation in FeOB acts as a carbon source for FeRB.

To address the above two hypotheses, the objectives were:

- (i) Profiling the metabolic potentials of the key iron snow isolates.
- (ii) Profiling the activities of autotrophic CO₂ fixation and heterotrophic organic carbon utilization by the *in-situ* iron snow microbiome.
- (ii) Protein-based ¹³CO₂ metabolic labeling of oxic and anoxic microcosms to track the carbon flow between the members of the iron snow microbiome.

Hypothesis III The secondary metabolite, 2-phenethylamine (PEA), produced by *Acidithrix* sp. C25, targets the Fe(III)-reducing members to induce aggregation.

To test the third hypothesis, the objectives were:

- (i) Incubation-based experiments designed to monitor the effect of PEA amendment on aggregation morphologies by the acidophilic FeRB, *Acidiphilium* sp. C61, *Acidiphilium cryptum* JF-5, *Acidiphilium* SJH, *Acidocella* sp. C78.
- (ii) Elucidation of potential aggregation mechanisms (i.e., autoaggregation, biofilm formation, flagellar inhibition) in *Acidiphilium* sp. C61.

1.6 Structure of the thesis

In chapter 2, “Draft genome sequences of *Acidithrix* sp. strain C25 and *Acidocella* sp. strain C78, acidophilic Fe(III)-oxidizer and Fe(III)-reducers isolated from iron-rich pelagic aggregates (iron snow) (Li *et al.*, published in *Microbiology Resource*

Announcements), genomes were sequenced and annotated. Preliminary genome analysis provided genetic evidence about their contribution to iron snow formation, e.g., production of aggregation-inducing signals and hydrolysis of polysaccharides.

In chapter 3, “Insights into autotrophic activities and carbon flow in iron-rich pelagic aggregates” (Li et al., published in *Microorganisms*), metatranscriptomics was used to reveal the dominance of FeOB and FeRB and linked them to iron snow microbiome activities, e.g., CO₂ fixation, polysaccharide biosynthesis, and flagellar motility. Protein-based stable isotope probing (protein-SIP) justified that a small amount of the carbon fixed by the FeOB (*Leptospirillum*, *Ferrovum*) flew to FeRB (*Acidiphilium*, *Acidocella*) while a majority of carbon was converted to EPS to stabilize iron snow.

In chapter 4, “Molecular mechanisms underpinning aggregation in *Acidiphilium* sp. C61 isolated from iron-rich pelagic aggregates” (Li et al., 2020; published in *Microorganisms*), the specific effect of PEA on the aggregation of iron-reducing bacteria *Acidiphilium* spp. was investigated. Pangenomes of *Acidiphilium* spp. characterized 65 shared gene clusters linked to potential aggregation. Further comparative transcriptomics elucidated the essential motility underlying the aggregation formation in *Acidiphilium* sp. C61.

2. Draft genome sequences of *Acidithrix* sp. strain C25 and *Acidocella* sp. strain C78, acidophiles isolated from iron-rich pelagic aggregates (iron snow)

Published in *Microbiology Resource Announcements*. doi: 10.1128/MRA.00102-21

Qianqian Li, Rebecca E. Cooper, Carl-Eric Wegner, Shipeng Lu, and Kirsten Küsel

Abstract

We report the draft genome sequences of two acidophiles, the Fe-oxidizing bacterium *Acidithrix* sp. Strain C25 and the putative Fe-reducing bacteria *Acidocella* sp. Strain C78. Both strains were isolated from iron-rich pelagic aggregates (iron snow) collected below the redoxcline at a 5-m depth in an acidic pit lake located in Germany (51°31'8.2"N, 13°41'34.7"E).



GENOME SEQUENCES



Draft Genome Sequences of *Acidithrix* sp. Strain C25 and *Acidocella* sp. Strain C78, Acidophiles Isolated from Iron-Rich Pelagic Aggregates (Iron Snow)

Qianqian Li,^a Rebecca E. Cooper,^a Carl-Eric Wegner,^a Shipeng Lu,^b Kirsten Küsel^{1,c}

^aInstitute of Biodiversity, Aquatic Geomicrobiology, Friedrich Schiller University Jena, Jena, Germany

^bInstitute of Botany, Jiangsu Province and Chinese Academy of Sciences, Nanjing, China

^cThe German Centre for Integrative Biodiversity Research (iDiv) Halle-Jena-Leipzig, Leipzig, Germany

ABSTRACT We report the draft genome sequences of two acidophiles, the Fe-oxidizing bacterium *Acidithrix* sp. strain C25 and the putative Fe-reducing *Acidocella* sp. strain C78. Both strains were isolated from iron-rich pelagic aggregates (iron snow) collected below the redoxcline at a 5-m depth in an acidic pit lake located in Germany (51°31'8.2"N, 13°41'34.7"E).

Fe-cycling bacteria represent a large fraction of iron snow microbial communities in acidic pit lakes (1). *Acidithrix* sp. strain C25, a heterotrophic Fe(II)-oxidizing bacterium within the *Acidimicrobiaceae* family of the *Actinobacteria* phylum, is the second isolated and sequenced strain within the *Acidithrix* genus (2, 3). *Acidocella* sp. strain C78, a putative heterotrophic Fe(III)-reducing bacterium, belongs to the *Acetobacteraceae* family of the *Proteobacteria* phylum. *Acidocella* sp. strain YE4-N1-5-CH, isolated from this pit lake, and other *Acidocella* isolates have the capacity for dissimilatory Fe(III) reduction (4, 5). To further understand the metabolic potential and the contribution of these microbes to iron snow formation, we sequenced and analyzed these two genomes.

Both strains were isolated from 100 μ l of diluted lake water (10^{-1} to 10^{-3}) transferred to two types of overlay plates containing 25 mM FeSO₄—iFeo (without a carbon source) for *Acidithrix* sp. C25 and YEo (0.2% yeast extract) for *Acidocella* sp. C78 (6, 7). Single colonies, transferred at least five times to establish pure cultures, were lysed and used for 16S rRNA gene PCR and phylogenetic analysis (7). To obtain sufficient biomass for DNA extraction, cultures were incubated in artificial pilot-plant water medium (APPW) amended with yeast extract (0.2 g liter⁻¹). *Acidithrix* sp. C25 incubations were additionally amended with 25 mM FeSO₄ (8). Genomic DNA was extracted using a phenol-chloroform-based protocol (9). Whole-genome sequencing was performed by RTL Genomics (Lubbock, TX, USA). Needle-sheared DNA was used to prepare 10- to 20-kb sequencing libraries using the PacBio SMRTbell template prep kit v1.0 without further size selection and was subsequently sequenced using P6-C4 chemistry with an 180-min collection protocol using a PacBio RS II platform (Pacific Biosciences, Menlo Park, CA) according to the standard manufacturer's protocols. The raw reads were filtered and assembled *de novo* with the Hierarchical Genome Assembly Process v3 (HGAP3) (10) using default settings (<https://github.com/ben-ferch/HGAP-3.0>). Genome completeness and contamination were assessed with CheckM v1.0.13 using default parameters (11). Genome annotation was performed with RASTtk v2.0 using default parameters (12). The genome characteristics of both strains are listed in Table 1.

Analysis of the *Acidithrix* sp. C25 genome revealed genes encoding the complete Calvin-Benson-Bassham cycle, which indicates that the heterotrophic *Acidithrix* sp. C25 has the genetic potential for CO₂ fixation. We could not identify homologs linked to Fe(II) oxidation under acidic conditions, such as *cyc2*, *cyt572*, *cyt579*, sulfocyanin, and *foxCD*. We found a gene

Citation Li Q, Cooper RE, Wegner C-E, Lu S, Küsel K. 2021. Draft genome sequences of *Acidithrix* sp. strain C25 and *Acidocella* sp. strain C78, acidophiles isolated from iron-rich pelagic aggregates (iron snow). *Microbiol Resour Announc* 10:e00102-21. <https://doi.org/10.1128/MRA.00102-21>.

Editor J. Cameron Thrash, University of Southern California

Copyright © 2021 Li et al. This is an open-access article distributed under the terms of the [Creative Commons Attribution 4.0 International license](https://creativecommons.org/licenses/by/4.0/).

Address correspondence to Kirsten Küsel, kirsten.kuesel@uni-jena.de.

Received 28 January 2021

Accepted 27 May 2021

Published 24 June 2021

2. Draft genome sequences of *Acidithrix* sp. Strain C25 and *Acidocella* sp. Strain C78

Li et al.



TABLE 1 Characteristics and accession numbers of draft genomes

Strain name	Genome size (bp)	Total PacBio sequences (bp)	PacBio sequence N_50 (bp)	Coverage (x)	No. of contigs	G+C content (%)	N_50 (bp)	Completeness (%)	Redundancy (%)	No. of genes	BioProject accession no.	Assembly accession no.
<i>Acidithrix</i> sp. C25	4,102,129	313,121,275	5,524	72	5	47.72	1,351,828	98.29	3.00	4,499	PRJEB40539	CAJHC1020000000.2
<i>Acidocella</i> sp. C78	3,250,836	145,349,460	3,896	38	59	67.54	96,816	94.53	1.00	3,219	PRJEB40546	CAJQZK1010000000.1

Volume 10 Issue 25 e010102-21

ms.asm.org 2

Downloaded from <https://journals.asm.org/journal/nms> on 30 June 2021 by 2001:638:1558:e710:104.

encoding aromatic-L-amino-acid decarboxylase, which converts phenylalanine to phenethylamine, an aggregation-mediating infochemical within iron snow (7, 13).

The *Acidoceella* sp. C78 genome encodes the complete Calvin-Benson-Bassham cycle, indicating the genetic capacity for CO₂ fixation. Multiple genes encoding polysaccharide-degrading enzymes (e.g., glycosidase) and a gene encoding the methionine sulfoxide reductase heme-binding subunit, previously linked to Fe(III) reduction (14), were detected. These draft genome sequences are a valuable resource to understand iron snow functioning.

Data availability. The sequencing reads and assemblies of *Acidithrix* sp. C25 and *Acidoceella* sp. C78 for this whole-genome sequencing project are available in ENA under the BioProject accession numbers [PRJEB40539](https://www.ncbi.nlm.nih.gov/bioproject/PRJEB40539) and [PRJEB40546](https://www.ncbi.nlm.nih.gov/bioproject/PRJEB40546), respectively, and the assembly accession numbers are listed in Table 1. The versions described in this paper are the first versions.

ACKNOWLEDGMENTS

This work was supported by the Jena School for Microbial Communication (JSMC) graduate school and the Collaborative Research Centre Chemical Mediators in Complex Biosystems (SFB 1127/2 ChemBioSys, 239748522), which are both funded by the Deutsche Forschungsgemeinschaft. Additional support for JSMC was also kindly provided by the Carl Zeiss Foundation (Carl Zeiss Stiftung).

We thank Jiro F. Mori (Yokohama City University) for the extraction of genomic DNA used for genome sequencing.

REFERENCES

- Lu S, Chourey K, Reiche M, Nietzsche S, Shah MB, Neu TR, Hettich RL, Kisel K. 2013. Insights into the structure and metabolic function of microbes that shape pelagic iron-rich aggregates ("iron snow"). *Appl Environ Microbiol* 79:4272–4281. <https://doi.org/10.1128/AEM.00467-13>.
- Jones RM, Johnson DB. 2015. *Acidithrix ferrooxidans* gen. nov., sp. nov.; a filamentous and obligately heterotrophic, acidophilic member of the *Actinobacteria* that catalyzes dissimilatory iron-oxidation of iron. *Res Microbiol* 166:111–120. <https://doi.org/10.1016/j.resmic.2015.01.003>.
- Eisen S, Poehlein A, Johnson DB, Daniel R, Schlömann M, Mühling M. 2015. Genome sequence of the acidophilic ferrous iron-oxidizing isolate *Acidithrix ferrooxidans* strain Py-F3, the proposed type strain of the novel actinobacterial genus *Acidithrix*. *Genome Announc* 3:e00382-15. <https://doi.org/10.1128/genomeA.00382-15>.
- Coupland K, Johnson DB. 2008. Evidence that the potential for dissimilatory ferric iron reduction is widespread among acidophilic heterotrophic bacteria. *FEMS Microbiol Lett* 279:30–35. <https://doi.org/10.1111/j.1574-6968.2007.00998.x>.
- Lu S, Gschkat S, Reiche M, Akob DM, Hallberg KB, Kisel K. 2010. Ecophysiology of Fe-cycling bacteria in acidic sediments. *Appl Environ Microbiol* 76:8174–8183. <https://doi.org/10.1128/AEM.01931-10>.
- Johnson DB, Hallberg KB. 2007. Techniques for detecting and identifying acidophilic mineral-oxidizing microorganisms, p 237–261. In Rawlings DE, Johnson DB (ed), *Bio-mining*. 1st ed. Springer, Berlin, Germany.
- Mori JF, Uebeschaar N, Lu S, Cooper RE, Pohnert G, Kisel K. 2017. Sticking together: inter-species aggregation of bacteria isolated from iron snow is controlled by chemical signaling. *ISME J* 11:1075–1086. <https://doi.org/10.1038/ismej.2016.186>.
- Mori JF, Lu S, Händel M, Totsche KU, Neu TR, Iancu VV, Tarcea N, Popp J, Kisel K. 2016. Schwertmannite formation at cell junctions by a new filament-forming Fe(II)-oxidizing isolate affiliated with the novel genus *Acidithrix*. *Microbiology (Reading)* 162:62–71. <https://doi.org/10.1099/mic.0.000205>.
- Lueders T, Manefield M, Friedrich MW. 2004. Enhanced sensitivity of DNA- and rRNA-based stable isotope probing by fractionation and quantitative analysis of isopycnic centrifugation gradients. *Environ Microbiol* 6:73–78. <https://doi.org/10.1046/j.1462-2920.2003.00536.x>.
- Chin C-S, Alexander DH, Marks P, Klammer AA, Drake J, Heiner C, Clum A, Copeland A, Huddleston J, Eichler EE, Turner SW, Korlach J. 2013. Nonhybrid, finished microbial genome assemblies from long-read SMRT sequencing data. *Nat Methods* 10:563–569. <https://doi.org/10.1038/nmeth.2474>.
- Parks DH, Imelfort M, Skennerton CT, Hugenhoitz P, Tyson GW. 2015. CheckM: assessing the quality of microbial genomes recovered from isolates, single cells, and metagenomes. *Genome Res* 25:1043–1055. <https://doi.org/10.1101/gr.186072.114>.
- Aziz RK, Bartels D, Best AA, DeJongh M, Disz T, Edwards RA, Formosa K, Gerdes S, Glass EM, Kubal M, Meyer F, Olsen GJ, Olson R, Osterman AL, Overbeek RA, McNeil LK, Paarmann D, Paccian T, Parrello B, Pusch GD, Reich C, Stevens R, Vassieva O, Vonstein V, Wilke A, Zagnitko O. 2008. The RAST server: Rapid Annotations using Subsystems Technology. *BMC Genomics* 9:75. <https://doi.org/10.1186/1471-2164-9-75>.
- Li Q, Cooper RE, Wegner CE, Kisel K. 2020. Molecular mechanisms underpinning aggregation in *Acidiphilium* sp. C61 isolated from iron-rich pelagic aggregates. *Microorganisms* 8:314. <https://doi.org/10.3390/microorganisms8030314>.
- Juillan-Binard C, Picococchi A, Andrieu JP, Dupuy J, Petit-Hartlein I, Caux-Thang C, Vivès C, Nivière V, Fieschi F. 2017. A two-component NADPH oxidase (NOX)-like system in bacteria is involved in the electron transfer chain to the methionine sulfoxide reductase MsrP. *J Biol Chem* 292:2485–2494. <https://doi.org/10.1074/jbc.M116.752014>.

3. Insights into autotrophic activities and carbon flow in iron-rich pelagic aggregates (iron snow)

Published in *Microorganisms*. doi: 10.3390/microorganisms9071368

Qianqian Li, Rebecca E. Cooper, Carl-Eric Wegner, Martin Taubert, Nico Jehmlich, Martin von Bergen, and Kirsten Küsel





Abstract

Pelagic aggregates function as biological carbon pumps for transporting fixed organic carbon to sediments. In iron-rich (ferruginous) lakes, photoferrotrophic and chemolithoautotrophic bacteria contribute to CO₂ fixation by oxidizing reduced iron, leading to the formation of iron-rich pelagic aggregates (iron-snow). The significance of iron oxidizers in carbon fixation, their general role in iron snow functioning and the flow of carbon within iron snow is still unclear. Here, we combined a two-year metatranscriptome analysis of iron snow collected from an acidic lake with protein-based stable isotope probing to determine general metabolic activities and to trace ¹³CO₂ incorporation in iron snow over time under oxic and anoxic conditions. mRNA-derived metatranscriptome of iron snow identified four key players (*Leptospirillum*, *Ferrovum*, *Acidithrix*, *Acidiphilium*) with relative abundances (59.6%-85.7%) encoding ecologically relevant pathways, including carbon fixation and polysaccharide biosynthesis. No transcriptional activity for carbon fixation from archaea or eukaryotes was detected. ¹³CO₂ incorporation studies identified active chemolithoautotroph *Ferrovum* under both conditions. Only 1.0-5.3% relative ¹³C abundances were found in heterotrophic *Acidiphilium* and *Acidocella* under oxic conditions. These data show that iron oxidizers play an important role in CO₂ fixation, but the majority of fixed C will be directly exported to the sediment without feeding heterotrophs in the water column in acidic ferruginous lakes.

Supplementary data to this article can be found online at <https://www.mdpi.com/2076-2607/9/7/1368#supplementary-material>

Article

Insights into Autotrophic Activities and Carbon Flow in Iron-Rich Pelagic Aggregates (Iron Snow)

Qianqian Li ¹ , Rebecca E. Cooper ¹ , Carl-Eric Wegner ¹ , Martin Taubert ¹, Nico Jehmlich ² , Martin von Bergen ^{2,3} and Kirsten Küsel ^{1,4,*}

¹ Institute of Biodiversity, Friedrich Schiller University Jena, Dornburger Strasse 159, 07743 Jena, Germany; qianqian.li@uni-jena.de (Q.L.); rebecca.cooper@uni-jena.de (R.E.C.); carl-eric.wegner@uni-jena.de (C.-E.W.); martin.taubert@uni-jena.de (M.T.)

² Department of Molecular Systems Biology, Helmholtz Centre for Environmental Research—UFZ, Permoserstrasse 15, 04318 Leipzig, Germany; nico.jehmlich@ufz.de (N.J.); martin.vonbergen@ufz.de (M.v.B.)

³ Pharmacy and Psychology, Faculty of Biosciences, Institute of Biochemistry, University of Leipzig, Brüderstraße 32, 04103 Leipzig, Germany

⁴ The German Centre for Integrative Biodiversity Research (iDiv) Halle-Jena-Leipzig, Puschstraße 4, 04103 Leipzig, Germany

* Correspondence: kirsten.kuesel@uni-jena.de; Tel: +49-3641-949461

Abstract: Pelagic aggregates function as biological carbon pumps for transporting fixed organic carbon to sediments. In iron-rich (ferruginous) lakes, photoferrotrophic and chemolithoautotrophic bacteria contribute to CO₂ fixation by oxidizing reduced iron, leading to the formation of iron-rich pelagic aggregates (iron snow). The significance of iron oxidizers in carbon fixation, their general role in iron snow functioning and the flow of carbon within iron snow is still unclear. Here, we combined a two-year metatranscriptome analysis of iron snow collected from an acidic lake with protein-based stable isotope probing to determine general metabolic activities and to trace ¹³C₂ incorporation in iron snow over time under oxic and anoxic conditions. mRNA-derived metatranscriptome of iron snow identified four key players (*Leptospirillum*, *Ferroplasma*, *Acidithrix*, *Acidiphilium*) with relative abundances (59.6–85.7%) encoding ecologically relevant pathways, including carbon fixation and polysaccharide biosynthesis. No transcriptional activity for carbon fixation from archaea or eukaryotes was detected. ¹³C₂ incorporation studies identified active chemolithoautotroph *Ferroplasma* under both conditions. Only 1.0–5.3% relative ¹³C abundances were found in heterotrophic *Acidiphilium* and *Acidocella* under oxic conditions. These data show that iron oxidizers play an important role in CO₂ fixation, but the majority of fixed C will be directly transported to the sediment without feeding heterotrophs in the water column in acidic ferruginous lakes.

Keywords: iron snow; autotrophic iron oxidizing bacteria; heterotrophic iron reducing bacteria; carbon flow; metatranscriptomics; ¹³C₂; stable isotope probing; metaproteomics



Citation: Li, Q.; Cooper, R.E.; Wegner, C.-E.; Taubert, M.; Jehmlich, N.; von Bergen, M.; Küsel, K. Insights into Autotrophic Activities and Carbon Flow in Iron-Rich Pelagic Aggregates (Iron Snow). *Microorganisms* 2021, 9, 1368. <https://doi.org/10.3390/microorganisms9071368>

Academic Editor: Caroline M. Plugge

Received: 6 May 2021

Accepted: 21 June 2021

Published: 23 June 2021

Publisher's Note: MDPI stays neutral with regard to jurisdictional claims in published maps and institutional affiliations.



Copyright © 2021 by the authors. Licensee MDPI, Basel, Switzerland. This article is an open access article distributed under the terms and conditions of the Creative Commons Attribution (CC BY) license (<https://creativecommons.org/licenses/by/4.0/>).

1. Introduction

Pelagic aggregates, formed in the water column of lakes and oceans through adsorption of inorganic and organic matter (OM), are composed of microorganisms, phytoplankton, feces, detritus and biominerals [1,2]. These snow-like aggregates are usually larger than 500 µm and are held together by extracellular polymeric substances (EPS) [3]. Marine pelagic aggregates (marine snow) drive the biological carbon pump via the export of photosynthetically derived particulate organic carbon (POC) from the photic zone of the ocean to the deep aphotic zones, where carbon can be sequestered for years before reaching the sediment [4–6]. The long residence time of marine snow enables microbial degradation and zooplankton grazing activity, which are largely responsible for the attenuation of carbon flux to the deep sea [7].

In iron-rich ferruginous meromictic lakes, iron-rich pelagic aggregates (iron snow) are formed and dominated by an Fe(III)-rich fraction of more than 35%, rather than OM,

which speeds up their sinking velocity [8]. The world's largest ferruginous lakes, such as the 600 m deep Lake Matano or Lake La Cruz, serve as analogous representatives to conditions of the Archaean Ocean ecosystems [9]. Here, low productivity in surface water allows sunlight to penetrate to the chemocline, stimulating anoxygenic phototrophic Fe(II)-oxidizing bacteria (FeOB) and anoxygenic green sulfur bacteria to form iron-rich pelagic aggregates [10–13]. In shallow ferruginous lakes, such as the numerous lignite lakes that have emerged in Europe during the last decades [14,15], Fe(II) was or still is provided by groundwater or surface water influx from mine tailings. At low pH conditions, Fe(II) oxidation is mediated mainly by chemolithotrophic acidophilic microbes [16]. The adsorption of phosphorous to the Fe(III) minerals formed within the water column limits primary production by phytoplankton in these lakes [17,18]. These limitations on primary production by phytoplankton suggest that carbon fixation mediated by FeOB might be central for primary production, further trophic interactions within iron snow and carbon export to the sediments.

In this study, we sampled iron snow from the model lignite Lake 77 (Lusatian district of Brandenburg, Germany), which also has a meromictic basin [8]. RNA-based quantitative PCR assigned up to 60% of the metabolically active iron snow colonizing microbes to Fe(II)-oxidizing and Fe(III)-reducing bacteria (FeRB) [8,19]. Fe-cycling key players, the FeOB *Acidithrix* and the FeRB *Acidiphilium*, isolated from iron snow [20], showed inter-species aggregation controlled by chemical signaling [21]. The heterotrophic *Acidiphilium* often co-occurs with the chemolithoautotrophic, EPS-producing FeOB *Ferroplasma*, another iron snow key player [22,23].

To capture metabolic activities comprehensively and to follow the flow of carbon within iron snow, we used metatranscriptomics and a ^{13}C metabolic labeling approach. We collected iron snow below the redoxcline of lignite Lake 77 in two consecutive years (2017 and 2018) to profile the activities of the iron snow microbial community. Mapping mRNA sequences to the genomes of representative Fe-cycling bacteria helped to obtain gene expression profiling. Next, we incubated iron snow with ^{13}C - CO_2 under oxic and anoxic conditions and applied protein-based stable isotope probing (protein-SIP) over time to follow the labeling of peptides in the identified microbial community members. We hypothesized that dominant FeOB are mainly responsible for CO_2 fixation and polysaccharide biosynthesis and that ^{13}C -labeled organic carbon is rapidly utilized by the heterotrophic FeRB *Acidiphilium* and *Acidocella*, as well as other trophic levels. However, our results suggest the majority of fixed CO_2 in this system is not feeding other trophic levels in iron snow; instead, the majority of the fixed CO_2 is pumped into the sediment.

2. Materials and Methods

2.1. Lake Characteristics and Iron Snow Sampling

Lignite Lake 77 is an acidic coal mining lake located in the Lusatian mining area in eastern Germany. Iron snow sampling was conducted in both August 2017 and August 2018 at the central basin (CB, $51^{\circ}1'8.2''$ N, $13^{\circ}41'34.7''$ E) during lake stratification or at the very beginning of the 'mixing' period [8]. For lake samples used for Fe(II) and sulfate measurements, 1 mL of 5 M HCl was added to each 5 mL water sample collected from 0–6.5 m depth to prevent abiotic iron oxidation. Iron snow was collected directly onto glass fiber filters (0.9 μm ; Infiltec, Speyer, Germany) using an electronic water pump installed between 5 and 6 m depth just below the redoxcline. A volume of 150 L of water was collected in 2017 and 50 L of water were collected in 2018. Glass fiber filters with iron snow were immediately stored on dry ice, transported to the laboratory and stored at -80°C until nucleic acid extraction. For iron snow incubation experiments, additional lake water was collected (20 L of lake water from around 1 m depth and 100 L of water from 5–6 m depth) during the 2018 sampling campaign and stored in 20 L plastic bottles at 4°C until further use.

2.2. Geochemical Analysis

Temperature, pH, conductivity and dissolved oxygen content were measured with a multiparameter meter (YSI, Yellow Springs, OH, USA). Fe(II) concentrations were determined spectrophotometrically at 512 nm (Hach Lange, Düsseldorf, Germany) using the phenanthroline method [24]. Sulfate was measured spectrophotometrically at 420 nm, according to the barium chloride–gelatin method [25].

2.3. Nucleic Acid Extraction of Iron Snow Microbiome

A single glass fiber filter with collected iron snow was cut into 12 even pieces, from which two even portions of filter pieces were pooled into 650 mL conical tubes and served as biological replicates. Then, 40–50 mL of oxalate extraction buffer (197 mM ammonium oxalate, 119 mM oxalic acid dissolved in DEPC-treated water, pH 3.25) were added to tubes and incubated for 30 min at 4 °C to dissolve the ferric iron minerals during which the tubes were shaken 3–5 times to detach cells from filters. Next, the oxalate buffer solution was passed through a 0.2 µm membrane filter (PALL corporation, Dreieich, Germany). Nucleic acids were extracted from these glass fiber membrane filters according to the method described in Lueders, Manefield and Friedrich 2004, with slight modification. First, the biomass-carrying membrane filters were washed in 15 mL conical tubes with 2.25 mL of NaPO₄ buffer (120 mM, pH = 8) and 0.75 mL of TNS solution (500 mM Tris-HCl pH 8.0, 100 mM NaCl, 10% SDS *w/v*) and subsequently subjected to beadbeating at 6.5 m/s for 30 s with 0.6 g zirconia/silica beads ($\phi = 1$ mm) (Carl Roth, Karlsruhe, Germany) to facilitate detachment. Cell debris was separated by centrifugation (20,000 × *g* at 4 °C for 10 min) and the supernatant was first extracted with equal volumes of phenol-chloroform-isoamyl alcohol (25:24:1 *v/v/v*, AppliChem, Darmstadt, Germany), following centrifugation (20,000 × *g* at 4 °C for 20 min), and second with chloroform-isoamyl alcohol (24:1 *v/v*, AppliChem, Darmstadt, Germany), following centrifugation (20,000 × *g* at 4 °C for 20 min). The obtained aqueous phase was subjected to overnight precipitation at 4 °C with two volumes of polyethylene glycol 6000 (Carl Roth, Karlsruhe, Germany) and 5 µL of Glycogen (20 mg mL⁻¹, Sigma-Aldrich, Darmstadt, Germany). Total nucleic acids were collected by centrifugation (20,000 × *g* at 4 °C for 90 min). The resulting pellets were washed with 1.5 mL of ice-cold ethanol (70% *v/v*), following centrifugation (20,000 × *g* at 4 °C for 30 min), and resuspended in 50 µL of elution buffer (Qiagen, Hilden, Germany). Of the resulting 6 total nucleic acid replicates, 3 were used for DNA-based amplicon sequencing and 3 replicates were used for metatranscriptome sequencing.

2.4. 16S rRNA Gene Amplicon Sequencing

DNA concentrations were determined by a NanoDrop (Thermo Fisher Scientific, Waltham, MA, USA) and a fragment of the 16S rRNA gene was amplified using primers S-D-Bact-0341-b-S-17 (5'-CCTACGGGNGGCWGCAG-3') and S-D-Bact-0785-a-A-21 (5'-GACTACHVGGGTATCTAATCC-3') [26], using the following cycling conditions: 15 min initial denaturation, followed by 30 cycles of 45 s at 94 °C, 45 s at 55 °C, 45 s at 72 °C and a final extension at 72 °C for 10 min. PCR products were checked by agarose gel electrophoresis and the target gel bands were cut from gels and purified with the NucleoSpin gel and PCR clean-up kit (Macherey-Nagel, Düren, Germany). PCR products were prepared for Illumina sequencing using the NEBNext Ultra DNA Library Prep Kit for Illumina (New England Biolabs, Hitchin, UK), according to the manufacturer's protocol. Sequencing was carried out in-house using an Illumina MiSeq platform (Illumina, San Diego, CA, USA) in paired-end mode (2 × 300 bp).

2.5. Amplicon Sequencing Data Analysis

Demultiplexing of raw data was performed with bclfastq (v. 2.19) (Illumina). Read pairs were imported into QIIME2 (v. 2019.7) [27] and primers were trimmed off by cutadapt (v. 2.5) with default parameters [28], which cuts the 5' and 3'-end, taking into account respective primer sequences. Trimmed read pairs were subjected to paired-end assembly with

vsearch (v. 2.7.0) (`--fastq_mergepairs`, default settings) [29] and then the joined sequences were filtered based on a minimum quality score of 30. Filtered sequences were denoised and amplicon sequence variants (ASVs) were identified with `deblur` (v. 2019.7) [30]. ASVs were taxonomically assigned against SILVA (release 132) [31] using the feature-classifier plugin of QIIME2 and a fitted classifier with the `classify-sklearn` (v. 0.21.2) function [32]. After rare ASVs with a frequency of less than 0.05% were removed, data were exported as biom file for downstream analysis with `phyloseq` (v. 1.28.0) [33] in R (v. 3.5.3) (R Core Team, 2020).

2.6. Metatranscriptome Sequencing

RNA was purified from the previously described nucleic acid extracts through enzymatic digestion with DNase (ThermoFisher Scientific, Waltham, MA, USA) for 1 h at 37 °C. The digested RNA was checked by agarose gel electrophoresis and purified using the RNA Clean & Concentrator-5 kit (Zymo Research, Freiburg, Germany). Purity and quantity were determined by spectrophotometry and fluorometry. RNA-seq libraries were prepared using the NEBNext Ultra II Directional RNA Library Prep Kit for Illumina (New England Biolabs, Hitchin, UK) according to the manufacturer's protocol. Libraries were pooled equimolarly and sequenced in paired-end (2 × 150 bp) mode on an Illumina HiSeq 2000 instrument by Eurofins Genomics (Constance, Germany). Between 51 and 110 million read pairs were obtained for each library. Data were processed according to Li et al. (2020). Briefly, the quality of the demultiplexed sequencing data was assessed using `FastQC` (v. 0.11.7) (<http://www.bioinformatics.babraham.ac.uk/projects/fastqc/> (accessed on 10 January 2018)) followed by adapter trimming using `trim_galore` (v. 0.4.3, -q 20) (https://www.bioinformatics.babraham.ac.uk/projects/trim_galore/ (accessed on 25 January 2017)) and quality-filtering with `sickle` (v. 1.33, -q 20) (<https://github.com/najoshi/sickle>). The remaining read pairs were paired-end assembled with `PEAR` (v. 0.9.11) with default settings [34]. Sequences derived from mRNA were identified with `SortMeRNA` (v. 2.0) [35] with default settings using pre-compiled SILVA (release 132) [31] and Rfam databases (release 12.2) [36].

2.7. Taxonomic Annotation of rRNA-Derived Sequences

Subsets of 100,000 SSU rRNA-derived sequences were queried against NCBI RefSeq rRNA sequences (release 203) [37] using `blastn` (v. 2.9.0) [38] applying an e-value cutoff of 1×10^{-3} and collecting up to 10 database hits. The search output was then parsed in `MEGAN` (v. 6.17.0) [39] using the implemented lowest common ancestor (LCA) algorithm with default settings. Taxonomically assigned sequences were used to deduce relative abundances. Sequences of eukaryotic origin were extracted and imported into `QIIME2` (v. 2019.7) [27] for taxonomic analysis. 18S rRNA sequences were taxonomically classified against the SILVA database (release: 132) [31] using the `classify-consensus-vsearch` function of the feature-classifier plugin (v. 2019.7.0) of QIIME2 with an identity threshold of 95%. Data were exported as biom file, which was used for downstream analysis with `phyloseq` (v. 1.28.0) [33].

2.8. Taxonomic and Functional Profiling of mRNA Sequences

mRNA sequences were queried against NCBI RefSeq (release 203) [37] by `diamond` (v. 0.9.26.127) [40] in `blastn` mode applying an e-value cutoff of 1×10^{-3} and collecting the top database hit. The search output was imported into `MEGAN` (v. 6.17.0) [39] for taxonomic classification.

mRNA sequences belonging to bacteria were queried against the SwissProt database (release 2020_05) [41] with `diamond` (v. 0.9.26.127) [40] in `blastx` mode applying an e-value cutoff of 1×10^{-3} and collecting the top database hit. Sequences were annotated using the KEGG Orthology (KO) based on a custom mapping file that contains KO assignments for SwissProt sequences. KO assignments for SwissProt sequences were obtained using `GhostKoala` (v. 2.2) with default settings [42]. The numbers of mRNA sequences assigned

to individual KOs were used for deducing relative abundance information about mRNA sequences linked to metabolic pathways of interest.

2.9. Taxonomic Annotation of Functional Subsets

Sequences linked to functional categories of interest were extracted based on their KO assignment. These sequence subsets were subsequently queried against NCBI Refseq and taxonomically annotated using diamond and MEGAN as outlined above.

2.10. Metatranscriptome Read Recruitment Analysis of Dominant Fe-Cycling Microbes

All available genomes of highly abundant Fe-cycling microbes (*Leptospirillum* spp., *Acidithrix* spp., *Ferroplasma* spp., *Acidiphilium* spp., *Acidocella* spp., *Granulicella* spp.) were downloaded as nucleotide fasta files from the NCBI assembly database (accessions are given in Table S1). Anvi'o (v. 6.1) [43] was used to identify open reading frames with *prodigal* (v. 2.6.3) [44]. Identified genes were annotated based on *blastp* (v. 2.5.0), *hmmer* (v. 3.2.1) and *KofamScan* (v. 2020-03-02) [45–47] searches against the clusters of orthologous groups (COGs) database (release 2014) [48], *Pfam* (v. 32.0) [49] and *KEGG* (release 93.0) [50]. Metatranscriptome sequences derived from mRNA were mapped onto the collected genomes with *bowtie2* (v. 2.3.5) applying default settings [51]. The resulting sam files were converted to bam files using *SAMtools* (v. 1.9) [52] with default settings. Read count tables were generated using *featurecounts* (v. 1.6.4) [53] and gene expression analysis was performed using the package *edgeR* (v. 3.26.8) [54]. Genes with \log_2 counts per million (\log_2 CPM) were plotted as distribution plot and \log_2 CPM with the lowest values were set as cutoff values (Figure S1). Expressed genes were defined as genes featuring \log_2 CPM values above the defined cutoff in at least three samples. Determined KO assignments of the expressed genes were used to profile the expressed metabolic potential. The coverage ratios of pathways were calculated by dividing the number of expressed genes by the number of genes in individual bacterial genomes corresponding to the individual pathway.

2.11. Oxic and Anoxic Microcosm Incubation Experiments

A volume of 120 L of lake water (20 L of lake water from around 1 m depth and 100 L of water from 5–6 m depth) was stored overnight at 4 °C to allow precipitation of iron snow. The lake water was then centrifuged at $702\times g$ for 5 min at 4 °C and the iron snow-free lake water supernatant was separated from the iron snow precipitate. A total of 36 sterile 150 mL incubation serum bottles were set up with 1.1 mL of the collected iron snow and 120 mL of iron snow-free lake water each. FeSO_4 was added to each replicate microcosm to a final concentration of 3 mM and sealed with butyl rubber stoppers. In oxic microcosms, oxygen sensor spots (PreSens, Regensburg, Germany) were adhered to the wall of each bottle to monitor O_2 concentrations in the liquid phase. Anoxic microcosm incubations were flushed for two hours with sterile N_2 (Linde, Pullach, Germany). Lastly, 4.2 mL of either ^{13}C -labeled CO_2 or unlabeled $^{12}\text{CO}_2$ were added to each oxic and anoxic replicate. The microcosms were incubated in the dark at 15 °C for 28 days to induce chemoautotrophic CO_2 fixation. During incubation, Fe(II) concentrations were determined as described above. Additional FeSO_4 was added to oxic incubations to a final concentration of 3 mM, when measured concentrations reached 0 mM. The same incubations were spiked with additional 4.5 mL of 100% sterile O_2 (Linde, Pullach, Germany) to yield a final concentration of $\sim 250\ \mu\text{M}$, when the O_2 concentrations decreased to 1/3 of the initial concentration. A Student's t-test was used to compare the difference of microcosms under oxic and anoxic conditions and determine statistical significance ($p < 0.05$).

2.12. Nucleic Acid and Protein Extraction of Microcosms

Sets of triplicate microcosms from $^{12}\text{CO}_2$ and $^{13}\text{CO}_2$ incubations under both oxic and anoxic conditions were harvested after 7, 14 and 28 days. The content of the microcosms was centrifuged at $1500\times g$ for 5 min to separate iron snow from lake water. After that, iron snow pellets were washed with an oxalate buffer and incubated for 5–10 min until

the brownish ferric iron minerals were completely dissolved. Cells were then pelleted by centrifugation at $22,000 \times g$ for 5 min at 4°C , followed by transfer into 2.6 mL of SET buffer (0.75 M sucrose, 40 mM EDTA, 50 mM Tris base pH 9) in 15 mL conical tubes. Cell lysis was conducted by adding 350 μL 10% SDS and 20 μL 100 mM phenylmethylsulfonyl fluoride (PMSF) in 2-propanol and subsequent incubation for 2 h at 60°C , 800 rpm (HTA-BioTec, Bovenden, Germany). The obtained solution was extracted twice with 2 mL of phenol-chloroform-isoamyl alcohol (25:24:1 v/v/v, AppliChem, Darmstadt, Germany) and twice with 2 mL of chloroform-isoamyl alcohol (24:1 v/v, AppliChem, Darmstadt, Germany), centrifuging for 5 min at $3220 \times g$. The obtained aqueous phase was subjected to overnight precipitation at -20°C with 5 μL of glycogen (20 mg mL^{-1} , Sigma-Aldrich, Darmstadt, Germany), 1 mL of NH_4OAc and 8 mL of pure ethanol. Total nucleic acids were collected by centrifugation at $3220 \times g$ and 4°C for 30 min. The resulting pellets were washed with ice-cold ethanol (80% v/v), centrifuged at $16,260 \times g$ at 4°C for 20 min and suspended in 100 μL of TE buffer.

The phenol phase was collected in 15 mL falcon tubes, washed with 1 mL of SET buffer and centrifuged at $3220 \times g$ for 10 min at 4°C . The bottom phenol phase was transferred to a 50 mL falcon tube containing 20 mL of 0.1 M NH_4OAc (dissolved in MeOH), precipitated overnight at -20°C and pelleted by centrifugation ($3220 \times g$ at 4°C for 1 h). The protein pellets were washed twice with 0.1 M NH_4OAc , twice with 80% acetone and once with 70% EtOH. Each washing step of pellets was followed by incubation (-20°C for 20 min) and centrifugation ($16,260 \times g$, 4°C for 10 min.). The resulting protein pellets were air dried for 15 min and stored at -20°C .

2.13. Metaproteomics Analysis: Identification, Taxonomy, Function and ^{13}C Quantification of Peptides from Proteins

Protein extracts were subjected to one-dimensional SDS polyacrylamide gel electrophoresis, followed by tryptic digestion using Trypsin Gold (Promega, Madison, WI, USA), as previously described [55]. The resulting tryptic peptides were desalted and enriched using ZipTip- $\mu\text{C}18$ (Merck, Darmstadt, Germany). The obtained peptides were resuspended in 0.1% formic acid and analyzed on a Q Exactive HF instrument (Thermo Fisher Scientific, Waltham, MA, USA), equipped with a TriVersa NanoMate source (Advion Ltd., Ithaca, NY, USA) in LC chip coupling mode. Mass spectrometric raw data were analyzed using Proteome Discoverer (v1.4.1.14, Thermo Fisher Scientific, Waltham, MA, USA) with the Sequest HT search algorithm. Protein identification was performed using a self-built reference database based on microbial community composition of the microcosms determined by 16S rRNA gene and metatranscriptome analysis (see above). Protein sequences of respective microbial genera were downloaded from UniProt (release 2020_02) [56], or from NCBI, if no sequences from UniProt were available. Searches were conducted with the following parameters: Trypsin as enzyme specificity and two missed cleavages allowed. A peptide ion tolerance of 10 ppm and an MS/MS tolerance of 0.05 Da were used. As modifications, oxidation (methionine) and carbamidomethylation (cysteine) were selected. Peptides that scored a q-value $>1\%$ based on a decoy database and with a peptide rank of 1, were considered identified. Functional classification of identified proteins was conducted by mapping accession numbers from Uniprot to the KEGG Orthology (KO) database (Release 93.0) [50]. For proteins without mapped KO, amino acid sequences were classified using BlastKoala (v.2.2) [42].

The identification of ^{13}C -labelled peptides and the calculation of their ^{13}C relative incorporation abundance (RIA) were performed by comparing theoretical and experimental isotopologue patterns, chromatographic retention times and fragmentation patterns as previously described [57]. The RIA was used to distinguish between active autotrophs assimilating $^{13}\text{CO}_2$ (RIA above 90%), active heterotrophs potentially labeled by crossfeeding (RIA between 1.1% and 90%) and inactive microbes (RIA of 1.1%, i.e., natural abundance of ^{13}C). Generation times of *Leptospirillum*, *Ferroplasma* and *Acidiphilum* were calculated based on the relative intensity of the mass spectrometric signals of unlabeled and labeled peptides as previously described [57]. Firstly, the number of doublings n was calculated using

Equation (1), where I_{12c} is the signal intensity of the unlabeled peptide and I_{13c} is the signal intensity of the labeled peptide:

$$n = \log_2 \frac{I_{12c} + I_{13c}}{I_{12c}} \quad (1)$$

In case of overlapping signals of labeled and unlabeled peptides, the monoisotopic peak was used to determine the total abundance of unlabeled peptide based on the natural distribution of heavy isotopes, as previously described [58]. Finally, the generation time t_d was calculated using Equation (2), where Δt is the incubation time:

$$t_d = \frac{\Delta t}{n} \quad (2)$$

2.14. Statistics

Statistical analyses were performed with the R software framework (v. 3.5.3) (R Core Team, 2020). Permutational multivariate analysis of variance (PERMANOVA) was used to compare microbial communities between different years or different incubations. The Pearson correlation coefficient was calculated to determine if oxygen and iron consumption were correlating. All other testing was performed using a Student's *t*-test. Test results were considered significant if two-tailed *p* values were smaller than 0.05.

2.15. Figure Generation

The UpSetR package [59] was used to create the intersect plot depicting overlapping KOs between the 2017 and 2018 samples. Unless otherwise stated, all figures were produced using the R package ggplot2 (version) (Wickham 2016) and polished with Inkscape (v. 0.92) (<https://inkscape.org/> (accessed on 01 January 2017)).

3. Results

3.1. Physicochemical Characterization and Microbial Community Composition and Diversity of Lake 77

The sampling at Lake 77 in August 2017 and 2018 was conducted prior to the beginning of the mixing period between surface water (epilimnion) and the anoxic hypolimnion fed by Fe(II)-rich groundwater. In 2017, the stratification was beginning to diminish due to the onset of mixing, resulting in a downward shift of the redoxcline (3.5–5 m), while the stratification and redoxcline (3–4.5 m) were more defined in 2018 (Figure 1A). In both years, profiles of opposing gradients of Fe(II) and O₂ were observed with increasing depths. A decline in dissolved O₂ was observed at the upper depths of the redoxcline and decreased to ~0 mg L⁻¹ just below the redoxcline, while Fe(II) concentrations increased to 0.32 and 0.73 mmol L⁻¹ in 2017 and 2018, respectively, below the redoxcline. The acidic pH (2.3–2.4 in 2017, 2.5–2.6 in 2018) and conductivity (2.9–3.2 mS cm⁻¹ in 2017, 2.7–3.1 mS cm⁻¹ in 2018) remained stable across depth, whereas the temperature decreased with increasing depth (from 22 to 11 °C). Sulfate concentrations fluctuated over depths, ranging 16.17–19.64 mM in 2017 and 15.84–19.34 mM in 2018 (Table S2).

3. Insights into autotrophic activities and carbon flow in iron-rich pelagic aggregates

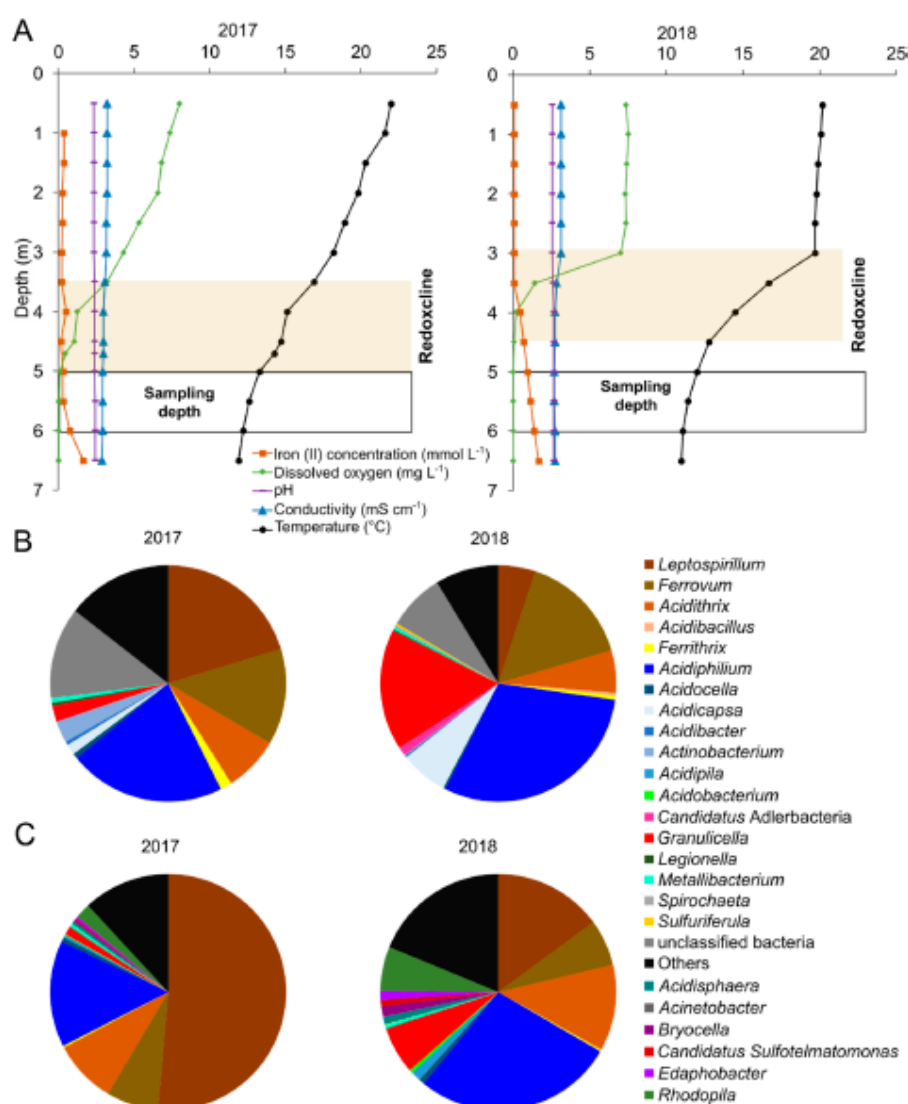


Figure 1. Water profile and microbial taxonomy of iron snow. **(A)** Water profiles of biogeochemical parameters measured at the sampling location in the central basin (CB) of Lake 77 in August 2017 and August 2018. The redoxcline is highlighted in yellow and the range of sampling depth is outlined in black. **(B)** Microbial community composition in iron snow based on 16S rRNA gene amplicon sequencing. Only bacteria classified to the genus level with relative abundance greater than 0.1% are shown. Others represent the sum of bacteria assigned at the genus level, but relative abundance is less than 0.1%. Unclassified bacteria represent bacteria not assigned to any given genus. Data represent the mean of three replicates per year. **(C)** Microbial community composition in iron snow based on mRNA sequences derived from metatranscriptome datasets. Only bacteria classified to genus level with relative abundance greater than 0.5% are plotted.

To profile the iron snow microbial community and to identify key players based on transcriptional activity, we performed 16S rRNA gene amplicon and total RNA sequencing. In addition, we were interested in investigating if outlined differences with respect to different sampling years were reflected in microbial community structure. Overall, the microbial compositions of the two different years were similar (PERMANOVA, $p > 0.05$) (Figure S2). Between 21.6 and 41.4% of SSU rRNA-derived metatranscriptome sequences were taxonomically assigned at the genus level (17.9%–37.2% of sequences linked to bacteria and 3.6–6.2% related to eukaryotes). Iron snow microbiome taxonomic profiles of 16S rRNA sequences showed the dominance of bacteria involved in Fe-cycling (72.6–92.2%) (Table S3), while high relative abundances were detected for *Stramenopile* (74.6–91.7%) in 18S rRNA sequences (Table S4). Both 16S rRNA gene amplicon sequencing and transcriptome sequencing showed that the microbial community was predominantly composed of FeOB (*Leptospirillum*, *Ferroplasma*, *Acidithrix*) and FeRB (*Acidiphilium*, *Acidoceles*) (Figure 1B,C, Table S3). The relative abundance of *Leptospirillum* in 2017 was significantly higher than the relative abundance of *Leptospirillum* in 2018 (51.4% and 15.0%, respectively), whereas the relative abundance of *Acidiphilium* was higher in 2018 in comparison to 2017 (27.5% and 14.5%, respectively) based on mRNA sequences (Figure 1C). In addition to Fe-cycling microbes, we also detected polysaccharide-degrading bacteria, such as *Granulicella* (1.1–6.4%), and the phototroph, *Rhodospira* (1.8–6.6%), in the metatranscriptome datasets (Figure 1C). The phototrophic Cyanobacteria (0.04–0.08%) were only detected in the 2017 16S rRNA amplicon datasets.

3.2. Gene Expression Analysis of Iron Snow Microbial Communities

The proportion of mRNA sequences ranged from 4.4% to 13.1% in the metatranscriptome datasets (Table S5). Between 18.1% and 41.6% of the mRNA sequences were assigned to bacteria. Substantially smaller fractions were linked to eukaryotes (0.16–0.75%) and archaea (0.11–0.23%). In total, 25.7–30.7% of bacterial mRNA sequences were functionally assigned based on KEGG orthology (KO). In total, 3427 and 3436 different functions were identified based on KOs for the 2017 and 2018 metatranscriptome datasets, respectively (Figure 2A). A total of 91.0% of the KOs was shared between the two datasets. In order to identify direct links between taxonomy and functions, mRNA sequences of representative KOs/gene functions based on metabolic pathways of interest were subsequently taxonomically assigned (Table S6). Genera classified as either FeOB (*Leptospirillum*, *Ferroplasma* and *Acidithrix*) or FeRB (*Acidiphilium*) showed the highest transcriptional activity for functions linked to CO₂ fixation, polysaccharide biosynthesis and motility (Figure 2B).

We were able to assign bacterial mRNA sequences to the following complete CO₂ fixation-related pathways: the Calvin–Benson–Bassham (CBB) cycle (2.0–2.8%) and the reverse tricarboxylic acid (rTCA) cycle (2.2–2.6%). The percentages are in relation to all other pathways. In total, 6.1–57.6% of sequences affiliated to key genes *rbcL* (ribulose-bisphosphate carboxylase large chain), *rbcS* (ribulose-bisphosphate carboxylase small chain), *frdABCD* (fumarate reductase gene cluster), *korABCD* (2-oxoglutarate/2-oxoacid ferredoxin oxidoreductase), *adABY* (ATP-citrate lyase), *ccsAB* (citryl-CoA synthetase), *ccp* (citryl-CoA lyase) of the two CO₂ fixation pathways mentioned above were assigned to *Leptospirillum*. However, few mRNA sequences of *Ferroplasma* were mapped to the above key genes. We only detected a few mRNA sequences linked to archaea and eukaryotes and did not detect transcriptional activity for carbon fixation from archaea or eukaryotes. Additionally, there were 0.06–0.26% of sequences linked to photosynthetic reaction centers (Figure S3) and 98% of these sequences were mapped to *Acidiphilium*. *Acidiphilium rubrum* was previously found to show light-stimulated CO₂ uptake [60,61]. Genes linked to anoxygenic photosystem II (*pufABLM*, *pufA*) were partially expressed. Of these mRNA sequences, only 1.08% were mapped to photosynthetic bacteria (*Rhodospira*, *Rhodospirillum rubrum*).

3. Insights into autotrophic activities and carbon flow in iron-rich pelagic aggregates

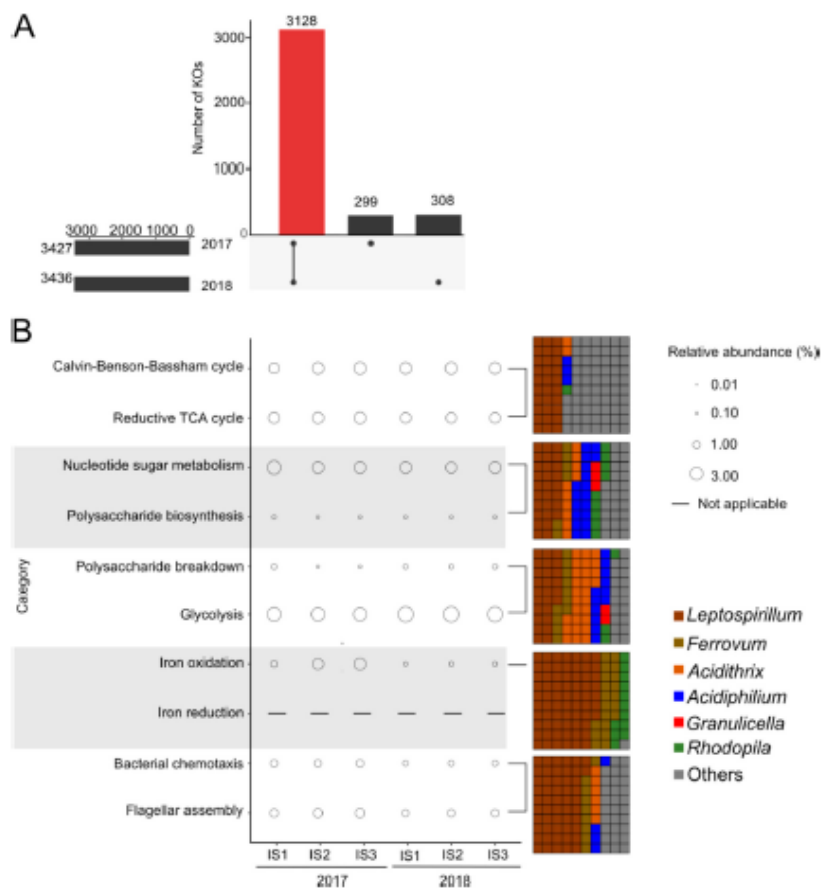


Figure 2. Functional profile of iron snow microbiome in metatranscriptome datasets. **(A)** The UpSetR package [59] was used to visualize shared and specific sets of KOs between the metatranscriptome datasets. Bar charts refer either to the total number of KOs in the datasets or the number of KOs for indicated intersects. **(B)** The relative abundances of functional categories in metatranscriptome datasets. Different colors represent different taxonomies linked to functional categories and only the top 6 taxonomic groups with the highest relative abundance are shown. Waffle charts represent relative abundances of assigned taxonomic groups within respective functional categories of interest. Others represent bacteria associated with one or two functional categories.

We identified mRNA sequences of genes predicted to be involved in the metabolism of nucleotide sugar, such as UDP-glucose, UDP-galactose and UDP-glucuronic acid, all of which may serve as precursors for the synthesis of exopolysaccharides. Additionally, we mapped mRNA sequences to the genes involved in the exopolysaccharides biosynthesis, such as *cysE* (serine O-acetyltransferase), involved in vibrio polysaccharide biosynthesis in *Vibrio cholerae*, *rfbN* (rhamnosyltransferase), involved in Psl polysaccharide biosynthesis in *Pseudomonas aeruginosa*, and *wza* (polysaccharide biosynthesis/export) and *pgaBC* (poly-N-acetyl-glucosamine biosynthesis) in *Escherichia coli*. Gene functions linked to EPS production (nucleotide sugar metabolism, exopolysaccharide biosynthesis) were present in 2.6–3.8% of the mRNA sequences. The FeOB *Leptospirillum*, *Ferrovum* encoded 24.9–75.2% of the mRNA sequences linked to EPS production.

We also mapped mRNA sequences to polysaccharide breakdown enzymes, such as β -glucosidase and endoglucanase. Bacterial gene functions linked to organic carbon utilization, for example glycolysis and polysaccharide breakdown, made up between 3.5% and 4.8% of the bacterial mRNA sequences. Of these mRNA sequences, 23.7–54.2% were assigned to the heterotrophs *Acidithrix* and *Acidiphilium*. Additionally, we found mRNA sequences mapped to genes linked to the Fe(II) oxidation (0.3–2.6%), of which 98.6% of sequences were mapped to *Leptospirillum*, *Ferroplasma* and *Rhodospila* in both datasets. mRNA sequences linked to Fe(III) reduction were not detected, due to a lack of knowledge of Fe(III) reduction machineries in acidophiles. Motility was essential in the iron snow microbiome with assignment rates (1.4–2.6%) to chemotaxis and flagellar assembly, of which 68.8% of sequences were assigned to *Leptospirillum*, *Ferroplasma*, *Acidithrix* and *Acidiphilium*.

3.3. Taxonomic Profiles of Active FeOB and FeRB Taxa in Oxidic and Anoxic Iron Snow Microcosm Incubations

To identify the active key players in the iron snow, we performed $^{13}\text{CO}_2$ SIP combined with metaproteomics in iron snow microcosm incubations, amended with iron snow samples collected in 2018. The microcosms were incubated under oxidic and anoxic conditions, similar to conditions above and below the redoxcline of Lake 77. In the oxidic microcosms, the rate of oxygen consumption increased (Student's *t*-test, $p < 0.001$) 15-fold, from 1.69 to 25.64 $\mu\text{M day}^{-1}$, from 1–7 days (T1) to 15–28 days (T3). The rate of Fe(II) oxidation increased (Student's *t*-test, $p < 0.05$) 2.6-fold from 0.56 to 1.48 mM day^{-1} in the same period (Figure S4A,B). Oxygen consumption rates showed a highly significant correlation to iron consumption rates (Pearson correlation, $p < 0.001$) (Figure S4C), demonstrating that active iron oxidizers were present in the microcosms. However, there were no significant changes in the Fe(II) concentration in anoxic microcosms.

The dominant Fe-cycling bacteria (*Leptospirillum*, *Ferroplasma*, *Acidithrix*, *Acidiphilium* and *Acidocella*) and the second most dominant bacteria (*Granulicella* and *Rhodospila*) in iron snow microcosms were consistent with the iron snow microbiome composition in the metatranscriptome datasets (Figure 3B). However, microbial compositions based on 16S rRNA amplicon sequencing and the relative abundances of peptides changed significantly between incubation conditions at three time points (PERMANOVA, $p < 0.001$) (Figure 3A, Figure S4D). Consistent with the absence of Cyanobacteria based on 16S rRNA amplicon sequencing of in situ iron snow in 2018, we did not detect 16S rRNA sequences assigned to Cyanobacteria in either the oxidic or anoxic microcosms. The relative abundances of the iron snow key player, *Acidithrix*, were significantly higher (Student's *t*-test, $p < 0.001$) under anoxic conditions in comparison to oxidic conditions, but the relative abundances did not differ over different incubation times. Among the top 10 bacteria which drive the difference between the microbial communities in the cluster of microcosms under oxidic and anoxic conditions, the different abundances of FeOB rather than FeRB contributed the most differences of microbial communities (Figure S5).

3.4. Carbon Flow of Dominant Iron Cycling Bacteria in Iron Snow Microcosms

Investigation of the C flux revealed *Ferroplasma* and *Leptospirillum* fixed CO_2 in the oxidic microcosms, leading to a ^{13}C relative isotope abundance (RIA) higher than 90% in their peptides (Figure 4A). These active chemolithoautotrophs showed generation times of 6 and 16 days within the first week of incubation, respectively (Figure S6). Peptides of *Acidocella* and *Acidiphilium* displayed a much lower ^{13}C RIA of 1.6% at T1, increasing to 2.7%, and 2.8% at T3. These incorporation patterns suggest heterotrophic growth on a mostly unlabeled source of organic carbon in the iron snow, receiving minor input of $^{13}\text{CO}_2$ -derived carbon from the chemolithoautotrophs. Interestingly, the generation times of *Acidiphilium* (9–20 days) were in the same range as those of the chemolithoautotrophs, indicating fast growth. Surprisingly, *Candidatus* Finniella and *Spirochaeta* showed RIA greater than 90% at T3. Both of these organisms are strictly heterotrophic, with *Candidatus* Finniella being an endosymbiont of a protist [62] and *Spirochaeta* is heterotrophic utilizing different mono-, di- and oligosaccharides (e.g., pentose, starch) [63]. This suggests that

these bacteria got labeled by cross-feeding of $^{13}\text{CO}_2$ -derived organic carbon directly from *Leptospirillum* and *Ferroplasma* and not the unlabeled organic carbon source in the iron snow that *Acidiphilium* and *Acidocella* were using. Their generation times were 17 and 12 days at T3, separately. *Acidithrix* and *Granulicella* were not found to be active in the microcosms, although they were highly abundant in the in situ iron snow microbiome and oxic and anoxic microcosms. The larger deviation of the RIA for *Ferroplasma* and *Leptospirillum* at T2 was caused by one replicate microcosm with a significantly lower RIA in the highly labeled organisms, likely due to a contamination with approximately 10% $^{12}\text{CO}_2$.

The generation time of *Ferroplasma* under anoxic conditions with average 32 days was significantly higher (Student's *t*-test, $p < 0.01$) than 6 days under oxic conditions within the time frame investigated, implying slower growth (Figure S6). In the anoxic microcosms, only *Ferroplasma* fixed CO_2 , leading to RIA greater than 90%. None of the remaining bacteria showed detectable metabolic activity within the time frame investigated (Figure 4B).

3.5. Metatranscriptomic and Metaproteomic Functional Profile of Dominant Microbes

The dominance of Fe-cycling bacteria and carbon transfer between FeOB and FeRB suggests the Fe-cycling key microbes play an important role in iron snow. In order to profile the functions of the key players in the in situ microbiome below the redoxcline and in microcosms under oxic and anoxic conditions, we mapped mRNA sequences to the available *Leptospirillum*, *Ferroplasma*, *Acidithrix*, *Acidiphilium*, *Acidocella* and *Granulicella* genomes in NCBI assembly database (Table S1) and profiled peptides linked to these key players in both the oxic and anoxic microcosms (Figure 5). Among these mapped genomes, iron snow isolates *Acidithrix* sp. C25, *Acidiphilium* sp. C61, *Acidocella* sp. C78 recruited most of the mRNA sequences. In total, 84.4%, 84.1% and 92.2% of their genomes were found to be expressed, respectively (Table S7). *Ferroplasma* expressed the whole set of CBB cycle genes for CO_2 fixation. While most of the rTCA cycle genes were expressed by *Leptospirillum*, we did not find any mRNA sequences mapped to the key genes in the *korABCD* (2-oxoglutarate/2-oxoacid ferredoxin oxidoreductase) and *adABY* (ATP-citrate lyase) operons. In agreement, peptides associated with the CBB cycle and rTCA cycle were mostly affiliated with *Ferroplasma* and *Leptospirillum* (Figure 5). Peptides linked to exopolysaccharide biosynthesis (e.g., *wza*) were found in chemolithoautotrophic *Leptospirillum* in oxic microcosms and *Ferroplasma* in both oxic and anoxic microcosms. However, peptides linked to polysaccharide breakdown were identified in *Acidiphilium* in oxic microcosms, but not *Acidocella*, despite the identification of peptides linked to organic carbon utilization in *Acidiphilium* and *Acidocella*. We observed peptides linked to flagellar assembly in *Acidithrix*, *Acidiphilium* and *Acidocella* in oxic microcosms, but not in the anoxic microcosms.

3. Insights into autotrophic activities and carbon flow in iron-rich pelagic aggregates

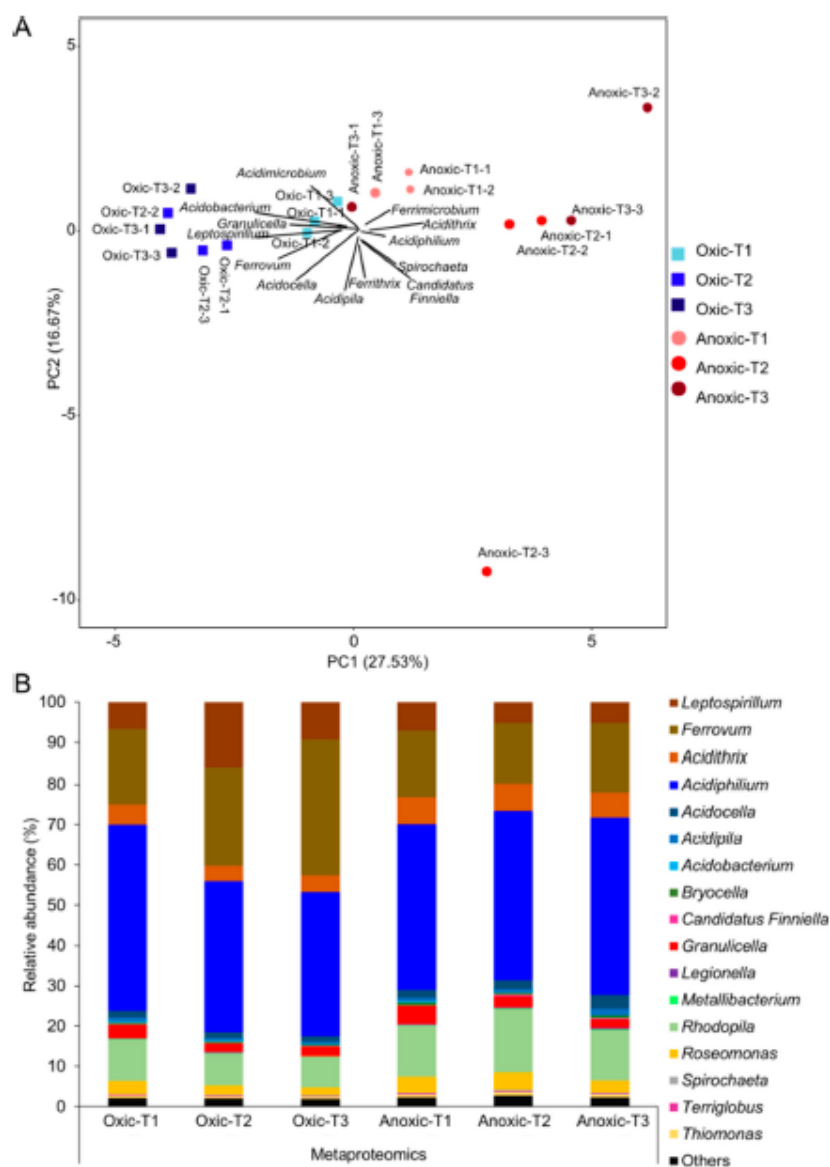


Figure 3. Taxonomic composition of iron snow microcosms in metaproteome datasets. **(A)** Principal component analysis of taxonomic profiles of iron snow microcosms over three time points at the genus level. Triangles represent oxic microcosm incubations and circles represent anoxic microcosm incubations. Different colors represent different time points. T1, T2 and T3 refer to predetermined sampling time points: 7, 14 and 28 days, respectively. **(B)** Microbial community composition based on the relative abundance of peptides of iron snow at the genus level. Only bacteria classified to the genus level with relative abundance greater than 0.1% are plotted.

3. Insights into autotrophic activities and carbon flow in iron-rich pelagic aggregates

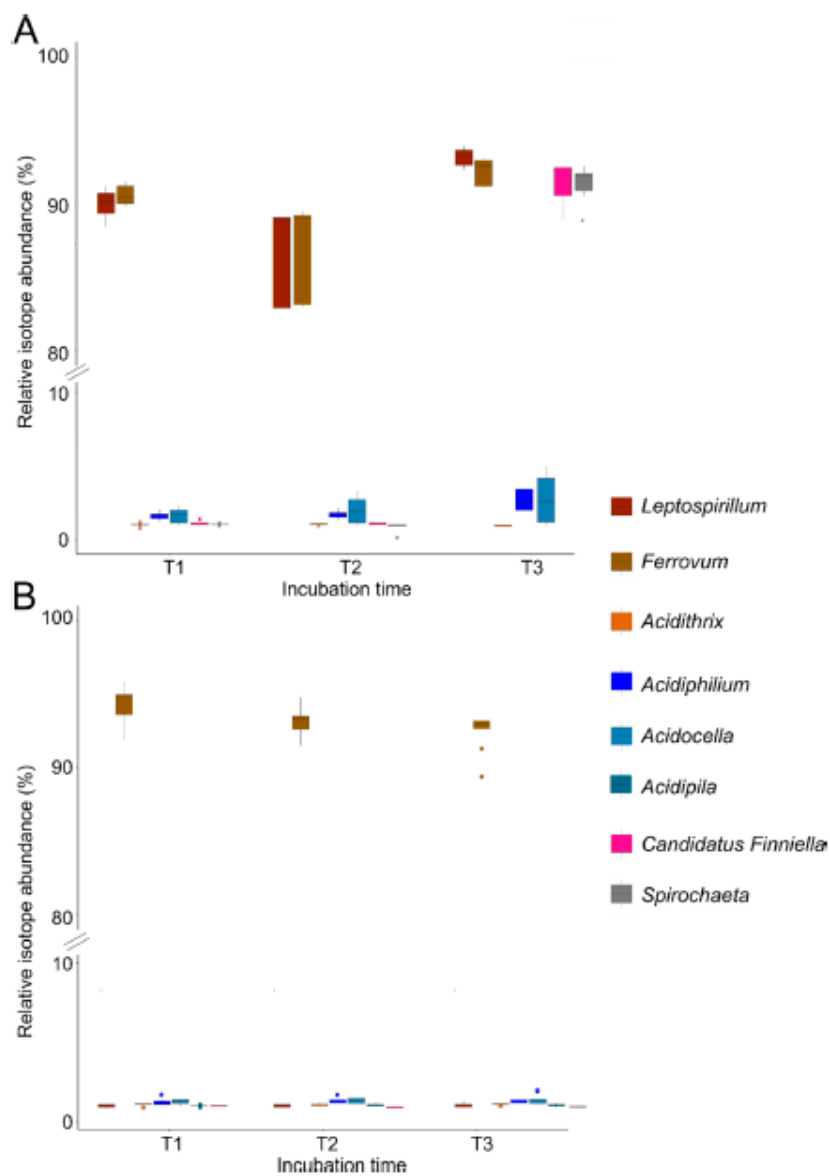


Figure 4. ^{13}C incorporation patterns of dominant iron cycling bacteria in iron snow microcosms. (A) Boxplot of bacterial ^{13}C incorporation pattern under oxic conditions. x axis represents three incubation times (T1: 7 days; T2: 14 days; T3: 28 days) and y axis shows the relative isotope abundance (RIA) starting from 0% to 100%. Different colors represent different genera. The dots represent outliers of ^{13}C incorporation value away from the median. (B) Boxplot of bacterial ^{13}C incorporation pattern under anoxic conditions.

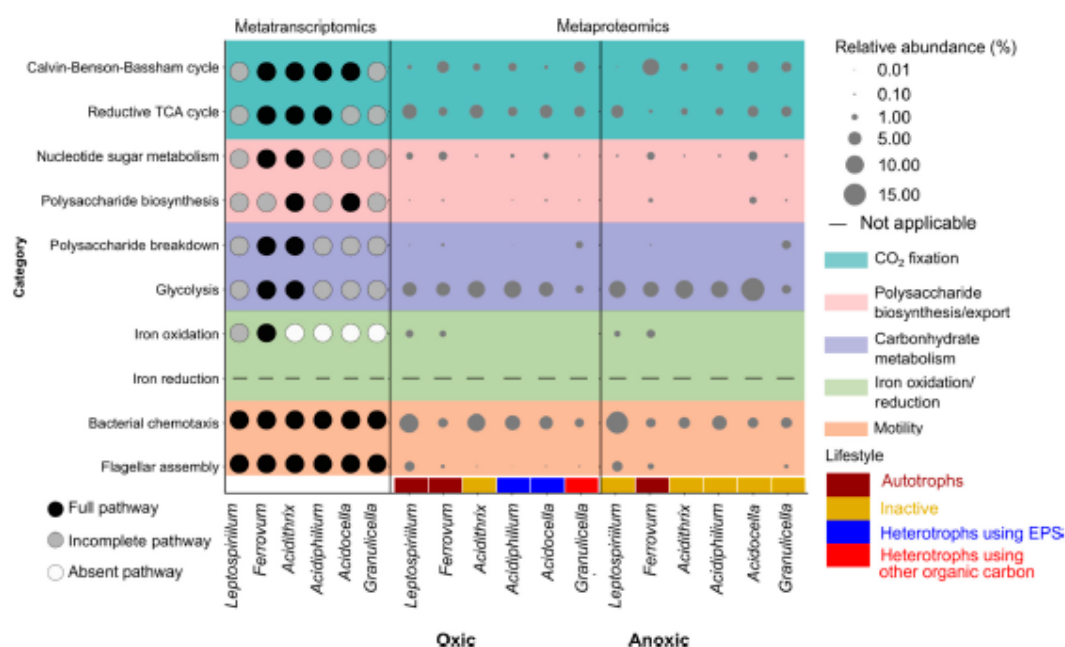


Figure 5. Functional profile of dominant iron cycling bacteria in the metatranscriptome and metaproteome datasets. The left panel represents the transcriptional activity of bacteria based on mapping of mRNA sequences to genomes in 2018 metatranscriptome datasets. The pathway coverage of each genome is shown in Figure S7. Dark, grey, white represent complete, incomplete, absent pathway separately based on mapping coverages of pathways. The right panel represents the proportion of functionally assigned peptides to any KEGG category in bacteria. The missing dot means that the number of peptides affiliated with the category equals to 0. Data represent the mean of replicates at three timepoints.

4. Discussion

The acidic ferruginous model Lake 77 provides ideal conditions to investigate the extent to which Fe(II) oxidation linked autotrophy (chemolithoautotrophy) contributes to the biological carbon pump versus the contribution from classical photoautotrophy. The Fe-cycling microbes found in Lake 77 mimic the previously characterized AMD and pit lake microbial communities [64,65]. Our molecular data consistently show the dominance of autotrophic FeOB (*Leptospirillum* and *Ferroplasma*) in iron snow, whereas autotrophic communities in marine or lake snow are dominated by phytoplankton (i.e., cyanobacteria and algae). Phytoplankton contributes to more than 50% of overall primary production in marine snow or lake snow [66–68]. The most abundant phototrophic bacterium, *Rhodospila*, accounted for 88.1–93.3% of all phototrophs detected in the iron snow of Lake 77. However, the relative abundances of mRNA sequences linked to *Rhodospila* ranged from 1.8 to 6.6%. Members of this genus are described as acidophilic anaerobic anoxygenic phototrophic purple bacteria [69]. After mapping mRNA sequences onto the *Rhodospila* genomes, we did not detect gene expression for all genes of the CBB-cycle. Transcripts linked to the small subunit of RuBisCO were not found. The mRNA sequences associated with eukaryotes were 31–388 times lower than the mRNA sequences mapped to bacteria in our samples. Several key genes of CO₂ fixation pathways were missing in mRNA sequences mapped to eukaryotes, including the small and large chain RuBisCO genes and a fumarate reductase gene cluster. Based on these findings, photosynthetic CO₂ fixation of eukaryotes and bacteria is of minor importance in iron snow, which further elucidates the difference

in microbially mediated processes across environments characterized by the presence of pelagic aggregates. For example, the dominant bacteria in marine or lake snow are members of the Bacteroidetes phylum, including the *Cytophaga* and *Flavobacteria* genera, and the Proteobacteria phylum, including α -, β - and γ -Proteobacteria, all of which are mainly associated with degrading OM during sinking of these pelagic aggregates [70,71].

Despite the differences in microbial community composition between iron snow and marine or lake snow, the functional properties of the aggregate communities were rather similar. In addition to genetic pathways responsible for CO₂ fixation, we also found evidence for other key microbially mediated processes found in marine snow, e.g., polysaccharide biosynthesis [72], organic carbon hydrolysis [73], nitrogen fixation [74], sulfate reduction [75] and motility [76]. The most abundant Fe-cycling microbes (*Leptospirillum*, *Ferroplasma*, *Acidithrix* and *Acidiphilium*) comprise more than 50% of the total iron snow community. These four microbes also represent the community members with the highest transcriptional activity based on mRNA abundances. Transcripts linked to CO₂ fixation, EPS biosynthesis, electron transfer processes, nitrogen fixation, sulfate reduction and flagellar-based motility were the most abundant. However, abundances of mRNA sequences involved in N₂ fixation were low (0.01%–0.09%). At the species level, two of our iron snow isolates, *Acidithrix* sp. C25 and *Acidiphilium* sp. C61, similarly expressed the most genes linked to these general activities. The high abundances of mRNA sequences mapped to *Leptospirillum* and *Ferroplasma* in our datasets were linked to CO₂ fixation and polysaccharide production, suggesting that these chemolithoautotrophic FeOB are the key species also driving EPS production. Conversely, in marine snow, phytoplankton (e.g., diatoms, cyanobacteria) produce transparent exopolymeric particles (TEP) or exopolysaccharides, which mediate cell aggregation and coagulation [77–79]. Cyanobacteria are mainly responsible for the marine or lake snow dinitrogen (N₂) fixation [80,81], with an annual contribution ranging from 26 to 47% in the North Pacific Subtropical Gyre [82], but do not play a significant role in iron snow.

Due to pyrite oxidation in Lake 77, concentrations of sulfate are high in the water column (up to ~20 mM), however, mRNA sequences linked to assimilatory/dissimilatory sulfate reduction were relatively low, ranging from 0.40% to 0.58%. The sulfate concentration is 11–16× higher than in meromictic Lake Cadagno [83]. Microbially mediated sulfate-reduction leading to the production of sulfide in marine and lake snow occurs in lower anoxic zones of the water column [75,84]. Sulfide concentrations within marine snow range from 1.3 to 25 $\mu\text{mol S L}^{-1}$ [75], while Lake Cadagno contains 1.5–1.9 mmol S L^{-1} in the monimolimnion [85]. We found evidence for the activity of sulfate reducers with extremely low relative abundance (~0.3%) in iron snow (e.g., *Desulfosporosinus*, *Desulfobulbus*). The low pH conditions in mining lakes limit sulfate reduction to sediment zones with higher pH [86,87], as only few sulfate reducers are known to tolerate low pH conditions [88,89].

Specific to iron snow microbiome activities, the chemical mediator-driven interactions observed between *Acidithrix* sp. C25 and *Acidiphilium* sp. C61 are in part due to the production and detection of PEA by these microbes, respectively [21]. We found 0.004–0.01% of mRNA sequences linked to amino-acid decarboxylase, which is linked to PEA production. PEA produced by *Acidithrix* sp. C25 induces aggregation in *Acidiphilium* strains [21,90]. Marine snow-associated bacteria produce acylated homoserine lactones (AHLs) to regulate microbial colonization and coordinated group behavior by quorum sensing (QS) [91,92]. We were able to map mRNA sequences to autoinducer-1 synthesis (i.e., acyl-homoserine lactose synthase AI-1) (up to 0.003%) in *Acidocella* spp. and receptor genes (i.e., LuxR transcriptional regulator, autoinducer sensor kinase) (up to 0.004%) in *Leptospirillum* spp., *Ferroplasma* spp., *Acidiphilium* spp. and *Granulicella* spp. [91,92]. However, QS is not required for lake snow-attached bacteria. They can rely on novel signal molecules to mediate cell-cell signaling in lake snow [93]. Taken together, microbially mediated communication appears to be driven by chemical mediators in iron snow.

Similar to marine and lake snow-attached bacteria, which are known to extracellularly hydrolyze the phytoplankton-derived fixed carbon, the iron snow microbiome can utilize

oligosaccharides produced via the extracellular hydrolysis of biological materials (i.e., fixed carbon, detritus) and function as common goods to promote cooperative growth. Since carbon sources are severely limited in acidic waters [94], obligate interactions between members of microbial consortia are probably critical in the optimization of microbial activity under acidic conditions [95]. To elucidate the importance of chemolithoautotrophic-mediated CO₂ fixation for the whole iron snow microbial community, rates of incorporation and the carbon flow were elucidated in oxic and anoxic microcosm incubations. ¹³C RIA values above 90%, demonstrating chemolithoautotrophic growth, were detected in peptides of *Ferroplasma* and *Leptospirillum*. Peptides specifically linked to the CBB pathway were predominantly affiliated with *Ferroplasma*. The ¹³CO₂ fixed by these taxa (i.e., the newly available organic carbon) could subsequently be transformed to polysaccharides and ultimately used for EPS production. We observed a slow increase in ¹³C quantification values in the heterotrophs *Acidiphilium* and *Acidocella*, but not *Granulicella*, in oxic microcosms, which suggested utilization of ¹³CO₂-derived organic carbon by these most abundant heterotrophic community members. *Acidiphilium* species have the capacity to break down EPS [90,96] and couple Fe(III) reduction to oxidation of sugars [97,98]. In the metatranscriptome dataset, we found *Acidiphilium* mRNA sequences linked to polysaccharide-breakdown enzymes, such as β-glucosidases and endoglucanases, which hydrolyze polysaccharides to monosaccharides. Overall, these results suggest that CO₂ fixed by the iron snow chemolithoautotrophic FeOB is converted to polysaccharides and EPS, which provide an organic C source to the heterotrophic members, as also described elsewhere [21]. In addition, EPS initiates the cohesiveness and contributes to the structural stability of iron snow [20].

In the anoxic microcosm incubations, only *Ferroplasma* had measurable ¹³C incorporation. *Ferroplasma* has the metabolic potential to oxidize Fe(II) and reduce NO₃⁻ [23,99] coupled to CO₂ fixation, which further explains why its growth was not restricted to oxic conditions. In addition, we detected mRNA sequences linked to nitrate reductase in iron snow which was collected below the redoxcline in 2018, although we could not identify proteins linked to the nitrate reductase in anoxic microcosms. Surprisingly, FeRB did not show any activity with regards to measurable ¹³C incorporation, suggesting a limited flow of carbon to other trophic levels when iron snow is sinking through the anoxic hypolimnion of Lake 77. Instead, our functional profile analysis and corresponding identification of peptides linked to flagellar motility indicate motility is still essential for the colonization of EPS-stabilized iron snow aggregates, consistent with natural assemblages of marine bacteria that express specific flagellin genes and exhibit motility [100,101].

Modern ferruginous meromictic lakes are important analogs to study microbial processes involved in carbon cycling in the Archean and Proterozoic oceans [102], where primary production was likely driven by anoxygenic photosynthetic Fe(II) oxidizing bacteria ("photoferrotrophs") [11,13]. In Lake Matano and Lake La Cruz, for example, phosphorus limitation controls primary production in the oxic layers of Lake Matano and Lake La Cruz [103,104], which allows light penetration below the oxic-anoxic interface. Here, sulfide-oxidizing phototrophic bacteria and anoxygenic photoferrotrophs drive photosynthetic CO₂ fixation and regulate OM export [13,105,106]. Similarly, sorption of phosphorus to the high amounts of ferric iron negatively affects the eukaryotic primary activity in Lake 77 and similar environments [105]. Despite the presence of sulfur oxidation genes (*soxA* and *dsrAB*) and iron oxidation genes (*cyc2*), incomplete anoxygenic photosynthetic reaction center genes in photosynthetic bacteria suggested anoxygenic photosynthesis coupling sulfide/Fe(II) oxidation was unlikely to happen in iron snow microbiome below the redoxcline. As microcosms were incubated in the dark, we might have missed ¹³C incorporation in the most abundant anoxygenic photosynthetic bacteria, *Rhodospira*. Low ¹³C incorporation by heterotrophs after the 28-day incubation period under oxic conditions provides strong evidence that the majority of fixed CO₂ produced by microbes colonizing iron snow aggregates rapidly sinks. Iron snow is characterized by a higher Fe fraction (35%) and lower organic carbon content (11%) compared to marine or lake snow, therefore the estimated iron snow C sedimentation rate (121–600 mg C m⁻² d⁻¹) in Lake 77 is 12× higher than C sedimentation

rates in ferruginous Lake Matano ($10.56\text{--}15.6\text{ mg C m}^{-2}\text{ d}^{-1}$) [8,9] and $10\text{--}20\times$ higher than C sedimentation rates in the North Atlantic ($12\text{--}30\text{ mg C m}^{-2}\text{ d}^{-1}$) [106], due to high velocity of iron snow ($\sim 2\text{ m h}^{-1}$). Conversely, the C sedimentation rate in Lake 77 is 1–2 orders of magnitude lower than in Lake Constance [8,107]. A previous study showed that anaerobic methanogenesis accounted for more than 50% of organic matter degradation in Lake Matano [9]. Thus, the absence of ^{13}C incorporation in heterotrophic FeRB under anoxic conditions in our microcosms suggests the majority of organic carbon was exported to the sediment without significant utilization in Lake 77. The rapid sinking of newly synthesized organic C results in a short residence time and enhanced contribution to the overall carbon pump from the surface to the anoxic sediments in acidic lakes.

Considering both the metatranscriptome and metaproteome profiles, our results show that *Ferroplasma* and *Leptospirillum* are responsible for the rapid fixation of CO_2 coupled to Fe(II) oxidation under oxic conditions and represent the main chemolithoautotrophic members of the community. The diversion of fixed CO_2 to the biosynthesis of EPS represents the organic carbon fraction of the iron snow aggregates. Furthermore, EPS is subsequently broken down again and likely used for biomass production by *Acidiphilium* sp. and other heterotrophic members of the community. The low labeling in these organisms shows that the EPS pool represents a relatively large pool of organic carbon compared to the new production of EPS, which is only slowly enriched in $^{13}\text{CO}_2$ by the autotrophs. Instead, other, more readily available and usable carbon compounds released by *Ferroplasma* spp. and *Leptospirillum* spp. are used by *Granulicella* spp. for heterotrophic growth, but not by *Acidiphilium* spp., which suggests that *Acidiphilium* spp. is highly specialized to strictly rely on EPS as an organic carbon source and cannot incorporate carbon coming directly from *Ferroplasma* and *Leptospirillum* spp.

5. Conclusions

FeOB and FeRB showed the highest transcriptional activity for functions linked to carbon fixation, polysaccharide biosynthesis and flagellar motility in the iron snow microbiome. The predominance of FeOB and FeRB in the iron snow aggregates, based on 16S rRNA amplicon sequencing and functional profiling, suggest Fe-cycling bacteria play a pivotal role in iron snow aggregation, stability and overall microbiome structure. Our study shows that chemolithotrophic CO_2 fixation is the main microbially mediated inorganic C fixation process by the iron snow microbial community, rather than photosynthetic CO_2 fixation which is the predominant process in marine and lake ecosystems. Dissimilar to oceans and lakes, only a small fraction of the fixed CO_2 is transferred to the heterotrophic FeRB under oxic conditions, thus indicating limited incorporation of fixed CO_2 by the heterotrophs in the water column. Thus, iron snow creates a very efficient carbon pump between the surface and the sediment in acidic, Fe-rich ferruginous lakes.

Supplementary Materials: The following are available online at <https://www.mdpi.com/article/10.3390/microorganisms9071368/s1>, Figure S1: Density distributions of log-transformed CPM values of gene expression levels, Figure S2: Principal coordinates analysis (PCoA) showing microbial community based on amplicon and mRNA sequences, Figure S3: Functional profile of iron snow microbiome in metatranscriptome datasets, Figure S4: Oxygen, Iron concentration and microbial community composition of incubated microcosms at three timepoints, Figure S5: Taxonomic groups contributing to PCA-based ordinations of iron snow microcosms under oxic and anoxic conditions, Figure S6: Growth rate of *Leptospirillum*, *Ferroplasma*, *Acidiphilium*, *Spirochaeta*, *Candidatus* Finniella based on labeling intensity, Figure S7: Pathway coverage in each genome based on mRNA sequences mapped to each genome, Table S1: Reference genomes for the metabolic potential of key players, Table S2: Concentrations of sulfate (mM) in 2017 and 2018, Table S3: Relative abundance of iron cycling bacteria based on 16S rRNA amplicon datasets, mRNA/rRNA sequences from metatranscriptome datasets, Table S4: Relative abundance of eukaryotes at class level based on 18S rRNA sequences from metatranscriptome datasets, Table S5: Sequence processing statistics of metatranscriptome datasets, Table S6: List of KOs for functional categories of interest based on assignments to KEGG, Table S7: Numbers of expressed genes in individual genomes of key players.

Author Contributions: K.K. and R.E.C. designed the experiments. Q.L. performed the laboratory experiments and data analysis. R.E.C. and C.-E.W. supervised the RNA extractions and metatranscriptome data analysis. M.T. supervised the protein extractions and metaproteome data analysis. N.J. and M.v.B. performed the identification of peptides. Q.L. wrote the original draft. K.K., R.E.C., C.-E.W., M.T., N.J. and M.v.B. reviewed and edited the manuscript. All authors have read and agreed to the published version of the manuscript.

Funding: This work was supported by the Jena School for Microbial Communication (JSMC) graduate school, which was funded by the Deutsche Forschungsgemeinschaft (DFG) and the Carl Zeiss Foundation (Carl Zeiss Stiftung). Additional support for this research was provided by the Collaborative Research Centre Chemical Mediators in Complex Biosystems (SFB 1127/2 ChemBioSys, 239748522) of the Friedrich Schiller University Jena, also funded by the Deutsche Forschungsgemeinschaft (DFG). M.T. gratefully acknowledges funding from the DFG under Germany's Excellence Strategy - EXC 2051 - Project-ID 390713860.

Institutional Review Board Statement: Not applicable.

Informed Consent Statement: Not applicable.

Data Availability Statement: The RNA-seq data have been submitted to the ArrayExpress under the accession number E-MTAB-9686. The 16S rRNA Illumina MiSeq amplicon sequencing data of in situ iron snow samples and iron snow microcosms have been deposited at the European Nucleotide Archive EBI-ENA under the accession numbers ERR4690399-4690404 and ERR4690405-4690440, respectively. Metaproteome data have been deposited at PRIDE under accession number PXID025534.

Acknowledgments: The authors thank Jens Wurlitzer and Falko Gutmann (Friedrich Schiller University Jena) for sampling and technical assistance in the laboratory.

Conflicts of Interest: The authors declare no conflict of interest.

References

1. Alldredge, A.L.; Silver, M.W. Characteristics, dynamics and significance of marine snow. *Prog. Oceanogr.* **1988**, *20*, 41–82. [\[CrossRef\]](#)
2. Thornton, D. Diatom aggregation in the sea: Mechanisms and ecological implications. *Eur. J. Phycol.* **2002**, *37*, 149–161. [\[CrossRef\]](#)
3. Simon, M.; Grossart, H.-P.; Schweitzer, B.; Ploug, H. Microbial ecology of organic aggregates in aquatic ecosystems. *Aquat. Microb. Ecol.* **2002**, *28*, 175–211. [\[CrossRef\]](#)
4. Hmelo, L.R.; Mincer, T.J.; Van Mooy, B.A.S. Possible influence of bacterial quorum sensing on the hydrolysis of sinking particulate organic carbon in marine environments. *Environ. Microbiol. Rep.* **2011**, *3*, 682–688. [\[CrossRef\]](#)
5. Passow, U.; Carlson, C. The biological pump in a high CO₂ world. *Mar. Ecol. Prog. Ser.* **2012**, *470*, 249–271. [\[CrossRef\]](#)
6. Ploug, H.; Grossart, H.-P.; Azam, F.; Jørgensen, B.B. Photosynthesis, respiration, and carbon turnover in sinking marine snow from surface waters of Southern California Bight: Implications for the carbon cycle in the ocean. *Mar. Ecol. Prog. Ser.* **1999**, *179*, 1–11. [\[CrossRef\]](#)
7. Turner, J.T. Zooplankton fecal pellets, marine snow, phytodetritus and the ocean's biological pump. *Prog. Oceanogr.* **2015**, *130*, 205–248. [\[CrossRef\]](#)
8. Reiche, M.; Lu, S.; Ciobotă, V.; Neu, T.R.; Nietzsche, S.; Rösch, P.; Popp, J.; Küsel, K. Pelagic boundary conditions affect the biological formation of iron-rich particles (iron snow) and their microbial communities. *Limnol. Oceanogr.* **2011**, *56*, 1386–1398. [\[CrossRef\]](#)
9. Crowe, S.A.; Katsev, S.; Leslie, K.; Sturm, A.; Magen, C.; Nomosatryo, S.; Pack, M.A.; Kessler, J.D.; Reeburgh, W.S.; Roberts, J.A.; et al. The methane cycle in ferruginous Lake Matano. *Geobiology* **2011**, *9*, 61–78. [\[CrossRef\]](#) [\[PubMed\]](#)
10. Posth, N.R.; Huelin, S.; Konhäuser, K.O.; Kappler, A. Size, density and composition of cell-mineral aggregates formed during anoxygenic phototrophic Fe(II) oxidation: Impact on modern and ancient environments. *Geochim. Cosmochim. Acta* **2010**, *74*, 3476–3493. [\[CrossRef\]](#)
11. Crowe, S.A.; Jones, C.A.; Katsev, S.; Magen, C.; O'Neill, A.H.; Sturm, A.; Canfield, D.E.; Haffner, G.D.; Mucci, A.; Sundby, B.; et al. Photoferrotrophs thrive in an Archean Ocean analogue. *Proc. Natl. Acad. Sci. USA* **2008**, *105*, 15938–15943. [\[CrossRef\]](#) [\[PubMed\]](#)
12. Walter, X.A.; Picazo, A.; Miracle, M.R.; Vicente, E.; Camacho, A.; Aragno, M.; Zopfi, J. Phototrophic Fe(II)-oxidation in the chemocline of a ferruginous meromictic lake. *Front. Microbiol.* **2014**, *5*, 713. [\[CrossRef\]](#)
13. Camacho, A.; Walter, X.A.; Picazo, A.; Zopfi, J. Photoferrotrophy: Remains of an ancient photosynthesis in modern environments. *Front. Microbiol.* **2017**, *8*, 323. [\[CrossRef\]](#) [\[PubMed\]](#)
14. Deshaies, M. Metamorphosis of Mining Landscapes in the Lower Lusatian Lignite Basin (Germany): New uses and new image of a mining region. *Calh. la Redh. Archit. Urbaine Paysagère* **2020**, *7*, 1–24. [\[CrossRef\]](#)

15. Geller, W.; Klapper, H.; Schultze, M. Natural and Anthropogenic Sulfuric Acidification of Lakes. In *Acidic Mining Lakes: Acid Mine Drainage, Limnology and Reclamation*; Geller, W., Klapper, H., Salomons, W., Eds.; Springer Berlin Heidelberg: Berlin, Heidelberg, 1998; pp. 3–14. ISBN 978-3-642-71954-7.
16. Johnson, D.B.; Kanao, T.; Hedrich, S. Redox Transformations of Iron at Extremely Low pH: Fundamental and Applied Aspects. *Front. Microbiol.* **2012**, *3*, 1–13. [[CrossRef](#)] [[PubMed](#)]
17. Nixdorf, B.; Krumbek, H.; Jander, J.; Beulker, C. Comparison of bacterial and phytoplankton productivity in extremely acidic mining lakes and eutrophic hard water lakes. *Acta Oecologica* **2003**, *24*, S281–S288. [[CrossRef](#)]
18. Saeed, H.; Hartland, A.; Lehto, N.J.; Baalousha, M.; Sikder, M.; Sandwell, D.; Mucalo, M.; Hamilton, D.P. Regulation of phosphorus bioavailability by iron nanoparticles in a monomictic lake. *Sci. Rep.* **2018**, *8*, 1–14. [[CrossRef](#)] [[PubMed](#)]
19. Lu, S.; Chourey, K.; Reiche, M.; Nietzsche, S.; Shah, M.B.; Neu, T.R.; Hettich, R.L.; Küsel, K. Insights into the structure and metabolic function of microbes that shape pelagic iron-rich aggregates (“Iron snow”). *Appl. Environ. Microbiol.* **2013**, *79*, 4272–4281. [[CrossRef](#)]
20. Mori, J.F.; Lu, S.; Händel, M.; Totsche, K.U.; Neu, T.R.; Iancu, V.V.; Tarcea, N.; Popp, J.; Küsel, K. Schwertmannite formation at cell junctions by a new filament-forming Fe(II)-oxidizing isolate affiliated with the novel genus *Acidithrix*. *Microbiology* **2016**, *162*, 62–71. [[CrossRef](#)]
21. Mori, J.F.; Ueberschaar, N.; Lu, S.; Cooper, R.E.; Pohnert, G.; Küsel, K. Sticking together: Inter-species aggregation of bacteria isolated from iron snow is controlled by chemical signaling. *ISME J.* **2017**, *11*, 1075–1086. [[CrossRef](#)]
22. Johnson, D.B.; Hallberg, K.B.; Hedrich, S. Uncovering a Microbial Enigma: Isolation and Characterization of the Streamer-Generating, Iron-Oxidizing, Acidophilic Bacterium “*Ferrofum mixofaciens*”. *Appl. Environ. Microbiol.* **2014**, *80*, 672–680. [[CrossRef](#)] [[PubMed](#)]
23. Ullrich, S.R.; Poehlein, A.; Tischler, J.S.; González, C.; Ossandon, E.J.; Daniel, R.; Holmes, D.S.; Schlömann, M.; Mühling, M. Genome analysis of the biotechnologically relevant acidophilic iron oxidizing strain JA12 indicates phylogenetic and metabolic diversity within the novel genus “*Ferrofum*”. *PLoS ONE* **2016**, *11*, e0146832. [[CrossRef](#)] [[PubMed](#)]
24. Tamura, H.; Goto, K. Spectrophotometric determination of iron(II) with 1,10-phenanthroline in the presence of large amounts of iron(III). *Talanta* **1974**, *21*, 314–318. [[CrossRef](#)]
25. Tabatabai, M.A. A Rapid Method for Determination of Sulfate in Water Samples. *Environ. Lett.* **1974**, *7*, 237–243. [[CrossRef](#)]
26. Klindworth, A.; Pruesse, E.; Schweer, T.; Peplies, J.; Quast, C.; Horn, M.; Glöckner, F.O. Evaluation of general 16S ribosomal RNA gene PCR primers for classical and next-generation sequencing-based diversity studies. *Nucleic Acids Res.* **2013**, *41*, 1–11. [[CrossRef](#)]
27. Bolyen, E.; Rideout, J.R.; Dillon, M.R.; Bokulich, N.A.; Abnet, C.C.; Al-Ghalith, G.A.; Alexander, H.; Alm, E.J.; Arumugam, M.; Asnicar, E.; et al. Reproducible, interactive, scalable and extensible microbiome data science using QIIME 2. *Nat. Biotechnol.* **2019**, *37*, 852–857. [[CrossRef](#)]
28. Saeidipour, B.; Bakhshi, S. Cutadapt Removes Adapter Sequences from High-throughput sequencing reads. *Adv. Environ. Biol.* **2013**, *7*, 2803–2809.
29. Rognes, T.; Flouri, T.; Nichols, B.; Quince, C.; Mahé, F. VSEARCH: A versatile open source tool for metagenomics. *PeerJ* **2016**, *2016*, 1–22. [[CrossRef](#)] [[PubMed](#)]
30. Amir, A.; McDonald, D.; Navas-Molina, J.A.; Kopylova, E.; Morton, J.T.; Zech Xu, Z.; Kightley, E.P.; Thompson, L.R.; Hyde, E.R.; Gonzalez, A.; et al. Deblur Rapidly Resolves Single-Nucleotide Community Sequence Patterns. *mSystems* **2017**, *2*, 1–7. [[CrossRef](#)] [[PubMed](#)]
31. Quast, C.; Pruesse, E.; Yilmaz, P.; Gerken, J.; Schweer, T.; Yarza, P.; Peplies, J.; Glöckner, F.O. The SILVA ribosomal RNA gene database project: Improved data processing and web-based tools. *Nucleic Acids Res.* **2012**, *41*, D590–D596. [[CrossRef](#)]
32. Pedregosa, F.; Varoquaux, G.; Gramfort, A.; Michel, V.; Thirion, B.; Grisel, O.; Blondel, M.; Prettenhofer, P.; Weiss, R.; Dubourg, V.; et al. Scikit-learn: Machine Learning in Python Fabian. *J. Mach. Learn. Res.* **2011**, *12*, 2825–2830.
33. McMurdie, P.J.; Holmes, S. Phyloseq: An R Package for Reproducible Interactive Analysis and Graphics of Microbiome Census Data. *PLoS ONE* **2013**, *8*, e61217. [[CrossRef](#)]
34. Zhang, J.; Kobert, K.; Flouri, T.; Stamatakis, A. PEAR: A fast and accurate Illumina Paired-End reAd mergeR. *Bioinformatics* **2014**, *30*, 614–620. [[CrossRef](#)]
35. Kopylova, E.; Noé, L.; Touzet, H. SortMeRNA: Fast and accurate filtering of ribosomal RNAs in metatranscriptomic data. *Bioinformatics* **2012**, *28*, 3211–3217. [[CrossRef](#)]
36. Argasinska, J.; Quinones-Olvera, N.; Nawrocki, E.P.; Finn, R.D.; Bateman, A.; Eddy, S.R.; Petrov, A.I.; Kalvari, I.; Rivas, E. Rfam 13.0: Shifting to a genome-centric resource for non-coding RNA families. *Nucleic Acids Res.* **2017**, *46*, D335–D342. [[CrossRef](#)]
37. Pruitt, K.D.; Tatusova, T.; Maglott, D.R. NCBI reference sequences (RefSeq): A curated non-redundant sequence database of genomes, transcripts and proteins. *Nucleic Acids Res.* **2007**, *35*, D61–D65. [[CrossRef](#)] [[PubMed](#)]
38. Camacho, C.; Coulouris, G.; Avagyan, V.; Ma, N.; Papadopoulos, J.; Bealer, K.; Madden, T.L. BLAST+: Architecture and applications. *BMC Bioinform.* **2009**, *10*, 1–9. [[CrossRef](#)] [[PubMed](#)]
39. Huson, D.H.; Beier, S.; Flade, I.; Górnska, A.; El-Hadidi, M.; Mitra, S.; Ruscheweyh, H.-J.; Tappu, R. MEGAN Community Edition—Interactive Exploration and Analysis of Large-Scale Microbiome Sequencing Data. *PLoS Comput. Biol.* **2016**, *12*, e1004957. [[CrossRef](#)] [[PubMed](#)]

40. Buchfink, B.; Xie, C.; Huson, D.H. Fast and sensitive protein alignment using DIAMOND. *Nat. Methods* **2015**, *12*, 59–60. [CrossRef] [PubMed]
41. Poux, S.; Arighi, C.N.; Magrane, M.; Bateman, A.; Wei, C.H.; Lu, Z.; Boutet, E.; Bye-A-Jee, H.; Famiglietti, M.L.; Roechert, B.; et al. On expert curation and scalability: UniProtKB/Swiss-Prot as a case study. *Bioinformatics* **2017**, *33*, 3454–3460. [CrossRef]
42. Kanehisa, M.; Sato, Y.; Morishima, K. BlastKOALA and GhostKOALA: KEGG tools for functional characterization of genome and metagenome sequences. *J. Mol. Biol.* **2016**, *428*, 726–731. [CrossRef]
43. Eren, A.M.; Esen, Ö.C.; Sogin, M.L.; Quince, C.; Delmont, T.O.; Morrison, H.G.; Vineis, J.H. Anvi'o: An advanced analysis and visualization platform for 'omics data. *PeerJ* **2015**, *3*, e1319. [CrossRef]
44. Hyatt, D.; Chen, G.L.; LoCascio, P.F.; Land, M.L.; Larimer, F.W.; Hauser, L.J. Prodigal: Prokaryotic gene recognition and translation initiation site identification. *BMC Bioinformatics* **2010**, *11*. [CrossRef] [PubMed]
45. Altschul, S.F.; Gish, W.; Miller, W.; Myers, E.W.; Lipman, D.J. Basic local alignment search tool. *J. Mol. Biol.* **1990**, *215*, 403–410. [CrossRef]
46. Eddy, S.R. Accelerated profile HMM searches. *PLoS Comput. Biol.* **2011**, *7*, e1002195. [CrossRef] [PubMed]
47. Aramaki, T.; Blanc-Mathieu, R.; Endo, H.; Ohkubo, K.; Kanehisa, M.; Goto, S.; Ogata, H. KofamKOALA: KEGG Ortholog assignment based on profile HMM and adaptive score threshold. *Bioinformatics* **2020**, *36*, 2251–2252. [CrossRef] [PubMed]
48. Tatusov, R.L. The COG database: New developments in phylogenetic classification of proteins from complete genomes. *Nucleic Acids Res.* **2002**, *29*, 22–28. [CrossRef] [PubMed]
49. El-Gebali, S.; Mistry, J.; Bateman, A.; Eddy, S.R.; Luciani, A.; Potter, S.C.; Qureshi, M.; Richardson, L.J.; Salazar, G.A.; Smart, A.; et al. The Pfam protein families database in 2019. *Nucleic Acids Res.* **2019**, *47*, D427–D432. [CrossRef]
50. Kanehisa, M.; Sato, Y.; Kawashima, M.; Furumichi, M.; Tanabe, M. KEGG as a reference resource for gene and protein annotation. *Nucleic Acids Res.* **2016**, *44*, D457–D462. [CrossRef]
51. Langmead, B.; Salzberg, S.L. Fast gapped-read alignment with Bowtie 2. *Nat. Methods* **2012**, *9*, 357–359. [CrossRef]
52. Li, H.; Handsaker, B.; Wysoker, A.; Fennell, T.; Ruan, J.; Homer, N.; Marth, G.; Abecasis, G.; Durbin, R. The sequence alignment/map format and SAMtools. *Bioinformatics* **2009**, *25*, 2078–2079. [CrossRef]
53. Liao, Y.; Smyth, G.K.; Shi, W. FeatureCounts: An efficient general purpose program for assigning sequence reads to genomic features. *Bioinformatics* **2014**, *30*, 923–930. [CrossRef]
54. Robinson, M.D.; McCarthy, D.J.; Smyth, G.K. edgeR: A Bioconductor package for differential expression analysis of digital gene expression data. *Bioinformatics* **2009**, *26*, 139–140. [CrossRef]
55. Taubert, M.; Stöckel, S.; Geesink, P.; Gimus, S.; Jehmlich, N.; von Bergen, M.; Rösch, P.; Popp, J.; Küsel, K. Tracking active groundwater microbes with D₂O labelling to understand their ecosystem function. *Environ. Microbiol.* **2018**, *20*, 369–384. [CrossRef]
56. Bateman, A. UniProt: A worldwide hub of protein knowledge. *Nucleic Acids Res.* **2019**, *47*, D506–D515. [CrossRef]
57. Taubert, M.; Vogt, C.; Wubet, T.; Kleinstaub, S.; Tarkka, M.T.; Harms, H.; Buscot, F.; Richnow, H.H.; Von Bergen, M.; Seifert, J. Protein-SIP enables time-resolved analysis of the carbon flux in a sulfate-reducing, benzene-degrading microbial consortium. *ISME J.* **2012**, *6*, 2291–2301. [CrossRef]
58. Taubert, M.; Baumann, S.; Von Bergen, M.; Seifert, J. Exploring the limits of robust detection of incorporation of ¹³C by mass spectrometry in protein-based stable isotope probing (protein-SIP). *Anal. Bioanal. Chem.* **2011**, *401*, 1975–1982. [CrossRef]
59. Conway, J.R.; Lex, A.; Gehlenborg, N. UpSetR: An R package for the visualization of intersecting sets and their properties. *Bioinformatics* **2017**, *33*, 2938–2940. [CrossRef] [PubMed]
60. Shimada, K.; Itoh, S.; Iwaki, M.; Nagashima, K.V.P.; Matsuura, K.; Kobayashi, M.; Wakao, N. Reaction Center Complex Based on Zn-Bacteriochlorophyll from *Acidiphilium Rubrum*. In *Photosynthesis: Mechanisms and Effects*; Springer: Dordrecht, The Netherlands, 1998; pp. 909–912.
61. Tomi, T.; Shibata, Y.; Ikeda, Y.; Taniguchi, S.; Haik, C.; Mataga, N.; Shimada, K.; Itoh, S. Energy and electron transfer in the photosynthetic reaction center complex of *Acidiphilium rubrum* containing Zn-bacteriochlorophyll a studied by femtosecond up-conversion spectroscopy. *Biochim. Biophys. Acta Bioenerg.* **2007**, *1767*, 22–30. [CrossRef] [PubMed]
62. Hess, S.; Suthaus, A.; Melkonian, M. "Candidatus Finniella" (*Rickettsiales, Alphaproteobacteria*), novel endosymbionts of viridiraptorid amoebiflagellates (*Cercozoa, Rhizaria*). *Appl. Environ. Microbiol.* **2016**, *82*, 659–670. [CrossRef] [PubMed]
63. Leschine, S.; Paster, B.J.; Canale-Parola, E. Free-Living Saccharolytic Spirochetes: The Genus *Spirochaeta*. In *The Prokaryotes: Volume 7: Proteobacteria: Delta, Epsilon Subclass*; Dworkin, M., Falkow, S., Rosenberg, E., Schleifer, K.-H., Stackebrandt, E., Eds.; Springer: New York, New York, NY, 2006; pp. 195–210. ISBN 978-0-387-30747-3.
64. Bomberg, M.; Mäkinen, J.; Salo, M.; Kinnunen, P. High Diversity in Iron Cycling Microbial Communities in Acidic, Iron-Rich Water of the Pyhäsalmi Mine, Finland. *Geofluids* **2019**, *2019*, 7401304. [CrossRef]
65. Santofimia, E.; González-Toril, E.; López-Pamo, E.; Gomariz, M.; Amils, R.; Aguilera, Á. Microbial Diversity and Its Relationship to Physicochemical Characteristics of the Water in Two Extreme Acidic Pit Lakes from the Iberian Pyrite Belt (SW Spain). *PLoS ONE* **2013**, *8*, e66746. [CrossRef]
66. Kaltenbock, E.; Herndl, G.J. Ecology of amorphous aggregations (marine snow) in the northern Adriatic Sea. IV. Dissolved nutrients and the autotrophic community associated with marine snow. *Mar. Ecol. Prog. Ser.* **1992**, *87*, 147–159. [CrossRef]
67. Simon, M.; Alldredge, A.; Azam, F. Bacterial carbon dynamics on marine snow. *Mar. Ecol. Prog. Ser.* **1990**, *65*, 205–211. [CrossRef]

68. Grossart, H.-P.; Simon, M.; Logan, B.E. Formation of macroscopic organic aggregates (lake snow) in a large lake: The significance of transparent exopolymer particles, phytoplankton, and Zooplankton. *Limnol. Oceanogr.* **1997**, *42*, 1651–1659. [CrossRef]
69. Imhoff, J.F.; Rahn, T.; Künzel, S.; Neulinger, S.C. New insights into the metabolic potential of the phototrophic purple bacterium *Rhodospira globiformis* DSM 161T from its draft genome sequence and evidence for a vanadium-dependent nitrogenase. *Arch. Microbiol.* **2018**, *200*, 847–857. [CrossRef] [PubMed]
70. Grossart, H.-P.; Berman, T.; Simon, M.; Pohlmann, K. Occurrence and microbial dynamics of macroscopic organic aggregates (lake snow) in Lake Kinneret, Israel, in fall. *Aquat. Microb. Ecol.* **1998**, *14*, 59–67. [CrossRef]
71. Schweitzer, B.; Huber, I.; Amann, R.; Ludwig, W.; Simon, M. α - and β -Proteobacteria Control the Consumption and Release of Amino Acids on Lake Snow Aggregates. *Appl. Environ. Microbiol.* **2001**, *67*, 632–645. [CrossRef]
72. Reichenbach, H. The Order Cytophagales. In *The Prokaryotes*; Springer New York: New York, NY, 2006; pp. 549–590.
73. Grossart, H.-P.; Ploug, H. Microbial degradation of organic carbon and nitrogen on diatom aggregates. *Limnol. Oceanogr.* **2001**, *46*, 267–277. [CrossRef]
74. Eigemann, F.; Vogts, A.; Voss, M.; Zoccarato, L.; Schulz-Vogt, H. Distinctive tasks of different cyanobacteria and associated bacteria in carbon as well as nitrogen fixation and cycling in a late stage Baltic Sea bloom. *PLoS ONE* **2019**, *14*, e0223294. [CrossRef]
75. Shanks, A.L.; Reeder, M.L. Reducing microzones and sulfide production in marine snow. *Mar. Ecol. Prog. Ser.* **1993**, *96*, 43–47. [CrossRef]
76. Dash, P.; Kashyap, D.; Mandal, S.C. Marine snow: Its formation and significance in fisheries and aquaculture. *World Aquac.* **2012**, *6*, 59–61.
77. Kierboe, T.; Hansen, J.L.S. Phytoplankton aggregate formation: Observations of patterns and mechanisms of cell sticking and the significance of exopolymeric material. *J. Plankton Res.* **1993**, *15*, 993–1018. [CrossRef]
78. Stoderegger, K.E.; Herndl, G.J. Production and release of bacterial capsular material and its subsequent utilization by marine bacterioplankton. *Limnol. Oceanogr.* **1998**, *43*, 877–884. [CrossRef]
79. Stoderegger, K.E.; Herndl, G.J. Production of exopolymer particles by marine bacterioplankton under contrasting turbulence conditions. *Mar. Ecol. Prog. Ser.* **1999**, *189*, 9–16. [CrossRef]
80. Olson, J.B.; Steppe, T.F.; Litaker, R.W.; Paer, H.W. N₂-Fixing Microbial Consortia Associated with the Ice Cover of Lake Bonney, Antarctica. *Microb. Ecol.* **1998**, *36*, 231–238. [CrossRef] [PubMed]
81. Klawonn, I.; Bonaglia, S.; Brüchert, V.; Ploug, H. Aerobic and anaerobic nitrogen transformation processes in N₂-fixing cyanobacterial aggregates. *ISME J.* **2015**, *9*, 1456–1466. [CrossRef] [PubMed]
82. Farnelid, H.; Turk-Kubo, K.; Ploug, H.; Ossolinski, J.E.; Collins, J.R.; Van Mooy, B.A.S.; Zehr, J.P. Diverse diazotrophs are present on sinking particles in the North Pacific Subtropical Gyre. *ISME J.* **2019**, *13*, 170–182. [CrossRef]
83. Tonolla, M.; Demarta, A.; Peduzzi, R. The chemistry of Lake Cadagno. *Doc. Ist. Ital. Idrobiol.* **1998**, *63*, 11–17.
84. Peduzzi, S.; Tonolla, M.; Hahn, D. Isolation and characterization of aggregate-forming sulfate-reducing and purple sulfur bacteria from the chemocline of meromictic Lake Cadagno, Switzerland. *FEMS Microbiol. Ecol.* **2003**, *45*, 29–37. [CrossRef]
85. Tonolla, M.; Peduzzi, S.; Demarta, A.; Peduzzi, R.; Hahn, D. Phototrophic sulfur and sulfate-reducing bacteria in the chemocline of meromictic Lake Cadagno, Switzerland. *J. Limnol.* **2004**, *63*, 161–170. [CrossRef]
86. Küsel, K. Microbial cycling of iron and sulfur in acidic coal mining lake sediments. *Water Air Soil Pollut. Focus* **2003**, *3*, 67–90. [CrossRef]
87. Meier, J.; Baberzien, H.-D.; Wendt-Potthoff, K. Microbial cycling of iron and sulfur in sediments of acidic and pH-neutral mining lakes in Lusatia (Brandenburg, Germany). *Biogeochemistry* **2004**, *67*, 135–156. [CrossRef]
88. Church, C.D.; Wilkin, R.T.; Alpers, C.N.; Rye, R.O.; Blaine, R.B. Microbial sulfate reduction and metal attenuation in pH 4 acid mine water. *Geochim. Trans.* **2007**, *8*, 1–14. [CrossRef] [PubMed]
89. Koschorneck, M. Microbial sulphate reduction at a low pH. *FEMS Microbiol. Ecol.* **2008**, *64*, 329–342. [CrossRef] [PubMed]
90. Li, Q.; Cooper, R.E.; Wegner, C.-E.; Küsel, K. Molecular Mechanisms Underpinning Aggregation in *Acidiphilium* sp. C61 Isolated from Iron-Rich Pelagic Aggregates. *Microorganisms* **2020**, *8*, 314. [CrossRef] [PubMed]
91. Gram, L.; Grossart, H.-P.; Schlingloff, A.; Kierboe, T. Possible quorum sensing in marine snow bacteria: Production of acylated homoserine lactones by *Roseobacter* strains isolated from marine snow. *Appl. Environ. Microbiol.* **2002**, *68*, 4111–4116. [CrossRef]
92. Dang, H.; Lovell, C. Microbial surface colonization and biofilm development in marine environments. *Microbiol. Mol. Biol. Rev.* **2016**, *80*, 91–138. [CrossRef] [PubMed]
93. Styp Von Rekowski, K.; Hempel, M.; Philipp, B. Quorum sensing by N-acylhomoserine lactones is not required for *Aeromonas hydrophila* during growth with organic particles in lake water microcosms. *Arch. Microbiol.* **2008**, *189*, 475–482. [CrossRef]
94. Méndez-García, C.; Peláez, A.I.; Mesa, V.; Sánchez, J.; Golyshina, O.V.; Ferrer, M. Microbial diversity and metabolic networks in acid mine drainage habitats. *Front. Microbiol.* **2015**, *6*, 475. [CrossRef]
95. Baker, B.J.; Banfield, J.F. Microbial communities in acid mine drainage. *FEMS Microbiol. Ecol.* **2003**, *44*, 139–152. [CrossRef]
96. Ullrich, S.R.; Poehlein, A.; Voget, S.; Hoppert, M.; Daniel, R.; Leimbach, A.; Tischler, J.S.; Schlömann, M.; Mühling, M. Permanent draft genome sequence of *Acidiphilium* sp. JA12-A1. *Stand. Genomic Sci.* **2015**, *10*, 1–10. [CrossRef]
97. Küsel, K.; Dorsch, T.; Acker, G.; Stackebrandt, E. Microbial reduction of Fe(III) in acidic sediments: Isolation of *Acidiphilium cryptum* JF-5 capable of coupling the reduction of Fe(III) to the oxidation of glucose. *Appl. Environ. Microbiol.* **1999**, *65*, 3633–3640. [CrossRef] [PubMed]

3. Insights into autotrophic activities and carbon flow in iron-rich pelagic aggregates

98. Küsel, K.; Roth, U.; Drake, H.L. Microbial reduction of Fe(III) in the presence of oxygen under low pH conditions. *Environ. Microbiol.* **2002**, *4*, 414–421. [[CrossRef](#)]
99. Mühling, M.; Poehlein, A.; Stuhr, A.; Voitel, M.; Daniel, R.; Schlömann, M. Reconstruction of the metabolic potential of acidophilic *Sideroxydans* strains from the metagenome of an microaerophilic enrichment culture of acidophilic iron-oxidizing bacteria from a pilot plant for the treatment of acid mine drainage reveals met. *Front. Microbiol.* **2016**, *7*, 2082. [[CrossRef](#)]
100. Winstanley, C.; Morgan, J.A.W. The bacterial flagellin gene as a biomarker for detection, population genetics and epidemiological analysis. *Microbiology* **1997**, *143*, 3071–3084. [[CrossRef](#)] [[PubMed](#)]
101. Mitchell, J.G.; Pearson, L.; Dillon, S.; Kantalis, K. Natural assemblages of marine bacteria exhibiting high-speed motility and large accelerations. *Appl. Environ. Microbiol.* **1995**, *61*, 4436–4440. [[CrossRef](#)]
102. Lambrecht, N.; Wittkop, C.; Katssev, S.; Fakhraee, M.; Swanner, E.D. Geochemical Characterization of Two Ferruginous Meromictic Lakes in the Upper Midwest, USA. *J. Geophys. Res. Biogeosci.* **2018**, *123*, 3403–3422. [[CrossRef](#)]
103. Crowe, S.A.; O'Neill, A.H.; Katssev, S.; Hehanussa, P.; Haffner, G.D.; Sundby, B.; Mucci, A.; Fowle, D.A. The biogeochemistry of tropical lakes: A case study from Lake Matano, Indonesia. *Limnol. Oceanogr.* **2008**, *53*, 319–331. [[CrossRef](#)]
104. Oswald, K.; Jegge, C.; Tischer, J.; Berg, J.; Brand, A.; Miracle, M.R.; Soria, X.; Vicente, E.; Lehmann, M.F.; Zopfi, J.; et al. Methanotrophy under versatile conditions in the water column of the ferruginous meromictic Lake La Cruz (Spain). *Front. Microbiol.* **2016**, *7*, 1762. [[CrossRef](#)]
105. Lu, S. Microbial Iron Cycling in Pelagic Aggregates (iron Snow) and Sediments of an Acidic Mine Lake. PhD's Thesis, Friedrich-Schiller-Universität Jena, Germany, 2012.
106. Reinthaler, T.; van Aken, H.M.; Herndl, G.J. Major contribution of autotrophy to microbial carbon cycling in the deep North Atlantic's interior. *Deep. Res. Part II Top. Stud. Oceanogr.* **2010**, *57*, 1572–1580. [[CrossRef](#)]
107. Grossart, H.-P.; Simon, M. Significance of limnetic organic aggregates (lake snow) for the sinking flux of particulate organic matter in a large lake. *Aquat. Microb. Ecol.* **1998**, *15*, 115–125. [[CrossRef](#)]

4. Molecular mechanisms underpinning aggregation in *Acidiphilium* sp. C61 isolated from iron-rich pelagic aggregates

Published in *Microorganisms*. doi: 10.3390/microorganisms8030314

Qianqian Li, Rebecca E. Cooper, Carl-Eric Wegner, and Kirsten Küsel

Abstract

Iron-rich pelagic aggregates (iron snow) are hot spots for microbial interactions. Using iron snow isolates, we previously demonstrated that the iron-oxidizer *Acidithrix* sp. C25 triggers *Acidiphilium* sp. C61 aggregation by producing the infochemical 2-phenethylamine (PEA). Here, we showed slightly enhanced aggregate formation in the presence of PEA on different *Acidiphilium* spp. but not other iron-snow microorganisms, including *Acidocella* sp. C78 and *Ferrovum* sp. PN-J47. Next, we sequenced the *Acidiphilium* sp. C61 genome to reconstruct its metabolic potential. Pangenome analyses of *Acidiphilium* spp. genomes revealed the core genome contained 65 gene clusters associated with aggregation, including autoaggregation, motility, and biofilm formation. Screening the *Acidiphilium* sp. C61 genome revealed the presence of autotransporter, flagellar, and extracellular polymeric substances (EPS) production genes. RNA-seq analyses of *Acidiphilium* sp. C61 incubations (+/- 10 μ M PEA) indicated genes involved in energy production, respiration, and genetic processing were the most upregulated differentially expressed genes in the presence of PEA. Additionally, genes involved in flagellar basal body synthesis were highly upregulated, whereas the expression pattern of biofilm formation-related genes was inconclusive. Our data shows aggregation is a common trait among *Acidiphilium* spp. and PEA stimulates the central cellular metabolism, potentially advantageous in aggregates rapidly falling through the water column.

Supplementary data to this article can be found online at <https://www.mdpi.com/2076-2607/8/3/314#supplementary-material>



Article

Molecular Mechanisms Underpinning Aggregation in *Acidiphilium* sp. C61 Isolated from Iron-Rich Pelagic Aggregates

Qianqian Li ¹ , Rebecca E. Cooper ¹, Carl-Eric Wegner ¹ and Kirsten Küsel ^{1,2,*}

¹ Institute of Biodiversity, Friedrich Schiller University Jena, 07743 Jena, Germany;

qianqian.li@uni-jena.de (Q.L.); rebecca.cooper@uni-jena.de (R.E.C.); carl-eric.wegner@uni-jena.de (C.-E.W.)

² The German Centre for Integrative Biodiversity Research (iDiv) Halle-Jena-Leipzig, 04103 Leipzig, Germany

* Correspondence: kirsten.kuesel@uni-jena.de; Tel.: +49-3641-949461

Received: 17 December 2019; Accepted: 23 February 2020; Published: 25 February 2020



Abstract: Iron-rich pelagic aggregates (iron snow) are hot spots for microbial interactions. Using iron snow isolates, we previously demonstrated that the iron-oxidizer *Acidithrix* sp. C25 triggers *Acidiphilium* sp. C61 aggregation by producing the infochemical 2-phenethylamine (PEA). Here, we showed slightly enhanced aggregate formation in the presence of PEA on different *Acidiphilium* spp. but not other iron-snow microorganisms, including *Acidocella* sp. C78 and *Ferroplasma* sp. PN-J47. Next, we sequenced the *Acidiphilium* sp. C61 genome to reconstruct its metabolic potential. Pangenome analyses of *Acidiphilium* spp. genomes revealed the core genome contained 65 gene clusters associated with aggregation, including autoaggregation, motility, and biofilm formation. Screening the *Acidiphilium* sp. C61 genome revealed the presence of autotransporter, flagellar, and extracellular polymeric substances (EPS) production genes. RNA-seq analyses of *Acidiphilium* sp. C61 incubations (+/− 10 μM PEA) indicated genes involved in energy production, respiration, and genetic processing were the most upregulated differentially expressed genes in the presence of PEA. Additionally, genes involved in flagellar basal body synthesis were highly upregulated, whereas the expression pattern of biofilm formation-related genes was inconclusive. Our data shows aggregation is a common trait among *Acidiphilium* spp. and PEA stimulates the central cellular metabolism, potentially advantageous in aggregates rapidly falling through the water column.

Keywords: 2-phenethylamine (PEA); microbial aggregation; iron snow; genomics; pangenomics; RNA-seq

1. Introduction

Pelagic aggregates, composed of microorganisms, phytoplankton, feces, detritus, and biominerals, are local hotspots for microbial interaction in nearly all aquatic habitats [1–3]. These snow-like aggregates are stabilized by a matrix of extracellular polymeric substances (EPS) and vary in size, ranging from micrometers to centimeters, depending on their residence time in the water column and the trophic state of the ecosystem [1,4,5]. Microbial colonization and coordinated group behavior within these pelagic aggregates are likely regulated by chemical signaling, including quorum sensing signaling molecules [6,7]; however, most chemical mediators involved in interspecies interaction are still unknown.

Iron-rich pelagic aggregates (iron snow), analogous to the more organic-rich marine or freshwater aggregates, are characterized by lower chemical and microbial complexity [5]. Iron snow forms at the redoxcline of stratified iron-rich lakes, where the oxygen-rich epilimnion water meets ferrous iron (Fe²⁺) of the anoxic hypolimnion [5]. Many of these lakes are acidic due to the inflow of protons in

addition to Fe^{2+} and sulfate (SO_4^{2-}) from mine tailings [8,9]. Under acidic conditions, Fe^{2+} is oxidized by microorganisms to ferric iron (Fe^{3+}), from which goethite and schwertmannite form via hydrolysis of Fe^{3+} cations [10,11]. In lignite mine lakes, these biominerals form the main inorganic component of pelagic aggregates [12,13]. These aggregates are stabilized by the adsorption of other metals, nutrients, and organic matter. Iron snow is an attractive habitat for heterotrophic microorganisms, especially those capable of using Fe^{3+} as an electron acceptor, such as *Acidiphilium* species [14]. Together, iron-oxidizing bacteria (FeOB) and iron-reducing bacteria (FeRB) can comprise up to 60% of the total microbial community found in iron snow aggregates [15]. To study the interactions between these iron-cycling bacteria, we isolated several key players from iron snow, including *Acidiphilium*, *Acidocella*, *Acidithrix*, and *Ferroplasma* species [13,16,17]. The iron-oxidizing isolate *Acidithrix* sp. C25 forms large cell-mineral aggregates in the late stationary phase [13]. When co-cultured with the iron-reducing isolate *Acidiphilium* sp. C61, motile cells of *Acidiphilium* also form cell aggregates with similar morphology to iron snow. Comparative metabolomics identified the aggregation-inducing signal, 2-phenethylamine (PEA), which also induced faster growth of *Acidiphilium* sp. C61 [17].

PEA is a small molecule that exhibits an array of seemingly unrelated functions, including roles as a neurotransmitter and in food processing [18]. PEA was found in the brains of humans and other mammals [19] and reportedly has stimulatory effects, resulting in the release of biogenic amines [20]. In high concentrations, PEA can act as an anti-microbial against *Escherichia coli* on beef meat [18]. Bacteria can produce PEA via decarboxylation of phenylalanine or as a by-product of the tyrosine decarboxylase reaction [21]. PEA is capable of inhibiting both swarming and the expression of the *flhDC* gene cluster, which encodes a flagellar regulon that regulates flagellar motility in *Proteus mirabilis* [22,23]. Swarmer cell differentiation is dependent on specific environmental conditions, including the presence of a solid surface, inhibition of flagellar rotation, and density-based cell–cell signaling by extracellular signals [24–26]. However, swarming is not known to exist in *Acidiphilium* spp. and this *flhDC* gene cluster is absent in all sequenced *Acidiphilium* spp. genomes [17]. Therefore, the molecular mechanisms underlying PEA-induced aggregate formation in *Acidiphilium* spp. remain unknown.

To broaden our understanding of chemical communication between iron-cycling bacteria shaping pelagic aggregates, we amended different *Acidiphilium* spp. and two other iron snow key players with PEA to see if this aggregation effect was isolate specific. We sequenced the genome of *Acidiphilium* sp. C61 to gain more insights into the metabolic pathways and potential behaviors (e.g., motility, chemotaxis) of this organism. Furthermore, we performed comparative transcriptomics of *Acidiphilium* sp. C61 amended with 10 μM PEA compared to cultures without PEA to elucidate the genetic mechanisms underlying aggregate formation.

2. Materials and Methods

2.1. Bacterial Strains, Growth Conditions, and Microscopic Characterization of Aggregate Formation in Acidophilic Bacteria

For incubation studies, three different Fe-reducing *Acidiphilium* spp. (*Acidiphilium* sp. C61, *Acidiphilium cryptum* JF-5, and *Acidiphilium* SJH) isolated from different environments were used. Briefly, *Acidiphilium* sp. C61 was isolated just below the redox cline in the water column of the central basin (pH 2.8–3.0) of lignite mine Lake 77 (Lusatian mining area in east-central Germany) [13,17], *A. cryptum* JF-5, isolated from Lake 77 sediments [14], and *Acidiphilium* SJH (strain kindly provided by Barrie Johnson, School of Natural Sciences, Bangor University) was originally isolated from an abandoned pyrite mine in North Wales [27]. In addition, we tested the FeRB *Acidocella* sp. C78, isolated from the Lake 77 water column [17], and the FeOB *Ferroplasma* sp. PN-J47 (strain kindly provided by Michael Schlömann, Technical University Bergakademie Freiberg) [28] to determine the effect of two different concentrations of 2-Phenethylamine (PEA) (Alfa Aesar, Kandel, Germany) (10 and 50 μM) on potential aggregate formation in monoculture incubations. Incubations were carried out using a defined medium, artificial pilot-plant water (APPW) medium (pH 2.5), and prepared as previously described (0.022 g L^{-1} K_2SO_4 , 3.24 g L^{-1} $\text{MgSO}_4 \cdot 7\text{H}_2\text{O}$, 0.515 g L^{-1} $\text{CaSO}_4 \cdot 2\text{H}_2\text{O}$, 0.058 g L^{-1} NaHCO_3 ,

0.010 g L⁻¹ NH₄Cl, 0.014 g L⁻¹ Al₂(SO₄)₃·18H₂O, 0.023 g L⁻¹ MnCl₂·4H₂O, 0.0004 g L⁻¹ ZnCl₂ [28] with the exception of added yeast extract (0.2 g L⁻¹) to ensure growth of *Acidiphilium* and *Acidocella* strains [14,17]. All incubations were grown aerobically at room temperature on a rotary shaker (100 rpm) for three days.

All incubations were prepared in triplicate and growth was monitored spectrophotometrically (OD_{600nm}) using a DR3900 spectrometer (Hach Lange, Düsseldorf, Germany) or indirectly using the 1,10-phenanthroline method [29] to monitor the oxidation of Fe²⁺ (*Ferroplasma* sp. PN-J47). *Acidiphilium* spp., *Acidocella* sp. C78, and *Ferroplasma* sp. PN-J47 were grown to exponential phase (OD_{600nm} = 0.03; A_{512nm} = 1.5) in the presence of 0, 10, or 50 µM PEA. Then, 10 µM SYTO 13 (Thermo Scientific, Schwerte, Germany) was used to stain nucleic acids of cells in all subsamples taken. Additionally, 8 µL of each cell culture was stained with SYTO 13 and placed on glass microscope slides. Aggregate formation was visually examined using an Axioplan fluorescence microscope (Zeiss, Oberkochen, Germany).

An additional 2 mM glucose was added to the above *Acidiphilium* sp. C61 culture supplemented with 0, 10, 50 µM PEA. Sterile pre-processed glass slides (Roth, Karlsruhe, Germany), which were immersed in H₂O₂: HNO₃ (1:1 v/v, Roth, Karlsruhe, Germany) overnight, were submerged in 50 mL conical tubes with 35 mL cultures. Glass slides were taken out and applied 50 µL SYTO 13 to stain nucleic acids of cells in the biofilm. Biofilm formation was visually examined using the above Axioplan fluorescence microscope.

2.2. Genomic DNA Extraction and Whole Genome Sequencing of *Acidiphilium* sp. C61

Acidiphilium sp. C61 genomic DNA was extracted using a phenol–chloroform based method from cultures grown to an OD_{600nm} of 0.060 in APPW+YE medium. Briefly, biomass was harvested by centrifugation at 12,000× g for 10 min at room temperature and subjected to bead beating (6.5 m s⁻¹ for 30 s with 0.6 g Zirconium/glass-Beadsbeads (ϕ = 1 mm, Carl Roth, Karlsruhe, Germany) in 750 µL sodium phosphate buffer (120 mM, pH 8.0) plus 250 µL TNS solution (500 mM Tris-HCl pH 8.0, 100 mM NaCl, 10% SDS w/v). Cell debris was separated by centrifugation. Nucleic acid extraction of the supernatant was performed in two sequential steps: first with phenol–chloroform–isoamyl alcohol (25:24:1 v/v/v, AppliChem, Darmstadt, Germany) and second with chloroform–isoamyl alcohol (24:1 v/v, AppliChem, Darmstadt, Germany). The aqueous phase was precipitated overnight at -20 °C with two volumes of polyethylene glycol 6000 (Carl Roth, Karlsruhe, Germany). Glycogen (20 mg mL⁻¹, Sigma-Aldrich, Darmstadt, Germany) was added to facilitate precipitation. DNA was collected by centrifugation (20,000× g at 4 °C for 90 min). The resulting pellets were washed with ice-cold ethanol (70% v/v), centrifuged, and resuspended in 50 µL elution buffer (Qiagen, Hilden, Germany). Genomic DNA was sent to RTL genomics (Lubbock, TX, USA) for library preparation and whole genome sequencing using PacBio[®] SMRTBell reagents (Pacific Biosciences, Menlo Park, CA, USA) and a PacBio RSII instrument.

2.3. Genome Assembly and Annotation

RTL genomics performed initial quality control and assembly of the *Acidiphilium* sp. C61 whole genome sequence. Raw data were subjected to quality control using FastQC (v. 0.11.7) (<http://www.bioinformatics.babraham.ac.uk/projects/fastqc/>) and assembled using HGAP3 (Hierarchical Genome Assembly Process 3) implemented in the SMRTLink software suite (v. 4.0) [30]. Basic genome characteristics were determined with QUAST (v. 4.0) [31]. Genome completeness and contamination level were estimated using the lineage-specific workflow of CheckM (v. 1.0.12) [32] with default settings, except for the “reduced_tree” parameter, which was applied to reduce the computational demand. The contamination percentage provided by CheckM represents the redundancy of single copy marker genes in this *Acidiphilium* sp. C61 genome sequence. The assembled genome was subsequently annotated using dfast (v. 1.1.0) [33] with default settings. This annotation was complemented by additional BlastKOALA searches [34] with default settings of encoded amino acid sequences against the KEGG GENES database. We collected amino acid sequences of known autotransporters and iron

reductases from the NCBI non-redundant protein database by text searches. These sequences were clustered based on a sequence identity of 90% using CD-HIT (v. 4.7) [35] and used as queries for diamond (v. 0.9.26.127) searches with default settings [36] against the genome of *Acidiphilium* sp. C61 to identify potential genes encoding known autotransporters and iron reductases.

2.4. Pangenomic Analysis

We collected six publically available genomes from the GenBank Assembly Database of related *Acidiphilium* spp., including *A. cryptum* JF-5 (GenBank assembly accession: GCA_000016725.1), *A. multivorum* AIU301 (GCA_000202835.1), *A. angustum* ATCC 35903 (GenBank assembly accession: GCA_000701585.1), *A. rubrum* ATCC 35905 (GCA_900156265.1), *Acidiphilium* sp. JA12-A1 (GCA_000724705.2), and *Acidiphilium* sp. PM (GCA_000219295.2). We performed a pangenomic analysis combining the six publically available *Acidiphilium* spp. genomes and our *Acidiphilium* sp. C61 isolate genome using anvi'o (v. 5.5), following a previously published workflow [37,38]. Briefly, the headers of the retrieved genome fasta files were simplified using the program "anvi-script-reformat-fasta". The "anvi-gen-contigs-database", which incorporates prodigal (v. 2.6.3) to identify open reading frames (ORFs), was used to profile *Acidiphilium* spp. genomes [39]. Genes were annotated with the program "anvi-run-ncbi-cogs" based on blastp (v. 2.5.0) [40], which searches against the December 2014 release of the Clusters of Orthologous Groups (COGs) database [41]. In this study, we define a pangenome as the whole gene set of all strains of *Acidiphilium* sp. We use the term "core genes" to describe all genes present in all *Acidiphilium* genomes and the term "accessory genes" when we discuss genes present in a single or multiple *Acidiphilium* genomes. The *Acidiphilium* pangenome was computed using the program "anvi-pan-genome" (settings: minbit: 0.5, mcl-inflation: 10), which relies on blastp for calculating amino acid sequence similarities across genomes, the minbit heuristic first implemented in ITEP [42] to identify and remove weak amino acid sequence matches, and the MCL algorithm [43] to identify clusters based on amino acid sequence similarity searches. The results were displayed using the program "anvi-display-pan" and analyzed using the interactive interface of anvi'o.

2.5. 16S rRNA Gene Phylogenetic Analysis

16S rRNA gene sequences from *Acidiphilium* sp. C61 (LN866588.1), *A. cryptum* JF-5 (Y18446.1), *A. multivorum* AIU301 (NR_074327.1), *A. SJH* (AY040740.1), *A. rubrum* (D30776.1), *A. angustum* (D30772.1), *Acidocella* sp. C78 (LN866590.1), *Acidocella aminolytica* (D30771.1), and *Acidocella facilis* (D30774.1), *Acidisphaera rubrifaciens* (NR_037119.1), *Acidicaldus organivorans* strain Y008 (NR_042752.1) from Acetobacteraceae, *Magnetospirillum gryphiswaldense* MSR-1 (NR_121771.1), *Magnetospirillum marisnigri* strain SP-1 (NR_149242.1), *Magnetospirillum magnetotacticum* strain DSM 3856 (NR_026381.1), *Magnetospirillum caucaseum* strain SO-1 (NR_149241.1) from Rhodospirillaceae, *Acidobacterium capsulatum* (D26171.1), *Acidobacterium ailaui* strain PMMR-2 (NR_153719.1) from Acidobacteriaceae were identified and obtained from the NCBI Genbank database. The 16S rRNA sequences were aligned using ClustalW [44] in mega (v. X) [45]. A phylogenetic tree was constructed using maximum likelihood to estimate the relatedness of the aforementioned species. The maximum likelihood tree was constructed using the following settings: bootstrapping (100 replicates), substitution type (nucleotide), model (Tamura-Nei), ML heuristics (nearest-neighbor-interchange), initial tree (NJ/BioNJ).

2.6. RNA Extraction

RNA was extracted from triplicate *Acidiphilium* sp. C61 cultures grown to exponential phase ($OD_{600nm} = 0.3$) in APPW+YE medium with 0 or 10 μ M PEA. Glucose (2 mM) was added to the medium to enhance growth. Biomass was harvested after 4 days and RNA was extracted using a modified version of the DNA extraction method described above. DNA was removed from 50 μ L total nucleic acid extracts through enzymatic digestion with 2.5 μ L ($2 \text{ U } \mu\text{L}^{-1}$) TURBO DNase (ThermoFisher Scientific, Waltham, MA, USA), 0.5 μ L ($20 \text{ U } \mu\text{L}^{-1}$) RNase inhibitor and 5 μ L 10X DNase buffer (ThermoFisher Scientific, Waltham, MA, USA) for 1 h at 37 °C. After digestion, successful DNA digestion was checked

by agarose gel electrophoresis. Total RNA was purified using the RNA Clean & Concentrator-5 kit (Zymo Research, Freiburg, Germany), according to the manufacturer's instructions. RNA purity was assessed by spectrophotometry, and RNA quantities were determined by fluorometry using Qubit RNA HS Assay (Life Technologies, Carlsbad, CA, USA) and a Qubit® 3.0 fluorometer (Life Technologies, Carlsbad, CA, USA). RNA integrity was additionally assessed by agarose gel electrophoresis.

2.7. RNA-seq Library Preparation and Sequencing

Total RNA was subjected to library preparation using the NEBNext Ultra II directional RNA library prep kit for Illumina (New England Biolabs, Beverly, MA, USA), according to the manufacturer's instructions. Size selection was used to select for fragments ranging between 150–200 bp in length. RNA libraries were quantified using a Qubit® 3.0 fluorometer as described above and their fragment size range was assessed by high-resolution, chip-based gel electrophoresis with a Bioanalyzer 2100 instrument (Agilent Technologies, Waldbronn, Germany) and the Agilent DNA7500 Kit (Agilent Technologies, Waldbronn, Germany). Libraries were pooled equimolarly and sequenced in paired-end (2 × 150 bp) mode on a HiSeq 2000 instrument (Illumina, Munich, Germany). Transcriptome sequencing (RNA-seq) was performed by Eurofins Genomics (Constance, Germany).

2.8. RNA-seq Data Pre-Processing

Demultiplexing of raw data was done with bclfastq (v. 2.19) (Illumina). The quality of raw, demultiplexed RNA-seq datasets was assessed using FastQC (v. 0.11.7) (<http://www.bioinformatics.babraham.ac.uk/projects/fastqc/>). Raw data (raw reads) was adapter trimmed using trimgalore (v. 0.4.3, cutoff: 20) (https://www.bioinformatics.babraham.ac.uk/projects/trim_galore/) and filtered using sickle (v. 1.33, quality threshold: 20) (<https://github.com/najoshi/sickle>). Ribosomal RNA-derived sequences, as well as non-coding RNA sequences, were filtered out with SortMeRNA (v. 2.1) [46] using pre-compiled databases of SILVA [47] and Rfam [48]. The remaining, mRNA-derived sequences were mapped onto the assembled and annotated genome of *Acidiphilium* sp. C61 using bbmap (v. 38.12, settings: slow, k = 11) [49]. The resulting bam files were sorted and indexed with SAMtools (v. 1.3.1) [50]. Read count tables were generated from sorted and indexed bam files using featureCounts (v. 1.6.0) [51].

2.9. Differential Gene Expression Analysis

Differential gene expression analysis was carried out in the R framework for statistical computing (v. 3.5.1) (R Core Development Team, 2018) [52], using the package edgeR (v. 3.20.9), including all dependencies [53]. The analysis started from merged read count data of the two tested experimental conditions (10 µM PEA vs. 0 µM PEA supplementation). Pseudocounts, generated by log₂-transforming counts+1 (where counts are equivalent to the raw counts per feature), were used for preliminary data exploration by generating M-A plots and multidimensional scaling. The biological coefficient of variation was calculated for each gene to assess biology-derived variation within replicate groups. Genes identified to be differentially expressed were false discovery rate (FDR) corrected and filtered with respect to log fold change, FDR-corrected *p*-value, and gene expression in counts per million (CPM).

2.10. Quantitative PCR

Total gene copy numbers of the *Acidiphilium* sp. C61 16S rRNA gene with and without PEA (0, 10, 50 µM; *n* = 3) were determined using quantitative PCR (qPCR), an Mx3000P instrument (Agilent Technologies, Waldbronn, Germany) and Maxima SYBR Green qPCR Mastermix (Agilent Technologies, Waldbronn, Germany). *Acidiphilium* sp. C61 16S rRNA gene copy numbers were determined using the primer set Bac8Fmod/Bac338Rabc [54,55] and previously published cycling conditions [56]. Genomic DNA was diluted to a range of 1–10 ng µL⁻¹ and 0.6 to 6 ng of DNA was used as template. Standard curves were made using serial dilutions of plasmid-based standards carrying the amplicon defined by the used primer pair. These curves were linear for primer sets from 5 × 10⁸ to 5 × 10¹ with R² values of

0.999–1.000, and the qPCR performed with efficiencies between 80% and 90%. Welch's *t*-test was used to compare treatments using the calculated quantification results and determine statistical significance ($p < 0.05$).

2.11. Quantification of eDNA Concentrations

eDNA concentrations were determined according to Tang et al. [57] in *Acidiphilium* sp. C61 incubations grown with increasing concentrations of PEA (0, 10, 50 μ M; $n = 3$). Bacterial cells were removed from samples (approximately 900 μ L) via centrifugation (4 min, 6800 \times *g*). The supernatant (700 μ L) was transferred to a sterile 1.5 mL Eppendorf tube and mixed with 50 μ L protein precipitation solution (ThermoFisher Scientific, Waltham, MA, USA) by inverting (10 times) and centrifuged again (10 min, 12,100 \times *g*). Then, 700 μ L of the supernatant was subsequently mixed with 70 μ L 2.5 M NaCl and 1400 μ L 96% ethanol prior to incubation at -20 $^{\circ}$ C for at least 24 h. DNA was precipitated by centrifugation (25 min, 4 $^{\circ}$ C, 18,300 \times *g*) and washed once in 70% (*v/v*) ice-cold EtOH. The pellet was air dried and resuspended in 50 μ L TE buffer (10 mM Tris, 1 mM EDTA, pH 7.5) by vortexing for 25 s. The eDNA concentration was determined by fluorimetric quantitation.

2.12. Data Deposition

The *Acidiphilium* sp. C61 genome sequence has been deposited at the European Nucleotide Archive EBI-ENA under the Bioproject number PRJEB35789. The RNA-seq sequencing data has been deposited at the ArrayExpress under the accession E-MTAB-8619.

3. Results

3.1. Effect of PEA on Phenotype and Growth of Iron Snow Key Players

Given the previously observed, aggregation-inducing effect of PEA on *Acidiphilium* sp. C61 [17], we were interested in assessing the extent to which this phenotype is conserved across different *Acidiphilium* species and other iron reducers and oxidizers present in iron snow. Using three closely related *Acidiphilium* strains (Figure 1), we applied increasing concentrations of PEA (up to 50 μ M) and used fluorescence microscopy to monitor any aggregate formation (Figure 2a). PEA induced aggregation in all tested *Acidiphilium* strains, with the greatest response observed in *Acidiphilium* SJH and *A. cryptum* JF-5, compared to *Acidiphilium* sp. C61. Higher concentrations of PEA resulted in increased numbers of aggregates formed (Figure 2a). In addition, biofilm formation of *Acidiphilium* sp. C61 on glass slides was enhanced in the presence of 10, 50, and 100 μ M PEA after 5 days but not after 7 days.

For comparison, we also tested a potential response to PEA by the more distantly related *Acidocella* sp. C78 and the iron oxidizer *Ferroplasma* sp. PN-J47, but we did not observe any aggregation (Figure 2a). Although PEA led to a distinct physiological response by *Acidiphilium* spp. following the addition of increasing concentrations of PEA, it did not have any effect on growth over time for the three tested *Acidiphilium* spp. or *Acidocella* sp. C78 (Figure 2b). However, rates of *Ferroplasma* sp. PN-J47 iron oxidation increased 1.2- and 1.6-fold in the presence of 10 and 50 μ M PEA, respectively (Figure S1).

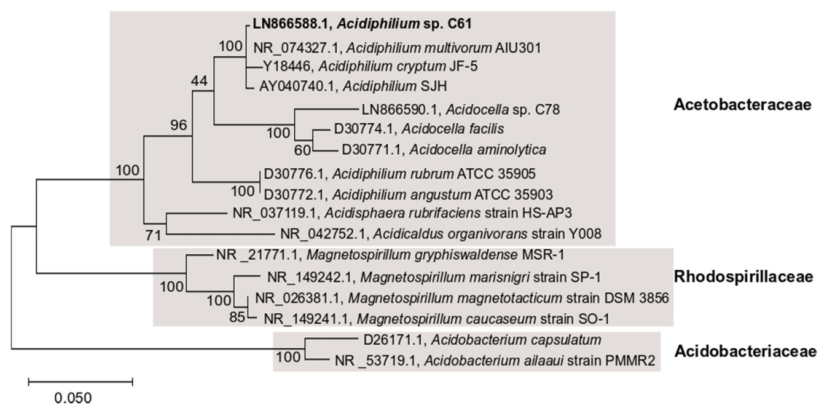


Figure 1. 16S rRNA gene phylogenetic tree of *Acidiphilium* sp. C61 (bold) with other closely related isolates. The tree was reconstructed using the maximum likelihood method. GeneBank accession numbers for sequences are given. Scale bar shows 0.05 change per nucleotide position.

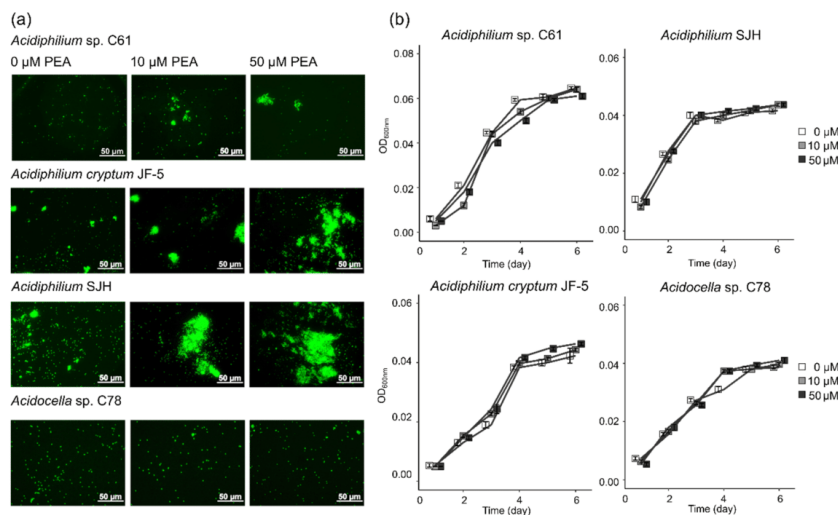


Figure 2. Effect of phenethylamine (PEA) on cell phenotype and growth of bacteria. (a) Fluorescence microscopy images of PEA-induced aggregate formation in *Acidiphilium* sp. C61, *Acidiphilium cryptum* JF-5, *Acidiphilium* SJH, and *Acidocella* sp. C78 incubations amended with increasing concentrations of PEA (0, 10, 50 μM) during aerobic growth. Total nucleic acids in subsamples taken after 3–4 days were stained with SYTO 13. (b) Aerobic growth curves (OD_{600nm}) of *Acidiphilium* sp. C61, *Acidiphilium cryptum* JF-5, *Acidiphilium* SJH, and *Acidocella* sp. C78 (see methods for growth conditions) incubations grown with increasing PEA concentrations (0 μM, white square; 10 μM, grey square; and 50 μM, black square). Values represent means of triplicate samples ($n = 3$); error bars represent one standard deviation.

3.2. Genome Sequencing, Assembly and Annotation of *Acidiphilium* sp. C61

We sequenced the genome of *Acidiphilium* sp. C61 to reconstruct its metabolic potential and to identify potential mechanisms enabling aggregate formation. Genome assembly led to a draft genome

comprising six contigs (Table S1). The longest contig (326,6126 bp) accounted for 84.8% of the total assembly. Based on the presence and copy numbers of single-copy marker genes, the genome was 100% complete and showed a contamination of 2.24%. The assembled genome sequence of *Acidiphilium* sp. C61 has a size of 3.85 Mbp, a GC content of 66.1%, and contains 3700 open reading frames (ORF), of which 3604 are protein-coding genes and 96 are non-coding RNA genes (6 ribosomal RNA genes and 90 transfer RNA genes). Ninety transfer RNA genes comprised one tmRNA and multiple copies for all tRNA-genes except tRNA-Cys and tRNA-Trp. Among the 3604 protein-coding genes, 2155 genes were assigned a putative function and 1333 encode hypothetical proteins. In addition, we identified 116 transposase genes.

3.3. Potential Mechanisms of Aggregate Formation in *Acidiphilium* sp. C61

Given the previously observed phenotype of *Acidiphilium* sp. C61 forming aggregates upon exposure to PEA, our genome analysis focused on identifying mechanisms potentially involved in facilitating aggregate formation, including autoaggregation, motility, and biofilm formation. Since the aggregation effect was not specific to *Acidiphilium* sp. C61, we performed initial pangenome analyses of seven *Acidiphilium* spp. available in the GenBank Assembly database. The core genome of all *Acidiphilium* spp. analyzed included 1701 gene clusters, which comprised 52.1% of the gene clusters in the *Acidiphilium* sp. C61 genome (Figure 3a).

After screening the core genome for gene clusters relevant to aggregation, we observed that the seven strains shared 65 gene clusters (3.8% of overlapped gene clusters). These functions of these gene clusters are commonly associated with bacterial autoaggregation (autotransporter), motility (flagellar assembly, chemotaxis), and biofilm formation (exopolysaccharide biosynthesis and transport) (Figure 3b, Table S2-1) since the exact genes and mechanisms of three potential aggregations were not elucidated in previous studies. Out of the gene clusters, 541 were unique to *Acidiphilium* sp. C61, with the majority encoding hypothetical proteins (60%) (Table S2-2). Other strain-specific gene clusters encoded proteins involved in capsular polysaccharide biosynthesis, capsular polysaccharides transport (*kps*), the import of urea, and CRISPR/Cas systems, which function to protect against viral attack.

The inhibition of flagellar motility represents one mechanism of aggregation. Bacterial flagella consist of six components: basal body, motor, switch, hook, filament, and export apparatus, and screening the genome of *Acidiphilium* sp. C61 revealed genes for all six components (Table S3). Modulation of flagellar-based motility is facilitated in *Acidiphilium* sp. C61 by an intact chemotaxis pathway, including genes for methyl-accepting chemotaxis proteins (*mcp*) and two-component systems (*cheAW*, *cheY*) that transduce environmental signals and interact with the flagellar basal body (*fliGMN*) and motor proteins (*motAB*).

Next, we screened the genome for genes encoding autotransporters, which are outer membrane proteins that facilitate aggregation by binding to extracellular matrix components and the surface of other cells. One autotransporter gene and two genes coding for autotransporter modification proteins were identified in the *Acidiphilium* sp. C61 genome. In addition, we identified genes with a homology (amino acid sequence identity >30%) to other putative autotransporter genes (Table S3).

Extracellular polymeric substances (EPS) are considered to be one of the major structural components of the biofilm matrix that form on solid surfaces as well as non-surface attached aggregates, for example, pellicle biofilms that form at the air–liquid interface. Genes encoding proteins involved in the synthesis and secretion of exopolysaccharides, such as glycosyltransferases, the putative polysaccharide biosynthesis/export protein (*wza*), and the capsular polysaccharide export protein (*kps*) were identified. The presence of different pathways involved in exopolysaccharide precursor production suggests that EPS biosynthesis plays a role in *Acidiphilium* sp. C61 aggregate formation. Lastly, we looked for genes related to quorum sensing based biofilm formation and aggregation. Quorum sensing can induce aggregate formation through coordinated changes in gene expression mediated by autoinducers in response to cell density fluctuations, which can regulate biofilm formation. However, the *Acidiphilium* sp. C61 genome lacks autoinducer synthesis and receptor genes.

4. Molecular mechanisms underpinning aggregation in *Acidiphilium* sp. C61

Microorganisms 2020, 8, 314

9 of 20

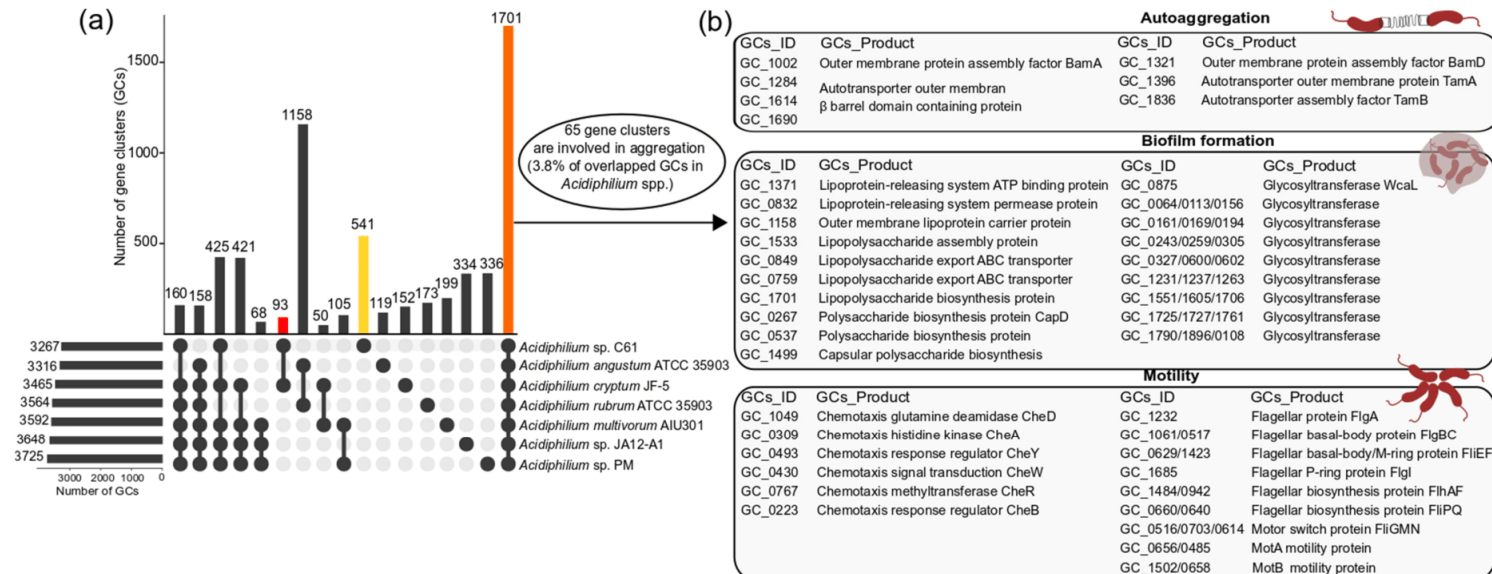


Figure 3. Genome comparison and identification of overlapping gene clusters (GCs) involved in bacterial aggregation of *Acidiphilium* sp. C61. (a) Intersect plot of the genome comparison of *Acidiphilium* sp. C61 with 6 other *Acidiphilium* sp. The horizontal bar chart in panel (a) corresponds to the total number of GCs found in each *Acidiphilium* strain. The vertical bar chart in panel (a) depicts the number of shared or unique GCs of intersected set under the corresponding species name and dark connected dots on the bottom panel indicate which *Acidiphilium* sp. is linked to each intersected set. The orange bar corresponds to the total number of overlapping GCs in all 7 *Acidiphilium* spp., the yellow bar corresponds to the total number of unique GCs found in *Acidiphilium* sp. C61, and the red bar corresponds to the total number of unique overlapping GCs between *Acidiphilium* sp. C61 and *Acidiphilium cryptum* JF-5, both of which were isolated from the same acidic lake (Lake77). Note, only overlapping GCs with a value greater than 50 are shown. (b) Schematic representation of a subset of overlapping GCs involved in aggregation. The GCs linked to these 3 categories (autoaggregation, biofilm formation, motility) were identified based on homologous functions to genes encoding for known aggregation mechanisms. Briefly, the 1701 shared GCs present in all *Acidiphilium* spp. were manually inspected based on annotated gene functions. Amino acid sequences of overlapping GCs linked to autoaggregation, biofilm formation, and motility were subset and compared to the *Acidiphilium* sp. C61 genome using BLAST (autoaggregation) or annotated using *dfast* (biofilm formation and motility). The IDs (GCs_ID) and corresponding annotated functions (GCs_Product) for the identified GCs are shown. In some cases, multiple GCs encode for the same function.

3.4. Central Metabolism and Iron Reduction Machinery in *Acidiphilium* sp. C61

The lack of genomic information available for acidophilic FeRB prompted us to investigate the metabolic potential of *Acidiphilium* sp. C61 as a whole. The *Acidiphilium* sp. C61 genome encodes an incomplete glycolysis pathway but features full sets of genes required for the tricarboxylic acid (TCA) cycle and oxidative phosphorylation (Figure 4, Table S4). The lack of an intact glycolysis pathway is compensated by a complete pentose phosphate pathway. We found no genes related to major carbon fixation pathways, but *Acidiphilium* sp. C61 appears to be able to fix carbon dioxide heterotrophically since its genome encodes a pyruvate carboxylase (*pyc*) and a pyruvate orthophosphate dikinase (*ppdk*) similar to *Acidiphilium* sp. JA12-A1 [58]. *Acidiphilium* sp. C61 possesses genes encoding all pathways for the biosynthesis of proteinogenic amino acids, nucleotide and fatty acid biosynthesis (Figure 4). Multiple encoded transporters enable the transport and utilization of inorganic nutrients (e.g., *afuABC*) and organic substrates (e.g., *kpsET*). Among others, we identified genes encoding ribose (*rbsABC*), fructose (*frcABC*) and xylose (*xylFGH*) transporters. We also found seven genes of two complete pathways (starting from acetyl-CoA) responsible for the biosynthesis and accumulation of poly-β-hydroxybutyrate (PHB), a common storage material in prokaryotic cells typically synthesized in the presence of excess organic carbon and previously identified in *Acidiphilium cryptum* JF-5 [14,59] and *Acidiphilium* sp. JA12-A1 [58].

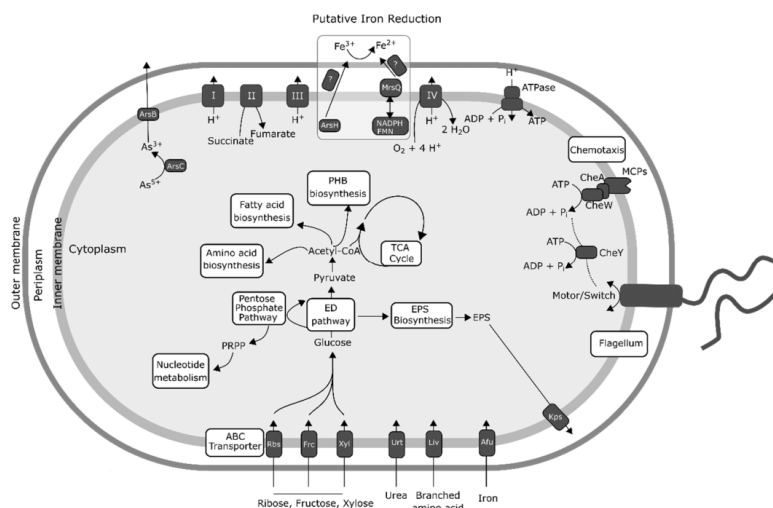


Figure 4. Genomic potential of *Acidiphilium* sp. C61, based on gene annotations described in the newly sequenced *Acidiphilium* sp. C61 genome. Here, the energy production pathway, oxidative phosphorylation pathway, sugar transporters, as well as all potential mechanisms (exopolysaccharide production, flagellar motility) of aggregate formation are included. Also shown are potential mechanisms of iron reduction derived from (1) previous publications [59,60] describing potential iron-reduction machinery in other acidic iron reducers, and (2) genes identified in the *Acidiphilium* sp. C61 genome with significant homology to iron reduction machinery described in other well-characterized iron-reducing bacteria, for example, *Shewanella*. ArsBC = arsenate reductase subunits B/C, MCPs = methyl-accepting chemotaxis proteins, CheA = chemotaxis protein CheA, CheY = chemotaxis protein CheY, EPS = extracellular polymeric substance, ED pathway = Entner–Doudoroff pathway, Rbs = ribose transport protein, Frc = fructose transport protein, Xyl = xylose transport protein, Urt = urea transport protein, Liv = branched-chain amino acid transport protein, Afu = iron transport protein, Kps = capsular polysaccharide export protein.

In comparison to neutrophilic and alkaliphilic FeRBs, our knowledge about the iron-reducing machinery in acidophiles is limited [60]. *Acidiphilium* sp. C61 possesses genes encoding for cytochrome *c* (Table S5-1), which is a outer-membrane cytochrome suggested to be involved in iron respiration of *A. cryptum* JF-5 [61]. No other conclusive iron reductases in acidophilic FeRB, such as *Acidocella* or *Acidiphilium* spp., have been identified to date [58,60]. We also identified a complete set of genes involved in oxidative phosphorylation and genes coding proteins known to be involved in electron transfer using a variety of electron donors such as NADH, NADPH, glutathione, and electron transfer mediators such as FMN and FAD (Table S5-2). These electron donors and electron transfer mediators are necessary to transfer electrons to Fe³⁺.

Furthermore, we searched for candidate iron reductase involved in iron reduction based on knowledge on other FeRB and electron transfer in general (Figure 4, Table S5-3). A homology search using all available iron reductases found in the NCBI non-redundant protein database against the genome of *Acidiphilium* sp. C61 was performed. Homology searches identified only one gene with a homology of 45.8% compared to *msrQ* (methionine sulfoxide reductase heme-binding subunit) from the neutrophilic FeRB *Shewanella* sp. Sh95 that could play a role in iron reduction. In addition, we identified a gene encoding an arsenate reductase (AcpC61_1183), which might function as iron reductase under acidic conditions [62].

3.5. Differential Gene Expression Analysis

We performed RNA-seq analysis on *Acidiphilium* sp. C61 with and without PEA exposure to examine transcriptome-wide responses to this aggregate-inducing chemical mediator. Under these specific growth conditions, we detected gene expression for 3598 out of 3604 genes encoded in the genome of *Acidiphilium* sp. C61. Gene expression ranged from 1.0 and 14.3 log₂ counts per million (log₂CPM). A detailed analysis of overall highly expressed genes (log₂CPM >9) revealed primarily genes linked to carbohydrate metabolism, electron transfer, ATP synthesis, amino acid metabolism, and genetic information processing (DNA replication, transcription, protein biosynthesis) (Table S6). Except for a few seemingly random genes, genes linked to potential aggregation mechanisms were not among those featuring highest gene expression values. Gene expression for flagella biosynthesis, for instance, ranged between 6 and 10 log₂CPM and between 5 and 9 log₂CPM for chemotaxis.

PEA addition triggered a pronounced shift in gene expression. Out of 3598 expressed genes, 45.3% were differentially expressed in *Acidiphilium* sp. C61 plus PEA incubations (log₂ fold change (FC) >0.58 or <-0.58, log₂ counts per million (CPM) >6 and false discovery rate (FDR <0.05) (Figure 5a, Table S7). Additionally, 896 genes were upregulated and 734 genes were downregulated, which equates to 55% and 45%, respectively, of all differentially expressed genes. Among these differentially expressed genes, 254 (26.5% of upregulated genes) and 216 (28.6% of downregulated genes) genes encode hypothetical proteins (Table S7). We focused on genes linked to potential aggregation mechanisms (Figure 5b, Table S8). Out of 29 genes involved in flagella biosynthesis, 6 were upregulated, including *fliC* (coding for the flagella filament), *flgI* (flagella P-ring protein precursor), *flgB*, *flgC*, *flgG* (encoding flagella proximal and distal rod proteins), *fliL* (flagella basal body rod protein). Only two genes, *fliR* (flagellar biosynthetic protein), *flgA* (flagella basal body P-ring formation, AcpC61_0944) were downregulated and the other *flgA* gene copy (AcpC61_1269) remained unchanged (Figure 5b, Table S8). Chemotaxis related genes ranged in expression between 4 and 8 log₂CPM. We observed that multiple *mcp* genes were downregulated, while other components of the chemotaxis machinery, for example, two-component systems, were not affected by PEA. For exopolysaccharide synthesis genes, the majority of genes involved in the exopolysaccharide precursor biosynthesis pathways (e.g., UDP-glucose, UDP-galactose) were upregulated, whereas genes involved in capsular polysaccharide biosynthesis were downregulated (e.g., glycosyltransferase, capsular polysaccharide biosynthesis protein) (Figure 5b, Table S8). Genes linked to capsular polysaccharide export (*kpsE*, *kpsT*) were upregulated.

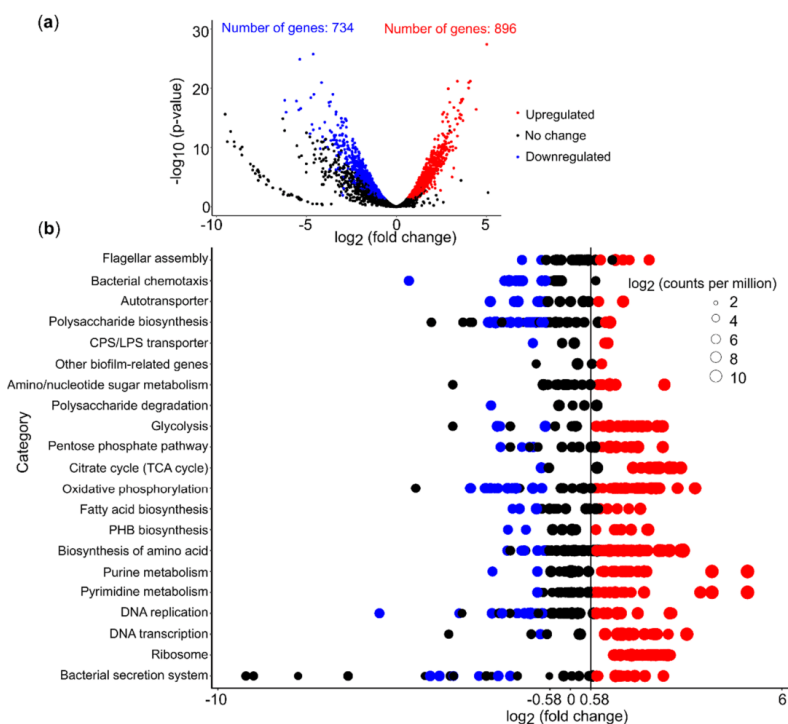


Figure 5. Differential gene expression profiling of *Acidiphilium* sp. C61 upon PEA (10 μM) supplementation. (a) Volcano plot of differentially expressed genes (DEGs) with statistical significance and fold change in the control and treatment group. Significantly differentially expressed genes are defined by a $\log_2\text{FC}$ (\log_2 fold change) > 0.58 or $\log_2\text{FC} < -0.58$, \log_2 counts per million (\log_2 CPM) > 6 , and an adjusted p -value FDR (false discovery rate) < 0.05 . Each dot represents a single expressed gene. Red dots represent upregulated genes, blue dots represent downregulated genes, and black dots represent genes not upregulated or downregulated. (b) Gene expression patterns of selected KEGG pathways in *Acidiphilium* sp. C61 incubations with 10 μM PEA. Each bubble denotes one gene and the bubble size indicates \log_2 CPM values. Red and blue bubbles represent up- and downregulated genes, while black bubbles represent non-significantly differentially expressed.

3.6. PEA Induced Upregulation of Central Cellular Metabolism

We also used RNA-seq data to assess the effect of PEA on genes linked to central cellular metabolism. More than 50% of the genes involved in glycolysis, the TCA cycle, and oxidative phosphorylation were upregulated (Figure 5b). Although we found that genes involved in energy production, for example, genes involved in DNA precursor biosynthesis, were highly expressed, we did not observe an increase in bacterial growth or production of eDNA (Figure 6). We did not detect a significant increase in bacterial 16S rRNA gene copies nor eDNA concentration in cultures of *Acidiphilium* sp. C61 in incubations supplemented with PEA despite enhanced aggregate formation. We also observed no change in the activity of DNA replication. However, we found that most genes involved in amino acid biosynthesis and transcription were upregulated (Figure 5b). Genes involved in the synthesis of ribosomes and genes encoding signal peptidases, which are involved in the removal of signal peptides from secretory proteins, were also upregulated. Genes linked to the Sec translocation pathway, which

provides a major pathway of protein translocation from the cytosol across the cytoplasmic membrane in bacteria, were also upregulated (Table S8).

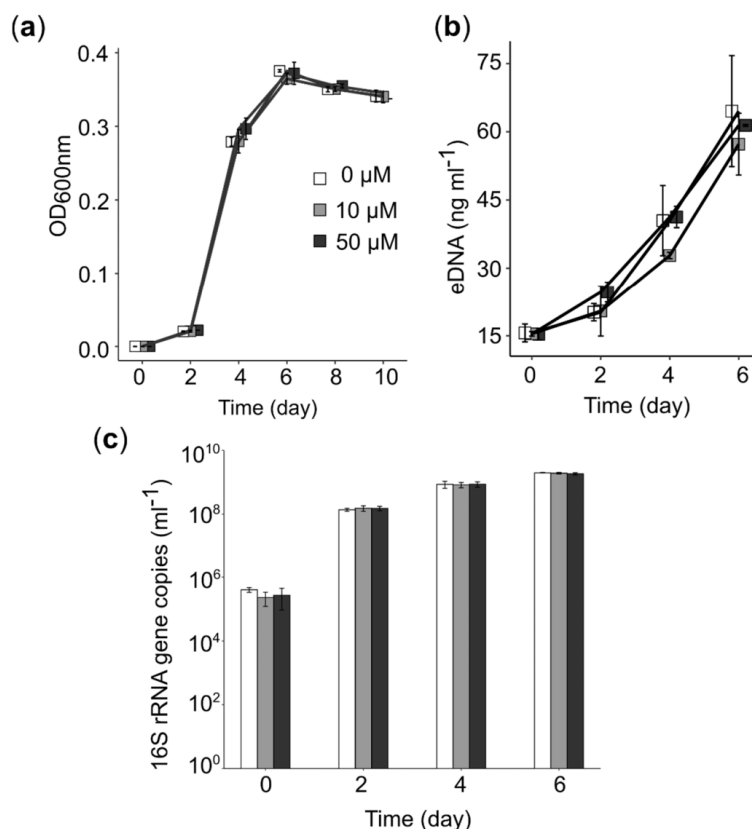


Figure 6. Effect of PEA on eDNA release and growth in *Acidiphilium* sp. C61. (a) Growth curve of *Acidiphilium* sp. C61 culture supplemented with different concentrations of PEA (0 μM, white; 10 μM, grey; 50 μM, black), $n = 3$. (b) eDNA concentration in cultures of *Acidiphilium* sp. C61 supplemented with different PEA concentrations. (c) Bacterial 16S rRNA gene copies numbers mL⁻¹ on days 0, 2, 4, 6 of the incubation were quantified and compared among *Acidiphilium* sp. C61 cultures with and without PEA.

4. Discussion

Bacteria of the heterotrophic alphaproteobacterial genus *Acidiphilium* are ubiquitous in acidic environments [63]. These heterotrophs are often isolated as contaminants from iron-oxidizing mixed cultures composed of acidophiles like *Acidithiobacillus ferrooxidans* [64,65] or species related to *Ferroplasma myxofaciens* P3G [58]. In these iron-oxidizing mixed cultures, *Acidiphilium* spp. enhance the activities of these chemolithoautotrophs in bioleaching. In return, *Acidiphilium* spp. seem to benefit from their secreted metabolites and biomass remnants [28,66]. *Acidiphilium* spp. have been also directly isolated from acidic mine drainage waters and sediments [14,67] and from acidic hypersaline river sediments in Australia, where they can make up high relative fractions of the microbial community [68].

Independent of their original ecological niche, all seven *Acidiphilium* spp. analysed by pangenomics show high similarities regarding their functional genome organization. Not surprisingly, both strains isolated from the same lake share the highest number of accessory gene clusters (93 gene clusters), with most of them being related to hypothetical proteins except a few related to transporters. Genes encoding different mechanisms of aggregation were present in all seven genomes, i.e., genes involved in the synthesis and secretion of EPS, suggesting that these mechanisms of aggregation are common in *Acidiphilium* spp. Indeed, all three *Acidiphilium* isolates tested in this study were able to aggregate to some extent, even without PEA addition. This morphological feature observed in *Acidiphilium* isolates has been previously documented, for example, the salt-tolerant *Acidiphilium* strain, AusYE3-1, also forms flocs and alters cell shapes from rod-shaped or coccobacillus to filamentous structures when stressed under high salt concentrations [68].

Our study shows PEA enhanced aggregation of all *Acidiphilium* strains tested, but not of other acidophiles [15,17] also present in iron snow. However, the PEA enhanced aggregate formation of *Acidiphilium* sp. C61 was less pronounced (Figure 2a) compared to the high number of large macroscopic cell aggregates formed by cultures of *Acidiphilium* sp. C61 soon after isolation from iron snow [17]. In that previous study, increased growth in the presence of 10 μ M PEA was also observed, which could not be repeated in our study, suggesting adaptations during extended laboratory incubation of *Acidiphilium* sp. C61.

Based on our previous model [17], we anticipated that PEA induced gene expression changes would primarily be related to motility similar to its role in *Proteus mirabilis* [22,23]. However, the assembled genome of *Acidiphilium* sp. C61 lacks the *flhDC* gene cluster present in *P. mirabilis*, and flagellar motility was not negatively affected by PEA addition. Motility still seems to be essential for *Acidiphilium* sp. C61, as the six genes involved in flagella biosynthesis were even slightly upregulated. This finding agrees with the results of a metaproteomic approach, which detected many flagellin domain proteins from *Acidiphilium* spp. in iron snow samples [15]. Furthermore, chemotaxis sensor proteins were downregulated in the presence of PEA, enabling more smooth swimming. Thus, flagellar motility might help *Acidiphilium* sp. C61 join iron oxidizers, like *Acidithrix* sp. C25 in the growing aggregate, then again, there may not be sufficient time for the microorganism to switch from a pelagic to an attached lifestyle.

Acidiphilium, *Acidithrix*, *Acidocella*, and *Ferroplasma* spp. can make up 53% of the total bacterial community of aggregates formed in acidic lignite lakes [15]. In these shallow lakes, iron snow forms a continuous shower of iron minerals, (in)organic matter and microorganisms ($\sim 10^8$ – 10^{10} cells (g dry wt⁻¹)) rapidly falling through the water column to the sediment [5,69,70]. Thus, there is only a short lifespan of these pelagic aggregates, which consequently means there is only limited time for microbial-coordinated activities, and for energy and matter fluxes to occur within these aggregates. Although acyl-homoserine lactone (AHL) mediated gene regulation has been shown to influence EPS production and biofilm formation in many proteobacteria, including *A. ferrooxidans* [71], we could not find autoinducer synthesis or receptor genes linked to quorum sensing in the genome of *Acidiphilium* sp. C61. Thus, communication appears to occur via other interaction mechanisms mediated by diffusive exometabolites (infochemicals).

Bacterial EPS is usually composed of a mixture of polysaccharides, proteins, lipids, and extracellular DNA (eDNA) [72,73]; however, the main constituents of EPS extracted from *Acidiphilium* strain 3.2Sup(5) are proteins and carbohydrates mostly composed of carboxylic, hydroxylic, and amino groups [74]. Although we observed the upregulation of several genes for exopolysaccharide precursor synthesis (e.g., UDP-glucose, UDP-galactose) and capsular polysaccharide exporters in the presence of PEA, the overall expression pattern of genes involved in polysaccharide synthesis, as well as autotransporters, were inconsistent. Thus, we cannot conclude that biofilm formation, in general, is enhanced in the presence of PEA, nor can we explicitly conclude the mechanisms involved in *Acidiphilium* sp. C61 biofilm formation. Similarly, we did not detect significantly enhanced eDNA concentrations, indicating

eDNA is likely not a primary constituent of EPS secreted by *Acidiphilium* sp. C61 and *Acidiphilium* sp. C61 may prefer to aggregate with other cells over forming biofilms.

The high surface area of the poorly crystalline iron mineral schwertmannite, which forms the inorganic matrix of iron snow [13,69], favors adsorption of organic matter that are ideal substrates for *Acidiphilium* spp. [14,15]. The above mentioned metaproteomic approach also identified *Acidiphilium*-related glucose uptake proteins in iron snow [15]. The genome of *Acidiphilium* sp. C61 contains ABC transporters for the uptake of ribose, fructose, and xylose (Figure 4). In contrast to the genome of *Acidiphilium* sp. JA12-A1 that lives in co-culture with *Ferroplasma* sp. JA12 [58], we did not find polysaccharide-hydrolyzing enzymes, such as β -glucosidases, or break down EPS or cell envelope polysaccharides from decaying cells endoglucanases in *Acidiphilium* sp. C61. However, glycoside hydrolase, alpha-amylase, beta-N-acetylhexosaminidase, and glucoamylase were present in all *Acidiphilium* spp. based on the pangenomic analysis (GC_1878, GC_1672, GC_1296, GC_1827) (Table S2-3). In addition, *Acidiphilium* sp. C61 possesses one more unique glycoside hydrolase (GC_6119), whereas another glycosidase (GC_1572) is present in the other six *Acidiphilium* strains. The capacity for polysaccharide degradation seems to be a common trait for *Acidiphilium* spp., but individual differences exist between the strains. Thus, these individual differences allow for niche differentiation and also ensures complementarity, since a diverse mixture of strains will colonize specific habitats.

In general, sugar compounds appear to be the preferred carbon source for biomass production in all *Acidiphilium* sp. We identified full sets of genes of the pentose phosphate pathway, compensating for the incomplete glycolysis pathway, a complete tricarboxylic acid (TCA) cycle, and genes encoding all pathways necessary for the synthesis of proteinogenic amino acids, nucleotide, and fatty acid biosynthesis. *Acidiphilium* sp. C61 is capable of urea uptake, a unique trait among *Acidiphilium* sp. Thus, it can be characterized as a prototrophic cell, able to synthesize all the compounds needed for growth listed above without the need for a partner organism. Different *Acidiphilium* strains present in complex communities appears to release a diverse suite of glycoside hydrolases and glucosidases to utilize the organic substances secreted by other community members or derived from microbial cell decay. In return, *Acidiphilium* spp. provide the chemolithoautotrophs with elevated CO₂ concentrations locally, which is advantageous especially in low pH environments, such as acidic coal mining lakes. This type of interspecies carbon transfer has been previously described for acidophilic mixed cultures containing *Acidiphilium cryptum* and *Acidithiobacillus ferrooxidans* [75] and other mixed cultures derived from a pilot plant for remediation of acid mine drainage (AMD) containing *Acidiphilium* sp. JA12-A1 and an iron oxidizer related to *Ferroplasma myxofaciens* P3G [76].

To our surprise, PEA did not preferentially affect one or more mechanisms of aggregate formation in *Acidiphilium* but induced upregulation of the central cellular metabolism by affecting more than 50% of the genes involved in glycolysis, the TCA cycle, and oxidative phosphorylation. Similarly, the synthesis of ribosomes, amino acid biosynthesis and transcription, as well as secretion systems, were stimulated. This broad range of affected upregulated genes points to a more general stimulatory mechanism of PEA, similar to its general role as a neurotransmitter [18] and stimulator for the release of biogenic amines in humans [20]. Thus, it is probable that these *Acidiphilium* cells are just more active in iron snow in the presence of the infochemical PEA released by *Acidithrix* sp. C25.

After the formation of iron minerals at the oxic-anoxic interface, iron snow will reach anoxic conditions in the hypolimnion. Since Fe³⁺ is energetically much more favorable as an electron acceptor at acidic compared to pH neutral conditions [77], the majority of the chemolithoautotrophic Fe²⁺ oxidizers are also capable of Fe³⁺ reduction, including *Acidithrix* sp. C25 [13]. These heterotrophic *Acidiphilium* spp., as well as other heterotrophic acidophiles, are also capable of Fe³⁺ reduction even in the presence of oxygen [78–80]. Thus, single cells within the iron snow aggregates may begin to respire Fe³⁺ in the redoxcline, even at low oxygen concentrations. Switching to this anaerobic metabolism requires activation, as genes responsible for Fe³⁺ reduction in *Acidiphilium* spp. do not seem to be constitutively expressed [78]. Although the Fe³⁺ reduction mechanism in *Acidiphilium* spp. has not yet been revealed in detail, different membrane-associated proteins potentially related

to electron transport chain genes have been identified in iron snow, including OmpA/MotB domain proteins, TonB-dependent receptor, and ApcA [15]. Genome assembly of *Acidiphilium* sp. C61 reveals MsrQ that can bind to two b-type hemes via conserved histidine residues along with MsrP; these proteins form a methionine sulfoxide reductase operon functioning to repair oxidized periplasmic proteins [81]. Additionally, the cytosolic NAD(P)H flavin reductase (Fre) has been shown to function as a proficient electron donor to MsrQ moieties and the soluble dehydrogenase partner, in *Escherichia coli*, for example [81]. These findings suggest that Fre and MsrPQ might form a membrane-spanning two-component system for electron transfer (Figure 4). Because MsrPQ is involved in oxidative stress response, specifically in the repair of oxidized periplasmic proteins, such as oxidized methionine residues, there is a potential role for the MsrPQ operon in the maintenance of the activated methyl cycle, which can be remotely linked to iron reduction via the transsulfuration pathway. We also identified a gene coding for an arsenate reductase (AcpC61_1183). Previous studies suggest that TetH or ArsH have the potential to mediate Fe³⁺ reduction in acidophiles [62,82,83]. However, since we did not perform RNA-seq analysis of *Acidiphilium* sp. C61 under iron-reducing conditions, we do not know how PEA would affect its anaerobic metabolism.

5. Conclusions

Aggregation appears to be a common mechanism in all *Acidiphilium* spp., since nearly 4% of their shared gene clusters are associated with mechanisms responsible for aggregation, including autoaggregation, motility (flagellar assembly, chemotaxis), and biofilm formation (exopolysaccharide biosynthesis and secretion). All genes associated with these mechanisms were transcribed under our incubation conditions; however, RNA-seq data did not show clear evidence that PEA affected aggregate formation directly. Inconsistent gene expression patterns relating to the formation and secretion of EPS and flagellar-based motility, despite enhanced aggregate formation with the addition of PEA, suggests this compound functions as an infochemical regulating other cellular mechanisms, and not aggregation mechanisms directly. In fact, *Acidiphilium* cells seem to retain motility within the aggregates. We did observe induced upregulation of glycolysis, the TCA cycle, oxidative phosphorylation, and synthesis of ribosomes, although these activities were not linked to enhanced growth. Degradation of polysaccharides appears to be a major function within the heterotrophic Alphaproteobacterial genus *Acidiphilium*, which is optimized by the complementarity of specific genes present in unique strains in addition to shared core functions.

Supplementary Materials: Supplementary materials can be found at <http://www.mdpi.com/2076-2607/8/3/314/s1>. Figure S1: Fe(II) consumption of *Ferroplasma* sp. PN-J47 supplemented with different concentrations of PEA (0, 10 and 50 μ M), Table S1: Genome features of *Acidiphilium* sp. C61 in comparison to six other *Acidiphilium* spp., Table S2: Gene clusters (GCs) involved in aggregation, unique gene clusters, and polysaccharide degradation in *Acidiphilium* sp. C61 by Pangenomics, Table S3: Aggregation genes identified in the genome of *Acidiphilium* sp. C61, Table S4: Genes of central metabolism present in the genome of *Acidiphilium* sp. C61, Table S5: Iron-reduction related genes (cytochrome c, electron transfer, iron reductase) identified in *Acidiphilium* sp. C61, Table S6: Top 10% of highly expressed genes of *Acidiphilium* sp. C61 in the presence of 10 μ M PEA, Table S7: Summary of differential expressed genes in *Acidiphilium* sp. C61 after 10 μ M PEA addition, Table S8: General gene expression pattern in *Acidiphilium* sp. C61 supplemented with 10 μ M PEA addition.

Author Contributions: Q.L. performed the laboratory work and bioinformatics. R.E.C., and C.-E.W. supervised the lab work and data analysis. K.K. conceived and designed the experiments and acquired funding. Q.L. wrote the original draft. K.K., R.E.C., and C.-E.W. reviewed and edited the manuscript. All authors have read and agreed to the published version of the manuscript.

Funding: This work was supported in part by the Jena School for Microbial Communication (JSMC) graduate school and by the Collaborative Research Centre Chemical Mediators in Complex Biosystems (SFB 1127 ChemBioSys) of the Friedrich Schiller University Jena, both funded by the Deutsche Forschungsgemeinschaft (DFG). Additional support for this research was kindly provided by the German Centre for Integrative Biodiversity Research (iDiv) Halle-Jena-Leipzig, also funded by the Deutsche Forschungsgemeinschaft (DFG). Further support for this research was provided by the Carl Zeiss Foundation (Carl Zeiss Stiftung) to Q.L.

Acknowledgments: The authors thank Jens D. Wurlitzer (Friedrich Schiller University Jena) for technical assistance in the laboratory and Jiro F. Mori (Yokohama City University) for extraction of genomic DNA used for genome sequencing.

Conflicts of Interest: There is no conflict of interest claimed by the authors. The funders had no role in the design of the study; in the collection, analyses, or interpretation of data; in the writing of the manuscript, or in the decision to publish the results.

References

1. Alldredge, A.L.; Silver, M.W. Characteristics, dynamics and significance of marine snow. *Prog. Oceanogr.* **1988**, *20*, 41–82. [[CrossRef](#)]
2. Simon, M.; Grossart, H.-P.; Schweitzer, B.; Ploug, H. Microbial ecology of organic aggregates in aquatic ecosystems. *Aquat. Microb. Ecol.* **2002**, *28*, 175–211. [[CrossRef](#)]
3. Thornton, D. Diatom aggregation in the sea: Mechanisms and ecological implications. *Eur. J. Phycol.* **2002**, *37*, 149–161. [[CrossRef](#)]
4. Grossart, H.-P.; Simon, M. Limnetic macroscopic organic aggregates (lake snow): Occurrence, characteristics, and microbial dynamics in Lake Constance. *Limnol. Oceanogr.* **1993**, *38*, 532–546. [[CrossRef](#)]
5. Reiche, M.; Lu, S.; Ciobotă, V.; Neu, T.R.; Nietzsche, S.; Rösch, P.; Popp, J.; Küsel, K. Pelagic boundary conditions affect the biological formation of iron-rich particles (iron snow) and their microbial communities. *Limnol. Oceanogr.* **2011**, *56*, 1386–1398. [[CrossRef](#)]
6. Dang, H.; Lovell, C. Microbial surface colonization and biofilm development in marine environments. *Microbiol. Mol. Biol. Rev.* **2016**, *80*, 91–138. [[CrossRef](#)] [[PubMed](#)]
7. Gram, L.; Grossart, H.-P.; Schlingloff, A.; Kjørboe, T. Possible quorum sensing in marine snow bacteria: Production of acylated homoserine lactones by *Roseobacter* strains isolated from marine snow. *Appl. Environ. Microbiol.* **2002**, *68*, 4111–4116. [[CrossRef](#)]
8. Blodau, C. A review of acidity generation and consumption in acidic coal mine lakes and their watersheds. *Sci. Total Environ.* **2006**, *369*, 307–332. [[CrossRef](#)]
9. Küsel, K. Microbial cycling of iron and sulfur in acidic coal mining lake sediments. *Water Air Soil Pollut. Focus* **2003**, *3*, 67–90.
10. Bigham, J.M.; Schwertmann, U.; Traina, S.J.; Winland, R.L.; Wolf, M. Schwertmannite and the chemical modeling of iron in acid sulfate waters. *Geochim. Cosmochim. Acta* **1996**, *60*, 2111–2121. [[CrossRef](#)]
11. Wang, H.; Bigham, J.M.; Tuovinen, O.H. Formation of schwertmannite and its transformation to jarosite in the presence of acidophilic iron-oxidizing microorganisms. *Mater. Sci. Eng. C* **2006**, *26*, 588–592. [[CrossRef](#)]
12. Ciobotă, V.; Lu, S.; Tarcea, N.; Rösch, P.; Küsel, K.; Popp, J. Quantification of the inorganic phase of the pelagic aggregates from an iron contaminated lake by means of Raman spectroscopy. *Vib. Spectrosc.* **2013**, *68*, 212–219. [[CrossRef](#)]
13. Mori, J.F.; Lu, S.; Händel, M.; Totsche, K.U.; Neu, T.R.; Iancu, V.V.; Tarcea, N.; Popp, J.; Küsel, K. Schwertmannite formation at cell junctions by a new filament-forming Fe(II)-oxidizing isolate affiliated with the novel genus *Acidithrix*. *Microbiology* **2016**, *162*, 62–71. [[CrossRef](#)] [[PubMed](#)]
14. Küsel, K.; Dorsch, T.; Acker, G.; Stackebrandt, E. Microbial reduction of Fe(III) in acidic sediments: Isolation of *Acidiphilium cryptum* JF-5 capable of coupling the reduction of Fe(III) to the oxidation of glucose. *Appl. Environ. Microbiol.* **1999**, *65*, 3633–3640. [[CrossRef](#)]
15. Lu, S.; Chourey, K.; Reiche, M.; Nietzsche, S.; Shah, M.B.; Neu, T.R.; Hettich, R.L.; Küsel, K. Insights into the structure and metabolic function of microbes that shape pelagic iron-rich aggregates (“Iron snow”). *Appl. Environ. Microbiol.* **2013**, *79*, 4272–4281. [[CrossRef](#)] [[PubMed](#)]
16. Lu, S.; Gischkat, S.; Reiche, M.; Akob, D.M.; Hallberg, K.B.; Küsel, K. Ecophysiology of Fe-cycling bacteria in acidic sediments. *Appl. Environ. Microbiol.* **2010**, *76*, 8174–8183. [[CrossRef](#)]
17. Mori, J.F.; Ueberschaar, N.; Lu, S.; Cooper, R.E.; Pohnert, G.; Küsel, K. Sticking together: Inter-species aggregation of bacteria isolated from iron snow is controlled by chemical signaling. *ISME J.* **2017**, *11*, 1075–1086. [[CrossRef](#)]
18. Irsfeld, M.; Spadafore, M.; Prüß, B. β -Phenylethylamine, a small molecule with a large impact. *Webmedcentral* **2013**, *4*, 1–15.
19. Paterson, I.A.; Juorio, A.V.; Boulton, A.A. 2-Phenylethylamine: A modulator of catecholamine transmission in the mammalian central nervous system? *J. Neurochem.* **1990**, *55*, 1827–1837. [[CrossRef](#)]
20. Rothman, R.B.; Baumann, M.H. Balance between dopamine and serotonin release modulates behavioral effects of amphetamine-type drugs. *Ann. N. Y. Acad. Sci.* **2006**, *1074*, 245–260. [[CrossRef](#)]

21. Marcobal, A.; De las Rivas, B.; Landete, J.M.; Tabera, L.; Muñoz, R. Tyramine and phenylethylamine biosynthesis by food bacteria. *Crit. Rev. Food Sci. Nutr.* **2012**, *52*, 448–467. [[CrossRef](#)] [[PubMed](#)]
22. Stevenson, L.G.; Rather, P.N. A novel gene involved in regulating the flagellar gene cascade in *Proteus mirabilis*. *J. Bacteriol.* **2006**, *188*, 7830–7839. [[CrossRef](#)] [[PubMed](#)]
23. Stevenson, L.G.; Szostek, B.A.; Clemmer, K.M.; Rather, P.N. Expression of the DisA amino acid decarboxylase from *Proteus mirabilis* inhibits motility and class 2 flagellar gene expression in *Escherichia coli*. *Res. Microbiol.* **2013**, *164*, 31–37. [[CrossRef](#)] [[PubMed](#)]
24. Alavi, M.; Belas, R. Surface sensing, swarmer cell differentiation, and biofilm development. *Methods Enzymol.* **2001**, *336*, 29–40. [[PubMed](#)]
25. Belas, R.; Suvanasuthi, R. The ability of *Proteus mirabilis* to sense surfaces and regulate virulence gene expression involves FliL, a flagellar basal body protein. *J. Bacteriol.* **2005**, *187*, 6789–6803. [[CrossRef](#)] [[PubMed](#)]
26. Sturgill, G.; Rather, P.N. Evidence that putrescine acts as an extracellular signal required for swarming in *Proteus mirabilis*. *Mol. Microbiol.* **2004**, *51*, 437–446. [[CrossRef](#)]
27. Bridge, T.A.M.; Johnson, D.B. Reductive dissolution of ferric iron minerals by *Acidiphilium* SJH. *Geomicrobiol. J.* **2000**, *17*, 193–206.
28. Tischler, J.S.; Jwair, R.J.; Gelhaar, N.; Drechsel, A.; Skirl, A.M.; Wiacek, C.; Janneck, E.; Schlömann, M. New cultivation medium for “*Ferrovum*” and *Gallionella*-related strains. *J. Microbiol. Methods* **2013**, *95*, 138–144. [[CrossRef](#)]
29. Tamura, H.; Goto, K.; Yotsuyanagi, T.; Nagayama, M. Spectrophotometric determination of iron(II) with 1,10-phenanthroline in the presence of large amounts of iron(III). *Talanta* **1974**, *21*, 314–318. [[CrossRef](#)]
30. Chin, C.S.; Alexander, D.H.; Marks, P.; Klammer, A.A.; Drake, J.; Heiner, C.; Clum, A.; Copeland, A.; Huddleston, J.; Eichler, E.E.; et al. Nonhybrid, finished microbial genome assemblies from long-read SMRT sequencing data. *Nat. Methods* **2013**, *10*, 563–569. [[CrossRef](#)]
31. Gurevich, A.; Saveliev, V.; Vyahhi, N.; Tesler, G. QUAST: Quality assessment tool for genome assemblies. *Bioinformatics* **2013**, *29*, 1072–1075. [[CrossRef](#)]
32. Parks, D.H.; Imelfort, M.; Skennerton, C.T.; Hugenholtz, P.; Tyson, G.W. CheckM: Assessing the quality of microbial genomes recovered from isolates, single cells, and metagenomes. *Genome Res.* **2015**, *25*, 1043–1055. [[CrossRef](#)] [[PubMed](#)]
33. Tanizawa, Y.; Fujisawa, T.; Nakamura, Y. DFAST: A flexible prokaryotic genome annotation pipeline for faster genome publication. *Bioinformatics* **2018**, *34*, 1037–1039. [[CrossRef](#)] [[PubMed](#)]
34. Kanehisa, M.; Sato, Y.; Morishima, K. BlastKOALA and GhostKOALA: KEGG tools for functional characterization of genome and metagenome sequences. *J. Mol. Biol.* **2016**, *428*, 726–731. [[CrossRef](#)] [[PubMed](#)]
35. Huang, Y.; Niu, B.; Gao, Y.; Fu, L.; Li, W. CD-HIT Suite: A web server for clustering and comparing biological sequences. *Bioinformatics* **2010**, *26*, 680–682. [[CrossRef](#)] [[PubMed](#)]
36. Buchfink, B.; Xie, C.; Huson, D.H. Fast and sensitive protein alignment using DIAMOND. *Nat. Methods* **2015**, *12*, 59–60. [[CrossRef](#)]
37. Eren, A.M.; Esen, Ö.C.; Quince, C.; Vineis, J.H.; Morrison, H.G.; Sogin, M.L.; Delmont, T.O. Anvi’o: An advanced analysis and visualization platform for ‘omics data. *PeerJ* **2015**, *3*, e1319. [[CrossRef](#)]
38. Delmont, T.O.; Eren, E.M. Linking pangenomes and metagenomes: The *Prochlorococcus* metapangenome. *PeerJ* **2018**, *2018*, 1–23. [[CrossRef](#)]
39. Hyatt, D.; Chen, G.L.; LoCasio, P.F.; Land, M.L.; Larimer, F.W.; Hauser, L.J. Prodigal: Prokaryotic gene recognition and translation initiation site identification. *BMC Bioinformatics* **2010**, *11*. [[CrossRef](#)]
40. Altschul, S.F.; Gish, W.; Miller, W.; Myers, E.W.; Lipman, D.J. Basic local alignment search tool. *J. Mol. Biol.* **1990**, *215*, 403–410. [[CrossRef](#)]
41. Tatusov, R.L.; Natale, D.A.; Garkavtsev, I.V.; Tatusova, T.A.; Shankavaram, U.T.; Rao, B.S.; Kiryutin, B.; Galperin, M.Y.; Fedorova, N.D.; Koonin, E.V. The COG database: New developments in phylogenetic classification of proteins from complete genomes. *Nucleic Acids Res.* **2002**, *29*, 22–28. [[CrossRef](#)] [[PubMed](#)]
42. Benedict, M.N.; Henriksen, J.R.; Metcalf, W.W.; Whitaker, R.J.; Price, N.D. ITEP: An integrated toolkit for exploration of microbial pan-genomes. *BMC Genomics* **2014**, *15*, 8. [[CrossRef](#)] [[PubMed](#)]
43. Enright, A.J.; Dongen, S.V.; Ouzounis, C.A. An efficient algorithm for large-scale detection of protein families. *Nucleic Acids Res.* **2002**, *30*, 1575–1584. [[CrossRef](#)]

44. Larkin, M.A.; Blackshields, G.; Brown, N.P.; Chenna, R.; McGettigan, P.A.; McWilliam, H.; Valentin, F.; Wallace, I.M.; Wilm, A.; Lopez, R.; et al. Clustal W and Clustal X version 2.0. *Bioinformatics* **2007**, *23*, 2947–2948. [[CrossRef](#)] [[PubMed](#)]
45. Kumar, S.; Stecher, G.; Li, M.; Niyaz, C.; Tamura, K. MEGA X: Molecular evolutionary genetics analysis across computing platforms. *Mol. Biol. Evol.* **2018**, *35*, 1547–1549. [[CrossRef](#)]
46. Kopylova, E.; Noé, L.; Touzet, H. SortMeRNA: Fast and accurate filtering of ribosomal RNAs in metatranscriptomic data. *Bioinformatics* **2012**, *28*, 3211–3217. [[CrossRef](#)]
47. Quast, C.; Pruesse, E.; Yilmaz, P.; Gerken, J.; Schweer, T.; Yarza, P.; Peplies, J.; Glöckner, F.O. The SILVA ribosomal RNA gene database project: Improved data processing and web-based tools. *Nucleic Acids Res.* **2013**, *41*, 590–596. [[CrossRef](#)]
48. Kalvari, I.; Argasinska, J.; Quinones-Olvera, N.; Nawrocki, E.P.; Rivas, E.; Eddy, S.R.; Bateman, A.; Finn, R.D.; Petrov, A.I. Rfam 13.0: Shifting to a genome-centric resource for non-coding RNA families. *Nucleic Acids Res.* **2017**, *46*, D335–D342. [[CrossRef](#)]
49. Bushnell, B. BMAP: A fast, accurate, splice-aware aligner. In Proceedings of the Conference: 9th Annual Genomics of Energy & Environment Meeting, Walnut Creek, CA, USA, 19 March 2014.
50. Li, H.; Handsaker, B.; Wysoker, A.; Fennell, T.; Ruan, J.; Homer, N.; Marth, G.; Abecasis, G.; Durbin, R.; 1000 Genome Project Data Processing Subgroup. The sequence alignment/map format and SAMtools. *Bioinformatics* **2009**, *25*, 2078–2079. [[CrossRef](#)]
51. Liao, Y.; Smyth, G.K.; Shi, W. FeatureCounts: An efficient general purpose program for assigning sequence reads to genomic features. *Bioinformatics* **2014**, *30*, 923–930. [[CrossRef](#)]
52. R Core Team. *R: A Language and Environment for Statistical Computing*; R Foundation for Statistical Computing: Vienna, Austria, 2018.
53. Robinson, M.D.; McCarthy, D.J.; Smyth, G.K. edgeR: A Bioconductor package for differential expression analysis of digital gene expression data. *Bioinformatics* **2009**, *26*, 139–140. [[CrossRef](#)] [[PubMed](#)]
54. Daims, H.; Brühl, A.; Amann, R.; Schleifer, K.-H.; Wagner, M. The domain-specific probe EUB338 is insufficient for the detection of all bacteria: Development and evaluation of a more comprehensive probe set. *Syst. Appl. Microbiol.* **1999**, *22*, 434–444. [[CrossRef](#)]
55. Loy, A.; Lehner, A.; Lee, N.; Adamczyk, J.; Meier, H.; Ernst, J.; Schleifer, K.-H.; Wagner, M. Oligonucleotide microarray for 16S rRNA gene-based detection of all recognized lineages of sulfate-reducing prokaryotes in the environment. *Appl. Environ. Microbiol.* **2002**, *68*, 5064–5081. [[CrossRef](#)] [[PubMed](#)]
56. Herrmann, M.; Hädrich, A.; Küsel, K. Predominance of thaumarchaeal ammonia oxidizer abundance and transcriptional activity in an acidic fen. *Environ. Microbiol.* **2012**, *14*, 3013–3025. [[CrossRef](#)] [[PubMed](#)]
57. Tang, L.; Schramm, A.; Neu, T.R.; Revsbech, N.P.; Meyer, R.L. Extracellular DNA in adhesion and biofilm formation of four environmental isolates: A quantitative study. *FEMS Microbiol. Ecol.* **2013**, *86*, 394–403. [[CrossRef](#)] [[PubMed](#)]
58. Ullrich, S.R.; Poehlein, A.; Voget, S.; Hoppert, M.; Daniel, R.; Leimbach, A.; Tischler, J.S.; Schlömann, M.; Mühling, M. Permanent draft genome sequence of *Acidiphilium* sp. JA12-A1. *Stand. Genomic Sci.* **2015**, *10*, 1–10. [[CrossRef](#)]
59. Ciobotă, V.; Burkhardt, E.M.; Schumacher, W.; Rösch, P.; Küsel, K.; Popp, J. The influence of intracellular storage material on bacterial identification by means of Raman spectroscopy. *Anal. Bioanal. Chem.* **2010**, *397*, 2929–2937. [[CrossRef](#)]
60. Bird, L.J.; Bonnefoy, V.; Newman, D.K. Bioenergetic challenges of microbial iron metabolisms. *Trends Microbiol.* **2011**, *19*, 330–340. [[CrossRef](#)]
61. Magnuson, T.S.; Swenson, M.W.; Paszczyński, A.J.; Deobald, L.A.; Kerk, D.; Cummings, D.E. Proteogenomic and functional analysis of chromate reduction in *Acidiphilium cryptum* JF-5, an Fe(III)-respiring acidophile. *BioMetals* **2010**, *23*, 1129–1138. [[CrossRef](#)]
62. Mo, H.; Chen, Q.; Du, J.; Tang, L.; Qin, F.; Miao, B.; Wu, X.; Zeng, J. Ferric reductase activity of the ArsH protein from *Acidithiobacillus ferrooxidans*. *J. Microbiol. Biotechnol.* **2011**, *21*, 464–469. [[CrossRef](#)]
63. Johnson, D.B.; Hallberg, K.B. The microbiology of acidic mine waters. *Res. Microbiol.* **2003**, *154*, 466–473. [[CrossRef](#)]
64. Harrison, A.P.; Jarvis, B.W.; Johnson, J.L. Heterotrophic bacteria from cultures of autotrophic *Thiobacillus ferrooxidans*: Relationships as studied by means of deoxyribonucleic acid homology. *J. Bacteriol.* **1980**, *143*, 448–454. [[CrossRef](#)] [[PubMed](#)]

65. Harrison, A.P. The acidophilic *Thiobacilli* and other acidophilic bacteria that share their habitat. *Annu. Rev. Microbiol.* **1984**, *38*, 265–292. [[CrossRef](#)] [[PubMed](#)]
66. Johnson, D.B. Geomicrobiology of extremely acidic subsurface environments. *FEMS Microbiol. Ecol.* **2012**, *81*, 2–12. [[CrossRef](#)] [[PubMed](#)]
67. Hallberg, K.B.; Johnson, D.B. Biodiversity of acidophilic prokaryotes. *Adv. Appl. Microbiol.* **2001**, *49*, 37–84. [[PubMed](#)]
68. Lu, S.; Peiffer, S.; Lazar, C.S.; Oldham, C.; Neu, T.R.; Ciobota, V.; Náb, O.; Lillicrap, A.; Rösch, P.; Popp, J.; et al. Extremophile microbiomes in acidic and hypersaline river sediments of Western Australia. *Environ. Microbiol. Rep.* **2016**, *8*, 58–67. [[CrossRef](#)]
69. Miot, J.; Jézéquel, D.; Benzerara, K.; Cordier, L.; Rivas-Lamelo, S.; Skouri-Panet, F.; Féraud, C.; Poinso, M.; Duprat, E. Mineralogical diversity in Lake Pavin: Connections with water column chemistry and biomineralization processes. *Minerals* **2016**, *6*, 24. [[CrossRef](#)]
70. Peine, A.; Tritschler, A.; Küsel, K.; Peiffer, S. Electron flow in an iron-rich acidic sediment—Evidence for an acidity-driven iron cycle. *Limnol. Oceanogr.* **2000**, *45*, 1077–1087. [[CrossRef](#)]
71. Rivas, M.; Seeger, M.; Holmes, D.S.; Jedlicki, E. A Lux-like quorum sensing system in the extreme acidophile *Acidithiobacillus ferrooxidans*. *Biol. Res.* **2005**, *38*, 283–297. [[CrossRef](#)]
72. Stoodley, P.; Sauer, K.; Davies, D.G.; Costerton, J.W. Biofilms as complex differentiated communities. *Annu. Rev. Microbiol.* **2002**, *56*, 187–209. [[CrossRef](#)]
73. Zafra, O.; Lamprecht-Grandío, M.; de Figueras, C.G.; González-Pastor, J.E. Extracellular DNA release by undomesticated *Bacillus subtilis* is regulated by early competence. *PLoS ONE* **2012**, *7*. [[CrossRef](#)] [[PubMed](#)]
74. Tapia, J.M.; Muñoz, J.; González, F.; Blázquez, M.L.; Malki, M.; Ballester, A. Extraction of extracellular polymeric substances from the acidophilic bacterium *Acidiphilium* 3.2Sup(5). *Water Sci. Technol.* **2009**, *59*, 1959–1967. [[CrossRef](#)] [[PubMed](#)]
75. Kermer, R.; Hedrich, S.; Taubert, M.; Baumann, S.; Schlömann, M.; Johnson, D.B.; Seifert, J. Elucidation of carbon transfer in a mixed culture of *Acidiphilium cryptum* and *Acidithiobacillus ferrooxidans* using protein-based stable isotope probing. *J. Integr. OMICS* **2012**, *2*, 37–45.
76. Ullrich, S.R.; Poehlein, A.; Tischler, J.S.; González, C.; Ossandon, F.J.; Daniel, R.; Holmes, D.S.; Schlömann, M.; Mühling, M. Genome analysis of the biotechnologically relevant acidophilic iron oxidising strain JA12 indicates phylogenetic and metabolic diversity within the novel genus “*Ferroovum*”. *PLoS ONE* **2016**, *11*, e0146832. [[CrossRef](#)] [[PubMed](#)]
77. Nitschke, W.; Bonnefoy, V. Energy acquisition in low pH environments. In *Acidophiles: Life in Extremely Acidic Environments*; Quatrini, R., Johnson, D.B., Eds.; Caister Academic Press: Poole, UK, 2016; pp. 19–48.
78. Küsel, K.; Roth, U.; Drake, H.L. Microbial reduction of Fe(III) in the presence of oxygen under low pH conditions. *Environ. Microbiol.* **2002**, *4*, 414–421. [[CrossRef](#)]
79. Coupland, K.; Johnson, D.B. Evidence that the potential for dissimilatory ferric iron reduction is widespread among acidophilic heterotrophic bacteria. *FEMS Microbiol. Lett.* **2008**, *279*, 30–35. [[CrossRef](#)]
80. Johnson, D.B.; Kanao, T.; Hedrich, S. Redox transformations of iron at extremely low pH: Fundamental and applied aspects. *Front. Microbiol.* **2012**, *3*, 1–13. [[CrossRef](#)]
81. Juillan-Binard, C.; Picciocchi, A.; Andrieu, J.P.; Dupuy, J.; Petit-Hartlein, I.; Caux-Thang, C.; Vivès, C.; Nivière, V.; Fieschi, F. A two-component NADPH oxidase (NOX)-like system in bacteria is involved in the electron transfer chain to the methionine sulfoxide reductase MsrP. *J. Biol. Chem.* **2017**, *292*, 2485–2494. [[CrossRef](#)]
82. Osorio, H.; Mangold, S.; Denis, Y.; Ñancucheo, I.; Esparza, M.; Johnson, D.B.; Bonnefoy, V.; Dopson, M.; Holmes, D.S. Anaerobic sulfur metabolism coupled to dissimilatory iron reduction in the extremophile *Acidithiobacillus ferrooxidans*. *Appl. Environ. Microbiol.* **2013**, *79*, 2172–2181. [[CrossRef](#)]
83. Sugio, T.; Taha, T.M.; Takeuchi, F. Ferrous iron production mediated by tetrathionate hydrolase in tetrathionate-, sulfur-, and iron-grown *Acidithiobacillus ferrooxidans* ATCC 23270 cells. *Biosci. Biotechnol. Biochem.* **2009**, *73*, 1381–1386. [[CrossRef](#)]



5. General Discussion

Iron-rich pelagic aggregates formed from the collision and sticking together of particles function similarly to marine, lake, river snow as carriers bringing inorganic matter, organic carbon, and living microorganisms from the water column to the lake sediment (Reiche *et al.*, 2011). Its inhabiting environment (acidic ferruginous lakes) results in unique features of iron snow compared to marine/snow aggregates and Fe(III) mineral-cell aggregates in other ferruginous lakes. The low microbial complexity (Fe-cycling bacteria, ~ 60% of the total microbial community) enabled us to isolate the representative isolates and sequence their genomes. Pangenome analyses allowed us to expansively describe the metabolic potentials of each group. Nevertheless, for *Ferrovum*, there are reported difficulties related to the isolation and conservation, including contamination, high sensitivity to organic compounds released from the agar plates, and bacterial loss (Ullrich, Poehlein, *et al.*, 2016). Although the metatranscriptome approach enabled us to record expressed transcripts within a microbiome, including the uncultivated members, the high fraction of Fe makes it very challenging to extract enough RNA for sequencing. These and various challenges were addressed to integrate multiple omics data sets. Thus, this dissertation highlights the unique features distinguishing iron snow from marine/lake snow and Fe(III) mineral-cell aggregates in ferruginous lakes. Furthermore, the interaction features between FeOB and FeRB colonizing iron snow provide additional insights into the microbially-mediated driving forces behind aggregates formation and stabilization in iron snow.

Hypothesis I Chemolithoautotrophy is the driving factor for building biomass.

5.1 Bacterial, Eukaryotic and Archaeal diversity in iron snow

Metatranscriptome taxonomic profiles of *in-situ* iron snow microbiome revealed the dominance of FeOB (Nitrospirae, β -Proteobacteria, Actinobacteria) and FeRB (α -Proteobacteria) within the community (**Chapter 3; Figure 6**). The Fe-cycling microbes found in iron snow are similar to the previously characterized AMD and pit lake microbial communities (Santofimia *et al.*, 2013; Bomberg *et al.*, 2019). Additionally, eukaryotes and archaea were also detected in iron snow. In contrast to relatively high eukaryotic species richness in the Iron Mountain AMD and the Tinto River (Amaral-Zettler *et al.*, 2002; Baker *et al.*, 2009), the eukaryotic community biodiversity in iron snow was low and *Stramenopiles*, *Holozoa* accounted for 88.6-93.2% of the total eukaryotic community (**Chapter 3**). *Stramenopiles*, *Holozoa* were also detected in other AMD systems (Amaral-Zettler, 2013; Méndez-García *et al.*, 2015). The archaeal abundance was extremely low (rRNA rate, 0.10-0.12%), and the majority of rRNA sequences were assigned to *Euryarchaeota* (data not shown).

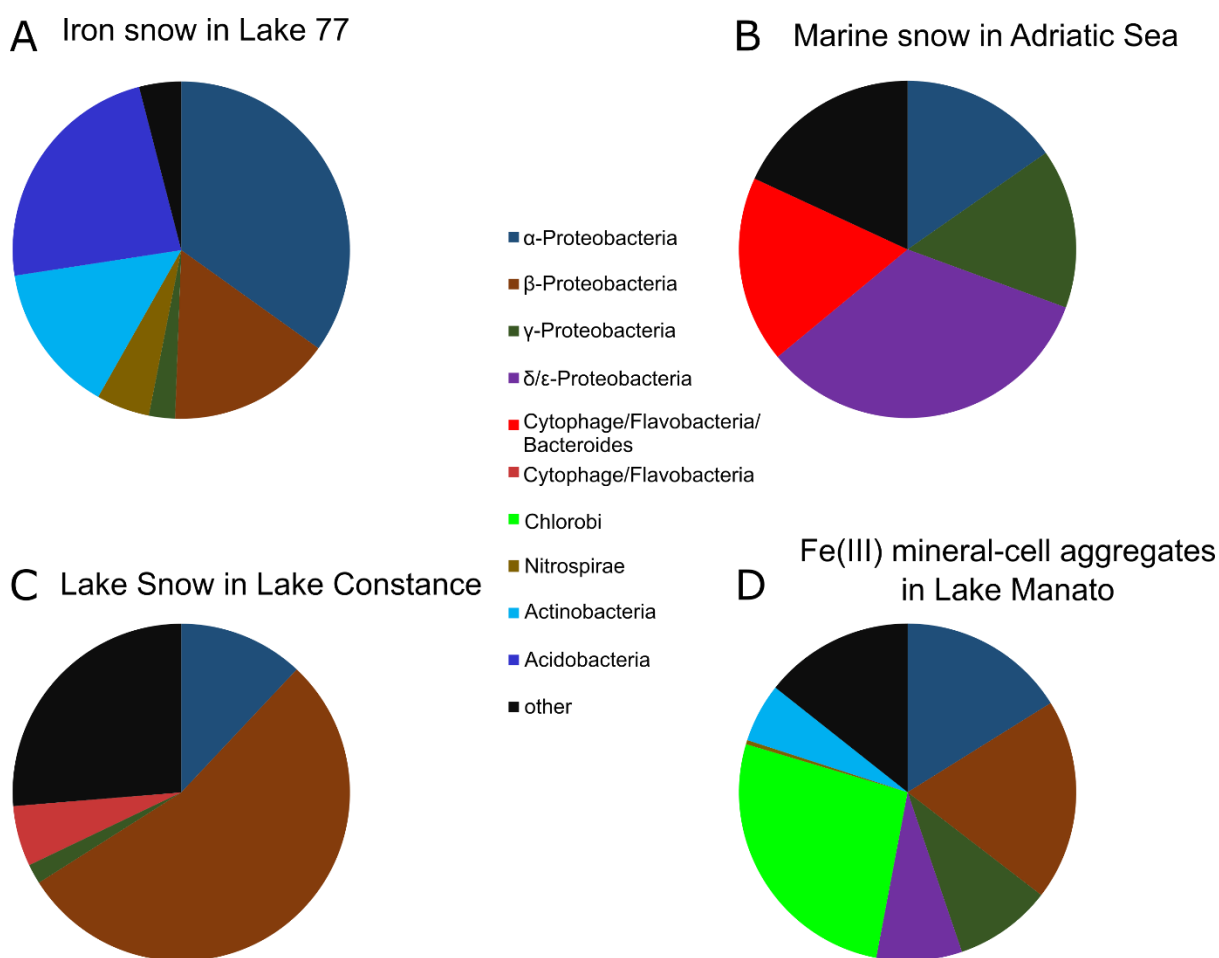


Figure 6. Bacterial community profile at phylum level in iron snow, marine snow, lake snow, and Fe(III) mineral-cell aggregates in ferruginous lakes.

(A) Relative abundances of iron snow samples collected at 5-6 m depth below redoxcline in 2018 based on 16S rRNA gene sequencing. (B) The relative percentages of bacterial 16S rRNA clones in marine snow at 13 m depth in 1991. (C) The mean proportions of bacterial groups detected by fluorescence in situ hybridization (FISH) with 16S rRNA-targeted oligonucleotide probes on lake snow at 50 m depth below redoxcline in 1995. (D) The percentage of metagenome reads mapped to bacterial 5S, 16S, and 23S rRNA genes from lake water at 117.5 m depth in 2010.

5.1.1 Bacterial classification in iron snow differs from that in marine/lake snow

The dominance of Fe-cycling bacteria is consistent with qPCR-based taxonomic analysis (Lu *et al.*, 2013). These Fe-cycling bacteria in iron snow are quite different from bacterial colonizers of marine snow or lake snow which are Bacteroidetes phylum, including the (*Cytophaga* and *Flavobacteria* genera cluster), and the members of

Proteobacteria phylum, most of which are α -, β -, γ -proteobacteria. These microbes are involved in the production of polysaccharides e.g., bacterioplankton (Stoderegger and Herndl, 1998, 1999; Reichenbach, 2006), hydrolysis of organic carbon e.g., *Alteromonas*, *Methylophaga* (Grossart and Ploug, 2001; Fontanez *et al.*, 2015), production of chemical signals e.g., *Roseobacter* (Gram *et al.*, 2002) and motility (Mitchell *et al.*, 1995; Dash *et al.*, 2012).

5.1.2 Bacterial classification in iron snow differs from that in Fe(III) mineral-cell aggregates in ferruginous lakes

Acidophilic Fe-cycling microbes inhabiting iron snow are also different from neutrophilic microbes in Fe(III) mineral-cell aggregates below redoxclines in different ferruginous lakes. In Lake Palvin, sulfur cycling microbes as well as FeOB (*Gallionella*), FeRB (*Geothrix*, *Geobacter*, *Rhodoferrax*) promoted the sulfur and iron cycling at lower depths of the lake, and Fe-phosphates precipitated within the water column profile in the particulate matter (Lehours *et al.*, 2007, 2010; Miot *et al.*, 2016; Berg *et al.*, 2019). In Lake Matano, Lake La Cruz, Kabuno Bay of Lake Kivu, anoxygenic phototrophic sulfur bacteria, anoxygenic photoferrotrophic bacteria (e.g., *Chlorobium ferrooxidans*), Fe(III) reducer (e.g., *Rhodoferrax*) were responsible for the cycling of iron, sulfur, and carbon as well as the formation of mineral particles with abundant Fe below the chemocline (Crowe, Jones, *et al.*, 2008; Crowe *et al.*, 2014; Lliros *et al.*, 2015; Morana *et al.*, 2016; Camacho *et al.*, 2017). Unlike dominant phototrophs in other ferruginous lakes, *Rhodospila* was the only phototrophy detected in the metatranscriptome sequences, and its relative abundance (0.25%-0.59%) was 77-323 times lower than that of chemolithoautotrophs (45.1%-83.2%). The low relative abundance of phototrophs is due to the high amount of iron snow, limiting light penetration in lake 77 (Lu, 2012).

5.2 Chemolithoautotrophic CO₂ fixation in iron snow

The dominant Fe-cycling groups showed the highest transcriptional activity for functions linked to CO₂ fixation, polysaccharide biosynthesis and degradation, and motility (**Chapter 3**). *Leptospirillum* and *Ferrovum*, represented the genera with the highest numbers of mRNA sequences linked to CO₂ fixation pathways (CBB cycle and rTCA cycle) as well as polysaccharide biosynthesis (**Chapter 3**). The dominant chemolithoautotrophic FeOB *Leptospirillum*, *Ferrovum* oxidize Fe(II) coupling with carbon and nitrogen fixation. Additional genome analysis of iron snow key isolates showed the presence of complete genes involved in the CBB cycle in *Acidithrix* and heterophilic *Acidiphilium*, *Acidocella* genome possessed genes (a pyruvate carboxylase (*pyc*) and a pyruvate orthophosphate dikinase (*ppdk*)) for anaplerotic CO₂ fixation (**Chapter 2**). 31-388 times lower mRNA sequences associated with eukaryotes than the mRNA sequences corresponding to bacteria as well as the absence of critical genes involved in CO₂ fixation pathways in eukaryotes suggest eukaryotes are unlikely to be involved in phototrophic CO₂ fixation in iron snow. Further protein-based ¹³C quantification confirmed that chemoautotrophic FeOB *Leptospirillum* and *Ferrovum* were responsible for ¹³CO₂ fixation (**Chapter 3; Figure 7**). Collectively, genomic, metatranscriptomic, protein-SIP findings confirm that chemolithoautotrophic CO₂ fixation is the primary production in iron snow.

5. General Discussion

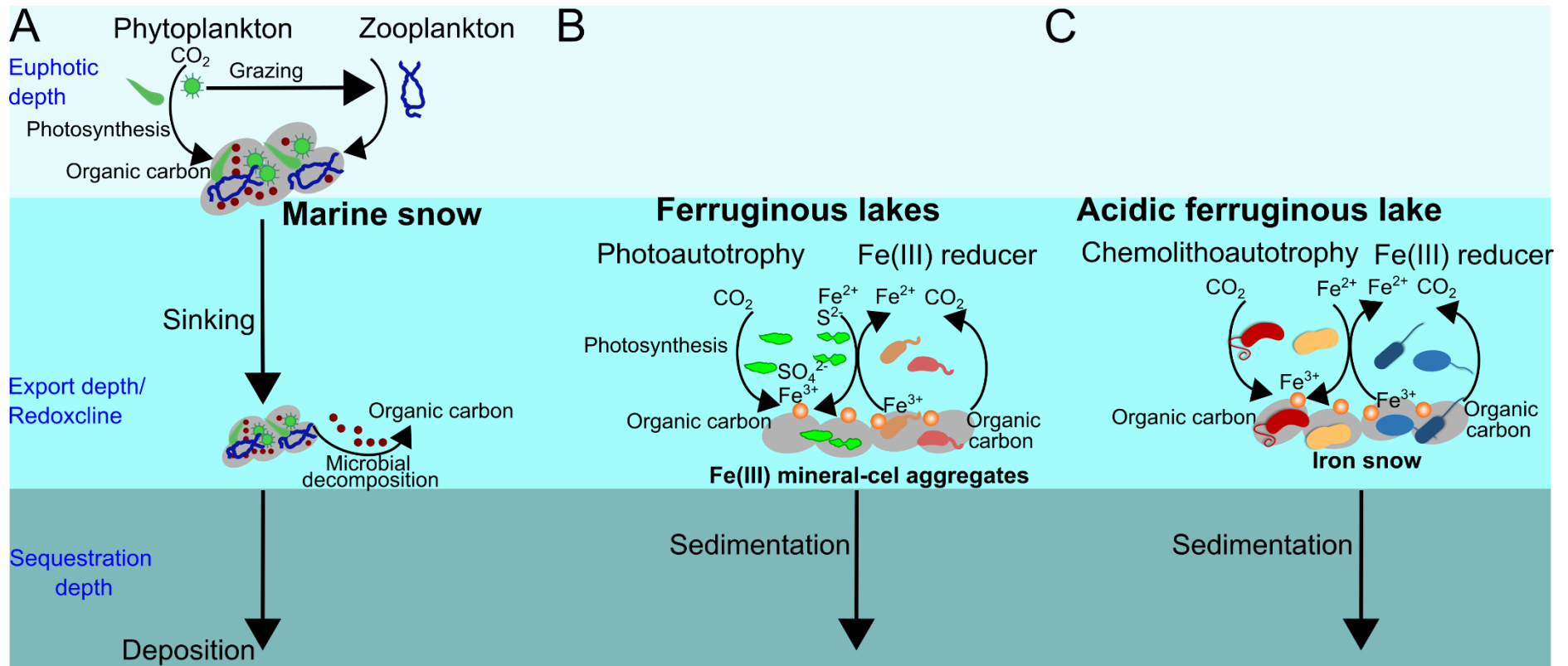


Figure 7. Schematic diagram illustrating different biological CO₂ fixation in marine snow, Fe(III) mineral-cell aggregates, iron snow.

(A) Dissolved inorganic carbon is transformed into organic biomass by phytoplankton through photosynthesis in the euphotic zone, and a fraction of it is pumped to the deep ocean, either in the particulate or dissolved phase. (B) CO₂ fixation by photoautotrophic bacteria couples microbial oxidation of Fe²⁺ or S²⁻. FeRB couple Fe³⁺ reduction to Fe²⁺ with the oxidation of organic carbon. (C) Chemolithoautotrophic FeOB couple CO₂ fixation with microbial oxidation of Fe²⁺ while FeRB reduce Fe³⁺ / O₂ using organic carbon as an electron donor.

5.2.1 Chemolithoautotrophic CO₂ fixation in iron snow is different from the photoautotrophic CO₂ fixation in marine/lake snow

The organic carbon content in iron snow is below 11%, while organic carbon constitutes 10 to 40% of the marine snow dry weight and up to 66% in lake snow (Simon *et al.*, 2002; Reiche *et al.*, 2011; Tang *et al.*, 2012). Phytoplankton are responsible for the light-driven primary production in marine/lake snow, and they contribute more than 50% of overall primary production in marine snow or lake snow (Simon *et al.*, 1990; Kaltenbock and Herndl, 1992; Grossart *et al.*, 1997). The lower organic carbon of iron snow suggests the lower fixed carbon amount by chemolithoautotrophs than the photoautotrophic fixed carbon in marine/lake snow. These aquatic particles composing organic carbon generally contribute to the sedimentary organic carbon pool in aquatic systems (de Vicente *et al.*, 2009). The higher velocity of iron snow than marine/lake snow in neutral aquatic systems compensates for the low organic carbon content contributing to the sedimentary organic carbon pool in acidic ferruginous lake 77 (Reiche *et al.*, 2011).

5.2.2 Chemolithoautotrophic CO₂ fixation in iron snow is different from photoautotrophic CO₂ fixation in Fe(III) mineral-cell aggregates in ferruginous lakes

Ferruginous lakes host a large community of anoxygenic phototrophic bacteria below the chemocline. They oxidize sulfide or Fe(II) as an electron donor to harness energy from sunlight and drive anoxygenic phototrophic CO₂ fixation into biomass. Due to phosphorus limitation, primary production limitation in the oxic layers enables light penetration down to a depth where oxygen is already absent (Crowe, O'Neill, *et al.*, 2008; Zegeye *et al.*, 2012; Camacho *et al.*, 2017). The organic carbon sedimentation rate of the phototrophic primary is 10.56–15.6 mg C m⁻² d⁻¹ in lake Matano, which is

10-40 times lower than C sedimentation rates (121-600 mg C m⁻² d⁻¹) estimated in Lake 77 (Reiche *et al.*, 2011; Crowe *et al.*, 2011).

Hypothesis II Organic carbon derived from the chemolithoautotrophic CO₂ fixation in FeOB acts as a carbon source for FeRB.

5.3 Carbon flow from autotrophic FeOB to heterotrophic FeRB in iron snow

Protein-based ¹³C quantification suggested that *Acidiphilium*, *Acidocella* slowly took in a small amount of the converted ¹³C-carbon under oxic conditions, but no detectable metabolic activity was in the remaining bacterial community under anoxic conditions within the time frame investigated (**Chapter 3; Figure 8**). Fe-cycling key players, e.g., *Ferrovum*, *Acidiphilium*, *Acidocella* in oxic and anoxic iron snow microcosms, have been found in iron snow at/below redoxcline and the lake sediments (Lu *et al.*, 2010). Thus, under oxic and anoxic conditions, the iron snow microbiome behaves similarly to in-situ iron snow microbiome sinking from oxic mixolimnion to anoxic hypolimnion in lake 77. *Leptospirillum* drives CO₂ fixation via the rTCA cycle, while *Ferrovum* performs CO₂ fixation via the CBB cycle. The fixed organic carbon can be converted to polysaccharides for EPS production. In agreement, 24.9%-75.2% of the EPS production mRNA sequences were assigned to *Leptospirillum*, *Ferrovum* (**Chapter 3**). Heterotrophic bacteria prefer iron snow with rich organic carbon, e.g., EPS at higher concentrations than the surrounding water in the lake. Of mRNA sequences linked to polysaccharide breakdown, 2.9%-7.5% were assigned to heterotrophic *Acidiphilium*. In addition, genes encoding polysaccharide breakdown enzymes (e.g., glycoside hydrolase, alpha-amylase) were present in all *Acidiphilium* spp. based on the pangenome analysis (**Chapter 4**). It suggests that *Acidiphilium* and *Acidocella* are dependent on derived organic carbon, e.g., EPS from *Leptospirillum* and *Ferrovum* (**Chapter 3**).

5. General Discussion

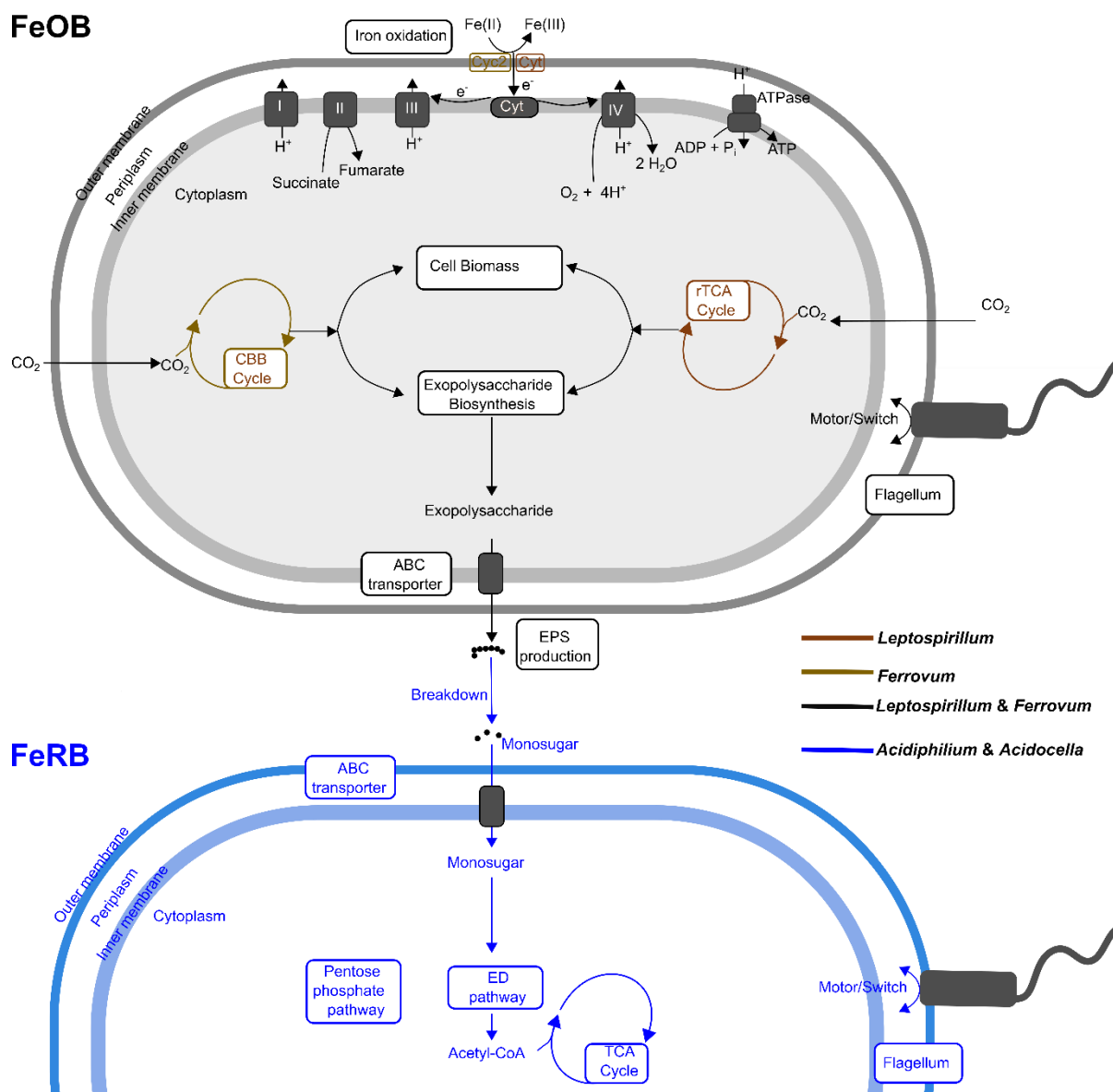


Figure 8. Schematic diagram showing carbon flow between FeOB (*Leptospirillum*, *Ferrofum*) and FeRB (*Acidiphilium*, *Acidocella*) in iron snow.

Metabolic traits only present in *Leptospirillum* or *Ferrofum* are shown in dark brown or golden, while traits shared by *Leptospirillum*/*Ferrofum* or *Acidiphilium*/*Acidocella* are colored in Black or Blue.

This type of interspecies carbon transfer has been previously described for acidophilic mixed cultures of *Acidiphilium cryptum* and *Acidithiobacillus ferrooxidans* (Kermer *et al.*, 2012). These heterotrophic Fe(III)-reducing members are often isolated as contaminants from FeOB mixed cultures, e.g., *Acidithiobacillus ferrooxidans* (Harrison *et al.*, 1980; Harrison, 1984), *Ferrofum* sp. JA12 (Kipry *et al.*, 2013; Ullrich, 2016).

Acidiphilium and *Acidocella* degrade EPS as electron donors and Fe(III) as electron acceptors for their growth, facilitating the growth of autotrophic FeOB (Méndez-García *et al.*, 2015; Ullrich *et al.*, 2015). The carbon flow from autotrophs to heterotrophs is similar to that in marine snow. Phytoplankton fix CO₂ to produce organic carbon. Heterotrophic bacteria colonizing marine snow exhibit a higher extracellular enzymatic hydrolysis rate than free-living bacteria to metabolize organic compounds (polysaccharides, di and monosaccharides, organic acids) (Grossart and Simon, 1998a; Simon *et al.*, 2002; Berkenheger *et al.*, 2003). The long residence time of marine snow enables the attenuation of carbon flux to the deep sea (Turner, 2015). Despite the low chemolithoautotrophic primary production in iron snow compared to phototrophic primary production in marine snow, the shorter residence time due to higher velocity, and the small amount of organic carbon from FeOB to FeRB in iron snow enhanced contribution to the sedimentary organic carbon pool from the surface to the anoxic sediments in acidic lakes.

Collectively, the first two hypotheses of this thesis are confirmed: “Chemolithoautotrophic FeOB fix CO₂, and the fixed organic carbon not only flows to FeRB but also is converted to EPS to stabilize iron snow”. Dissimilar to oceans and lakes, iron snow sinks quickly through the water column as an efficient carbon pump in the acidic Fe-rich ferruginous lakes.

Hypothesis III The secondary metabolite, 2-phenethylamine (PEA), produced by *Acidithrix* sp. C25, targets the Fe(III)-reducing members to induce aggregation.

Similar to marine snow-associated bacteria, which produce acylated homoserine lactones (AHLs) to trigger the community behavior by quorum sensing (QS), we mapped 0.005% of mRNA sequences to autoinducer-1 synthesis and receptor genes linked to QS (**Chapter 3**). This suggests that chemical communication appears to be at play in iron snow. ^{13}C quantification showed that *Acidithrix* did not fix CO_2 , nor did it derive organic carbon from *Ferrovum* or *Leptospirillum* in oxic and anoxic microcosms (**Chapter 3**). This suggests that heterotrophic *Acidithrix* functions differently from chemolithoautotrophic FeOB to interact with FeRB. Indeed, screening the exchanged supernatant of *Acidithrix* sp. C25 (FeOB) & *Acidiphilium* sp. C61 (FeRB) identified the secondary metabolite (PEA), which induced faster growth and triggered aggregates formation of *Acidiphilium* sp. C61 (Mori *et al.*, 2017). The absence of genes involved in PEA production and autoinducer receptor in *Acidiphilium* sp. C61 suggests that QS is unlikely to occur between *Acidithrix* and *Acidiphilium*. Screening the genome of *Acidithrix* sp. C25 identified genes encoding amino acid decarboxylase for PEA production (**Chapter 2**). In agreement, *Acidithrix* was also one of the top 5 bacteria with the most mRNA sequences linked to the above decarboxylase (**Chapter 3**). The produced PEA can be secreted by precursor/product exchangers or passive diffusion in bacteria (Konings *et al.*, 1994; Lolkema *et al.*, 1996; Marcobal *et al.*, 2012).

5.4 Genomic insights into aggregation in *Acidithrix* sp. C25, *Acidiphilium* sp. C61, *Acidocella* sp. C78

Comparative metabolomics identified PEA in the supernatant exchange experiment between *Acidithrix* and *Acidocella* (data not shown). However, the amendment of either *Acidithrix* supernatant (data not shown) or 10/50 μM exogenous PEA (**Chapter**

4) to *Acidocella* sp. C78 culture did not trigger the aggregate formation of *Acidocella* sp. C78. *Acidiphilium* sp. C61, on the other hand, formed aggregates not only in the presence of PEA (**Chapter 4**), but also in the co-culture of *Acidithrix* and *Acidiphilium*. 98% and 93% of genes in *Acidiphilium* sp. C61 and *Acidithrix* sp. C25, respectively, were not differentially expressed in co-culture vs. pure culture (data not shown), presumably due to no significant growth of *Acidiphilium*. It should be noted that *Acidiphilium* grew faster than *Acidithrix*, and the co-cultivation was carried out after two days of pre-incubation of *Acidithrix*. This result would support the high sensitivity of *Acidiphilium* at low cell numbers responding to PEA.

The cell aggregation effect induced by PEA is specialized in all tested *Acidiphilium* strains, but not *Acidocella* sp. C78 (**Chapter 4**). Therefore, genomes were examined to reveal their morphological differences. The same flagellar assembly pathway and the absence of *flhDC* in *Acidiphilium* and *Acidocella* (**Chapter 2**), imply that the PEA-triggered cell aggregation of *Acidiphilium* is induced by regulations of other physiological pathways rather than flagellar motility. This is despite the fact that PEA has been previously reported to block cell motility by inhibiting the assembly or activity of *flhDC*, a key regulator of flagellin in lateral flagellum systems in *Proteus mirabilis* (Stevenson and Rather, 2006; Stevenson *et al.*, 2013). Comparative genome analysis showed that shared genes accounted for 99.8%, 89.4% of total genes in *Acidocella* sp. C78 and *Acidiphilium* sp. C61 genome respectively (data not shown). Among the five unique genes in *Acidocella* sp. C78, four genes were uncharacterized, and one gene encoded dehydratase. Among the 377 unique genes in *Acidiphilium* sp. C61, 26.5% of unique genes with inconsistent expression patterns were differentially expressed in *Acidiphilium* sp. C61 after the addition of PEA (data not shown).

5.5 Transcriptomic insights into genes linked to aggregation mechanisms (autoaggregation, biofilm, and motility) in *Acidiphilium* sp. C61

Here, we focus on characterizing the expression patterns of genes involved in general aggregation mechanisms. The overall expression pattern of autoaggregation and biofilm, motility-related genes were inconsistent (**Chapter 4**). Motility still seems to be essential for *Acidiphilium* sp. C61, as genes involved in flagella biosynthesis, were even slightly upregulated. In agreement, metatranscriptome data of *in-situ* iron snow and metaproteome data of iron snow microcosms detected many flagellin domain transcripts and proteins from *Acidiphilium* (**Chapter 3**). This might help *Acidiphilium* sp. C61 join FeOB *Acidithrix* sp. C25, which contributed to the aggregates growth. However, the majority of genes (55%) for autotransporter and biofilm formation in *Acidiphilium* sp. C61 remained unchanged, although PEA was found to strongly inhibit biofilm formation in *E. coli* (Irsfeld *et al.*, 2013; Lynnes *et al.*, 2014). It suggests that *Acidiphilium* sp. C61 may prefer to aggregate over forming biofilms.

5.6 Potential unexamined aggregation mechanisms in *Acidiphilium* sp. C61

Higher concentrations of PEA resulted in increased numbers of aggregates formed (**Chapter 4**). PEA can diffuse into the cell without the transporter, similar to brain cells (Crupi *et al.*, 2016). Unlike AHLs, attractor or repellent molecules induce chemokinetic swimming behavior of bacteria toward the aggregates (Kjørboe and Jackson, 2001; Laganenka *et al.*, 2016). PEA can be utilized as a carbon or nitrogen source (Scarlett and Turner, 1976; Paterson *et al.*, 1990). However, qPCR showed that PEA did not promote bacterial growth as two mM glucose was added to the cultures of *Acidiphilium* sp. C61. Comparative transcriptomics showed that PEA stimulated the central metabolism, e.g., protein biosynthesis (**Chapter 4**). Likely, unknown synthesized protein, similar to the M protein found in *Streptococcus canis* (Nerlich *et al.*, 2019),

may occur (**Figure 9**). These proteins are known to exhibit homophilic protein interactions with self-binding activity via the N-terminal to facilitate bacterial aggregation (Nerlich *et al.*, 2019). Since higher concentrations of PEA led to more significant aggregates (**Chapter 4**), this suggests that *Acidiphilium* moves directionally towards PEA signals. Thus, different PEA concentrations gradient across the bacteria may function like polymer concentrations gradient which generates an osmotic pressure that physically holds aggregates together (Secor *et al.*, 2018).

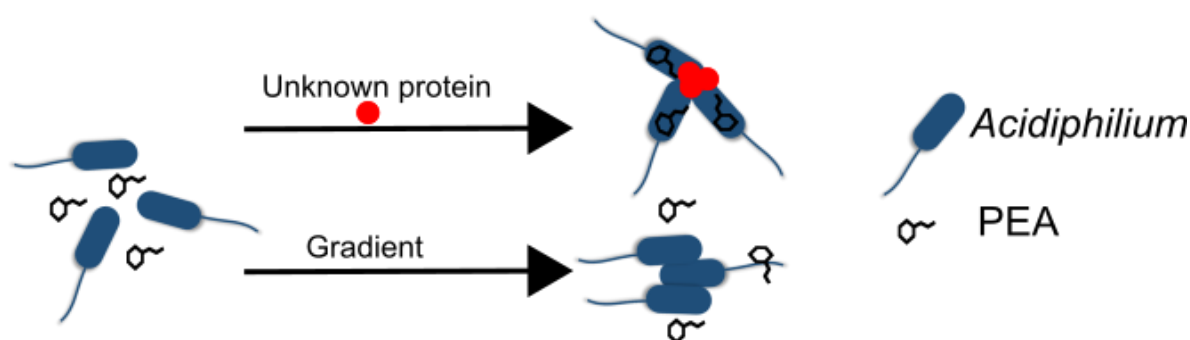


Figure 9. Conceptual illustration of aggregation mechanisms in *Acidiphilium* sp. C61.

The unknown protein interactions may facilitate bacterial aggregation. Additionally, the difference in PEA concentration across the cell generates an osmotic pressure that physically holds aggregates together.

The third hypothesis III, “The secondary metabolite, 2-phenethylamine (PEA), produced by Acidithrix sp. C25, targets the Fe(III)-reducing members to induce aggregation” is confirmed. PEA produced by Acidithrix has a specific aggregation effect on Acidiphilium, but not Acidocella, despite the high similarity of their genomes. Inconsistent gene expression patterns relating to the aggregation mechanisms suggest PEA functions as an infochemical regulating other cellular mechanisms, not aggregation mechanisms directly. This specific aggregation of PEA on the most dominant FeRB Acidiphilium can enhance primary iron snow formation.

5.7 Conclusion

Iron snow resembles marine/lake snow regarding carbon pump and chemical communication. This dissertation applied multi-omics approaches combined with experimental approaches to illustrate the functions and interactions of the key co-occurring Fe-cycling players (**Figure 10**). The specific aggregation of metabolite produced by FeOB (*Acidithrix*) on co-colonizing FeRB (*Acidiphilium*) contributes to initiating the aggregation of a particular iron snow bacterial community. Chemolithoautotrophically fixed carbon by FeOB (*Ferrovum*) subsequently flows to FeRB (*Acidiphilium*) as their energy sources or is converted to EPS to stabilize iron snow. These findings differentiate iron snow from well-known marine/lake snow and other Fe(III) mineral-cell aggregates in ferruginous lakes regarding the contribution of photosynthetic CO₂ fixation to the overall pool of fixed CO₂ found in these environments. Thus, two forces of microbial interactions were characterized to contribute to iron snow formation and stability between dominant FeOB and FeRB: bring together (PEA) and stuck together (organic carbon form, e.g., EPS) in this thesis.

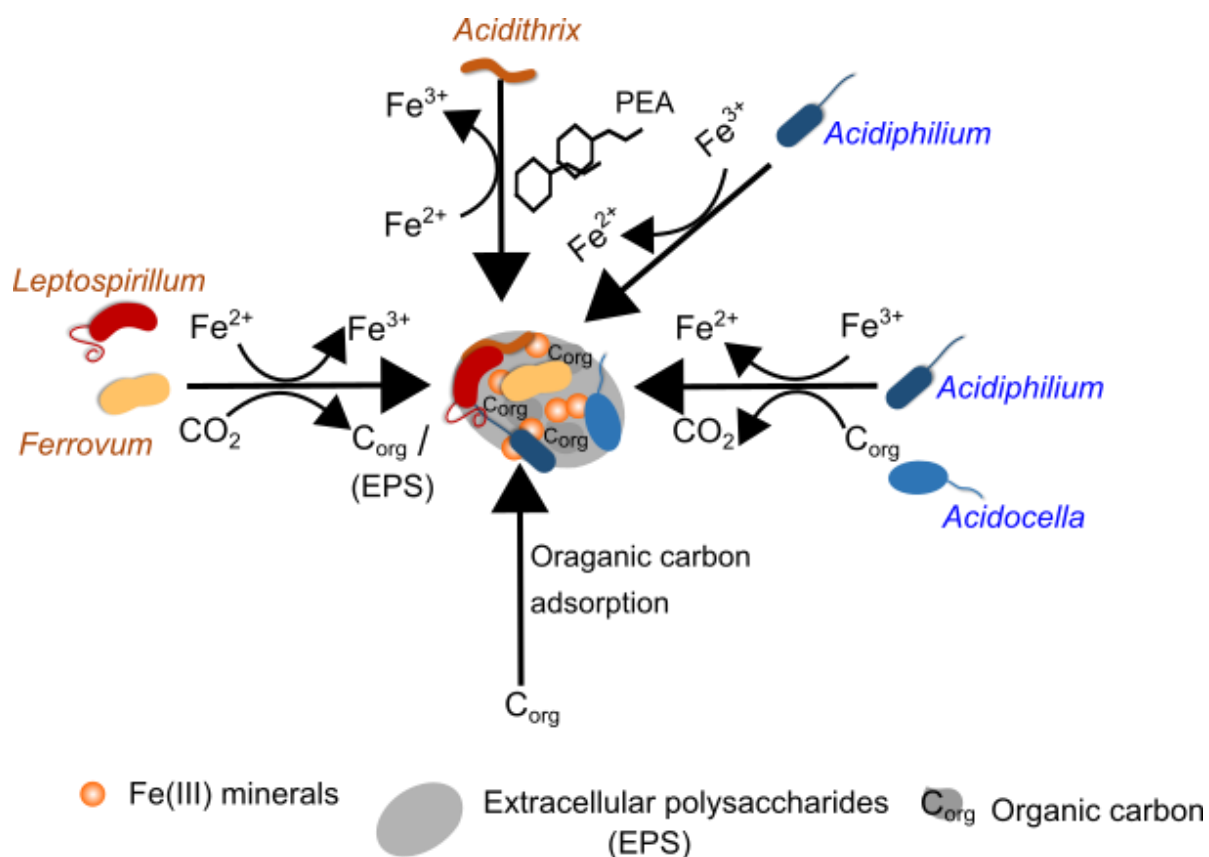


Figure 10. Schematic interaction model mediated by a chemical mediator and carbon flow between FeOB and FeRB in iron snow.

Iron snow is primarily formed by Fe(II) oxidation by FeOB *Acidithrix*. *Acidithrix* excretes PEA, which induces specific colonization of free-living *Acidiphilium*. *Leptospirillum*, *Ferrovum* fix CO₂ to produce organic carbon (e.g., EPS), of which a small amount of the fixed carbon serves as the carbon source for heterotrophic FeRB (*Acidiphilium*, *Acidocella*) colonization. The majority of fixed carbon favors the cohesiveness and additional growth of these pelagic aggregates

References

- Acosta, M., Galleguillos, P., Ghorbani, Y., Tapia, P., Contador, Y., Velásquez, A., et al. (2014) Variation in microbial community from predominantly mesophilic to thermotolerant and moderately thermophilic species in an industrial copper heap bioleaching operation. *Hydrometallurgy* **150**: 281–289.
- Alavi, M. and Belas, R. (2001) Surface sensing, swarmer cell differentiation, and biofilm development. *Methods in Enzymology* **336**: 29–40.
- Allredge, A.L., Cole, J.J., and Caron, D.A. (1986) Production of heterotrophic bacteria inhabiting macroscopic organic aggregates (marine snow) from surface waters. *Limnology and Oceanography* **31**: 68–78.
- Allredge, A.L. and Gotschalk, C.C. (1990) The relative contribution of marine snow of different origins to biological processes in coastal waters. *Continental Shelf Research* **10**: 41–58.
- Allredge, A.L. and Silver, M.W. (1988) Characteristics, dynamics and significance of marine snow. *Progress in Oceanography* **20**: 41–82.
- Altermann, E. (2014) Invited commentary: lubricating the rusty wheel, new insights into iron oxidizing bacteria through comparative genomics. *Frontiers in Microbiology* **5**: 1–4.
- Altschul, S.F., Gish, W., Miller, W., Myers, E.W., and Lipman, D.J. (1990) Basic local alignment search tool. *Journal of Molecular Biology* **215**: 403–410.
- Amaral-Zettler, L.A. (2013) Eukaryotic diversity at pH extremes. *Frontiers in Microbiology* **3**: 1–17.
- Amaral-Zettler, L.A., Gómez, F., Zettler, E., Keenan, B.G., Amils, R., and Sogin, M.L. (2002) Eukaryotic diversity in Spain's River of Fire. *Nature* **417**: 137–137.
- Amir, A., McDonald, D., Navas-Molina, J.A., Kopylova, E., Morton, J.T., Zech Xu, Z., et al. (2017) Deblur Rapidly Resolves Single-Nucleotide Community Sequence Patterns. *mSystems* **2**: 1–7.
- Aramaki, T., Blanc-Mathieu, R., Endo, H., Ohkubo, K., Kanehisa, M., Goto, S., and Ogata, H. (2020) KofamKOALA: KEGG Ortholog assignment based on profile HMM and adaptive score threshold. *Bioinformatics* **36**: 2251–2252.
- Argasinska, J., Quinones-Olvera, N., Nawrocki, E.P., Finn, R.D., Bateman, A., Eddy, S.R., et al. (2017) Rfam 13.0: shifting to a genome-centric resource for non-coding RNA families. *Nucleic Acids Research* **46**: 335–D342.
- Aziz, R.K., Bartels, D., Best, A.A., DeJongh, M., Disz, T., Edwards, R.A., et al. (2008) The RAST Server: Rapid Annotations using Subsystems Technology. *BMC Genomics* **9**: 75–89.
- Baker, B.J. and Banfield, J.F. (2003) Microbial communities in acid mine drainage. *FEMS Microbiology Ecology* **44**: 139–152.
- Baker, B.J., Tyson, G.W., Goosherst, L., and Banfield, J.F. (2009) Insights into the diversity of eukaryotes in acid mine drainage biofilm communities. *Applied and Environmental Microbiology* **75**: 2192–2199.

References

- Banks, D., Younger, P.L., Arnesen, R.T., Iversen, E.R., and Banks, S.B. (1997) Mine-water chemistry: The good, the bad and the ugly. *Environmental Geology* **32**: 157–174.
- Bastida, F., Rosell, M., Franchini, A.G., Seifert, J., Finsterbusch, S., Jehmlich, N., et al. (2010) Elucidating MTBE degradation in a mixed consortium using a multidisciplinary approach. *FEMS Microbiology Ecology* **73**: 370–384.
- Bateman, A. (2019). UniProt: A worldwide hub of protein knowledge. *Nucleic Acids Res*, **47**: 506–515.
- Belas, R. and Suvanasuthi, R. (2005) The ability of *Proteus mirabilis* to sense surfaces and regulate virulence gene expression involves FliL, a flagellar basal body protein. *Journal of Bacteriology* **187**: 6789–6803.
- Benedict, M.N., Henriksen, J.R., Metcalf, W.W., Whitaker, R.J., and Price, N.D. (2014) ITEP: An integrated toolkit for exploration of microbial pan-genomes. *BMC Genomics* **15**: 8.
- Berg, J.S., Jézéquel, D., Duverger, A., Lamy, D., Laberty-Robert, C., and Miot, J. (2019) Microbial diversity involved in iron and cryptic sulfur cycling in the ferruginous, low-sulfate waters of Lake Pavin. *PLoS ONE* **14**: e0212787.
- Berg, J.S., Michellod, D., Pjevac, P., Martinez-Perez, C., Buckner, C.R.T., Hach, P.F., et al. (2016) Intensive cryptic microbial iron cycling in the low iron water column of the meromictic Lake Cadagno. *Environmental Microbiology* **18**: 5288–5302.
- Berkenheger, I., Heuchert, A., de Silva, S., and Fischer, U. (2003) Heterotrophic Particle-Associated Bacteria from the South Atlantic: A Community of Marine Microorganisms with a High Organic Carbon Degradation Potential. In *The South Atlantic in the Late Quaternary*. Berlin, Heidelberg: Springer Berlin Heidelberg, pp. 65–79.
- Bigham, J.M., Schwertmann, U., Traina, S.J., Winland, R.L., and Wolf, M. (1996) Schwertmannite and the chemical modeling of iron in acid sulfate waters. *Geochimica et Cosmochimica Acta* **60**: 2111–2121.
- Bird, L.J., Bonnefoy, V., and Newman, D.K. (2011) Bioenergetic challenges of microbial iron metabolisms. *Trends in Microbiology* **19**: 330–340.
- Blodau, C. (2006) A review of acidity generation and consumption in acidic coal mine lakes and their watersheds. *Science of the Total Environment* **369**: 307–332.
- Böckelmann, U. (2000) Characterization of the microbial community of lotic organic aggregates ('river snow') in the Elbe River of Germany by cultivation and molecular methods. *FEMS Microbiology Ecology* **33**: 157–170.
- Bohrer, B., Dietz, S., Von Rohden, C., Kiwel, U., Jöhnk, K.D., Naujoks, S., et al. (2009) Double-diffusive deep water circulation in an iron-meromictic lake. *Geochemistry, Geophysics, Geosystems* **10**: 1-7.
- Bohrer, B. and Schultze, M. (2008) Stratification of lakes. *Reviews of Geophysics* **46**: 1–27.
- Bolyen, E., Rideout, J.R., Dillon, M.R., Bokulich, N.A., Abnet, C.C., Al-Ghalith, G.A., et al. (2019) Reproducible, interactive, scalable and extensible microbiome data science using QIIME 2. *Nature Biotechnology* **37**: 852–857.
- Bomberg, M., Mäkinen, J., Salo, M., and Kinnunen, P. (2019) High Diversity in Iron

References

- Cycling Microbial Communities in Acidic, Iron-Rich Water of the Pyhäsalmi Mine, Finland. *Geofluids* **2019**: 1–17.
- Boyd, P.W. and Ellwood, M.J. (2010) The biogeochemical cycle of iron in the ocean. *Nature Geoscience* **3**: 675–682.
- Bridge, T.A.M. and Johnson, D.B. (2000) Reductive Dissolution of Ferric Iron Minerals by *Acidiphilium* S.J.H. *Geomicrobiology Journal* **17**: 193–206.
- Brown, J.F., Jones, D.S., Mills, D.B., Macalady, J.L., and Burgos, W.D. (2011) Application of a Depositional Facies Model to an Acid Mine Drainage Site. *Applied and Environmental Microbiology* **77**: 545–554.
- Buchfink, B., Xie, C., and Huson, D.H. (2015) Fast and sensitive protein alignment using DIAMOND. *Nature Methods* **12**: 59–60.
- Bushnell, B. (2014) BBMap: a fast, accurate, splice-aware aligner. In *Conference: 9th Annual Genomics of Energy & Environment Meeting*. CA, USA.
- Caldwell, P.E., MacLean, M.R., and Norris, P.R. (2007) Ribulose biphosphate carboxylase activity and a Calvin cycle gene cluster in *Sulfobacillus* species. *Microbiology* **153**: 2231–2240.
- Camacho, A., Walter, X.A., Picazo, A., and Zopfi, J. (2017) Photoferrotrophy: Remains of an ancient photosynthesis in modern environments. *Frontiers in Microbiology* **8**: 323.
- Camacho, C., Coulouris, G., Avagyan, V., Ma, N., Papadopoulos, J., Bealer, K., and Madden, T.L. (2009) BLAST+: Architecture and applications. *BMC Bioinformatics* **10**: 1–9.
- Caron, D., Davis, P., Madin, L., and Sieburth, J. (1982) Heterotrophic Bacteria and Bacterivorous Protozoa in Oceanic Macroaggregates. *Science* **218**: 795–797.
- Chan, C.S., Fakra, S.C., Edwards, D.C., Emerson, D., and Banfield, J.F. (2009) Iron oxyhydroxide mineralization on microbial extracellular polysaccharides. *Geochimica et Cosmochimica Acta* **73**: 3807–3818.
- Chin, C.-S., Alexander, D.H., Marks, P., Klammer, A.A., Drake, J., Heiner, C., et al. (2013) Nonhybrid, finished microbial genome assemblies from long-read SMRT sequencing data. *Nature Methods* **10**: 563–569.
- Cho, B.C. and Azam, F. (1988) Major role of bacteria in biogeochemical fluxes in the ocean's interior. *Nature* **332**: 441–443.
- Christel, S., Herold, M., Bellenberg, S., El Hajjami, M., Buetti-Dinh, A., Pivkin, I. V., et al. (2017) Multi-omics Reveals the Lifestyle of the Acidophilic, Mineral-Oxidizing Model Species *Leptospirillum ferriphilum* T. *Applied and Environmental Microbiology* **84**: 1–17.
- Church, C.D., Wilkin, R.T., Alpers, C.N., Rye, R.O., and Blaine, R.B. (2007) Microbial sulfate reduction and metal attenuation in pH 4 acid mine water. *Geochemical Transactions* **8**: 1–14.
- Ciobotă, V., Burkhardt, E.M., Schumacher, W., Rösch, P., Küsel, K., and Popp, J. (2010) The influence of intracellular storage material on bacterial identification by means of Raman spectroscopy. *Analytical and Bioanalytical Chemistry* **397**: 2929–2937.

References

- Ciobotă, V., Lu, S., Tarcea, N., Rösch, P., Küsel, K., and Popp, J. (2013) Quantification of the inorganic phase of the pelagic aggregates from an iron contaminated lake by means of Raman spectroscopy. *Vibrational Spectroscopy* **68**: 212–219.
- Clark, D. a and Norris, P.R. (1996) *Acidimicrobium ferrooxidans* gen. nov., sp. nov.: mixed-culture ferrous iron oxidation with *Sulfobacillus* species. *Microbiology* **142**: 785–790.
- Clarke, W.A., Konhauser, K.O., Thomas, J.C., and Bottrell, S.H. (1997) Ferric hydroxide and ferric hydroxysulfate precipitation by bacteria in an acid mine drainage lagoon. *FEMS Microbiology Reviews* **20**: 351–361.
- Conway, J.R., Lex, A., and Gehlenborg, N. (2017) UpSetR: An R package for the visualization of intersecting sets and their properties. *Bioinformatics* **33**: 2938–2940.
- Cordero, O.X. and Datta, M.S. (2016) Microbial interactions and community assembly at microscales. *Current Opinion in Microbiology* **31**: 227–234.
- Cordero, O.X., Ventouras, L.A., DeLong, E.F., and Polz, M.F. (2012) Public good dynamics drive evolution of iron acquisition strategies in natural bacterioplankton populations. *Proceedings of the National Academy of Sciences of the United States of America* **109**: 20059–20064.
- Cosmidis, J., Benzerara, K., Morin, G., Busigny, V., Lebeau, O., Jézéquel, D., et al. (2014) Biomineralization of iron-phosphates in the water column of Lake Pavin (Massif Central, France). *Geochimica et Cosmochimica Acta* **126**: 78–96.
- Coupland, K. and Johnson, D.B. (2008) Evidence that the potential for dissimilatory ferric iron reduction is widespread among acidophilic heterotrophic bacteria. *FEMS Microbiology Letters* **279**: 30–35.
- Crowe, S.A., Jones, C.A., Katsev, S., Magen, C., O'Neill, A.H., Sturm, A., et al. (2008) Photoferrotrophs thrive in an Archean Ocean analogue. *Proceedings of the National Academy of Sciences* **105**: 15938–15943.
- Crowe, S.A., Katsev, S., Leslie, K., Sturm, A., Magen, C., Nomosatryo, S., et al. (2011) The methane cycle in ferruginous Lake Matano. *Geobiology* **9**: 61–78.
- Crowe, S.A., Maresca, J.A., Jones, C., Sturm, A., Henny, C., Fowle, D.A., et al. (2014) Deep-water anoxygenic photosynthesis in a ferruginous chemocline. *Geobiology* **12**: 322–339.
- Crowe, S.A., O'Neill, A.H., Katsev, S., Hehanussa, P., Haffner, G.D., Sundby, B., et al. (2008) The biogeochemistry of tropical lakes: A case study from Lake Matano, Indonesia. *Limnology and Oceanography* **53**: 319–331.
- Daims, H., Brühl, A., Amann, R., Schleifer, K.H., and Wagner, M. (1999) The domain-specific probe EUB338 is insufficient for the detection of all bacteria: Development and evaluation of a more comprehensive probe set. *Systematic and Applied Microbiology* **22**: 434–444.
- Dang, H. and Lovell, C. (2016) Microbial surface colonization and biofilm development in marine environments. *Microbiology and Molecular Biology Reviews* **80**: 91–138.
- Dash, P., Kashyap, D., and Mandal, S.C. (2012) Marine snow : Its formation and significance in fisheries and aquaculture. *World Aquaculture* **6**: 59–61.
- Datta, M.S., Sliwerska, E., Gore, J., Polz, M.F., and Cordero, O.X. (2016) Microbial

- interactions lead to rapid micro-scale successions on model marine particles. *Nature Communications* **7**: 11965.
- Delmont, T.O. and Eren, E.M. (2018) Linking pangenomes and metagenomes: The *Prochlorococcus* metapangenome. *PeerJ* **2018**: 1–23.
- Deshaies, M. (2020) Metamorphosis of Mining Landscapes in the Lower Lusatian Lignite Basin (Germany): New uses and new image of a mining region. *Cahiers de la recherche architecturale, urbaine et paysagère* **7**: 0–24.
- Ducklow, H. W., Steinberg, D. K., William, C., Point, M. G., & Buesseler, K. O. (2001). Upper Ocean Carbon Export and the Biological Pump, *Oceanography* **14**: 50-58.
- Ebrahimi, A., Schwartzman, J., and Cordero, O.X. (2019) Multicellular behaviour enables cooperation in microbial cell aggregates. *Philosophical Transactions of the Royal Society B* **374**: 20190077.
- Eddy, S.R. (2011) Accelerated profile HMM searches. *PLoS Computational Biology* **7**: e1002195
- Eigemann, F., Vogts, A., Voss, M., Zoccarato, L., and Schulz-Vogt, H. (2019) Distinctive tasks of different cyanobacteria and associated bacteria in carbon as well as nitrogen fixation and cycling in a late stage Baltic Sea bloom. *PLoS ONE* **14**: e0223294.
- Eisen, S., Poehlein, A., Johnson, D.B., Daniel, R., Schlömann, M., and Mühlhling, M. (2015) Genome Sequence of the Acidophilic Ferrous Iron-Oxidizing Isolate *Acidithrix ferrooxidans* Strain Py-F3, the Proposed Type Strain of the Novel Actinobacterial Genus *Acidithrix*. *Genome Announcements* **3**: e00382-15.
- El-Gebali, S., Mistry, J., Bateman, A., Eddy, S.R., Luciani, A., Potter, S.C., et al. (2019) The Pfam protein families database in 2019. *Nucleic Acids Research* **47**: 427–432.
- Emerson, D., Fleming, E.J., and McBeth, J.M. (2010) Iron-oxidizing bacteria: An environmental and genomic perspective. *Annual Review of Microbiology* **64**: 561–583.
- Engel, A. (2000) The role of transparent exopolymer particles (TEP) in the increase in apparent particle stickiness (α) during the decline of a diatom bloom. *Journal of Plankton Research* **22**: 485–497.
- Enright, A.J., Dongen, S.V., and Ouzounis, C.. (2002) An efficient algorithm for large-scale detection of protein families. *Nucleic Acids Research* **30**: 1575–1584.
- Eren, A.M., Esen, Ö.C., Sogin, M.L., Quince, C., Delmont, T.O., Morrison, H.G., and Vineis, J.H. (2015) Anvi'o: an advanced analysis and visualization platform for 'omics data. *PeerJ* **3**: e1319.
- Falagán, C., Sánchez-España, J., and Johnson, D.B. (2014) New insights into the biogeochemistry of extremely acidic environments revealed by a combined cultivation-based and culture-independent study of two stratified pit lakes. *FEMS Microbiology Ecology* **87**: 231–243.
- Farnelid, H., Turk-Kubo, K., Ploug, H., Ossolinski, J.E., Collins, J.R., Van Mooy, B.A.S., and Zehr, J.P. (2019) Diverse diazotrophs are present on sinking particles in the North Pacific Subtropical Gyre. *ISME Journal* **13**: 170–182.
- Farquhar, J., Bao, H., and Thiemens, M. (2000) Atmospheric influence of Earth's

- earliest sulfur cycle. *Science* **289**: 756–758.
- Fontanez, K.M., Eppley, J.M., Samo, T.J., Karl, D.M., and DeLong, E.F. (2015) Microbial community structure and function on sinking particles in the North Pacific Subtropical Gyre. *Frontiers in Microbiology* **6**: 1–14.
- Fortin, D., Leppard, G.G., and Tessier, A. (1993) Characteristics of lacustrine diagenetic iron oxyhydroxides. *Geochimica et Cosmochimica Acta* **57**: 4391–4404.
- Geller, W, Klapper, H, and Schultze, M. (1998) Natural and Anthropogenic Sulfuric Acidification of Lakes. In *Acidic Mining Lakes: Acid Mine Drainage, Limnology and Reclamation*. Geller, Walter, Klapper, Helmut, and Salomons, W. (eds). Berlin, Heidelberg: Springer Berlin Heidelberg, pp. 3–14.
- Ghiorse, W.C. (1984) Biology of iron- and manganese-depositing bacteria. *Annual Review of Microbiology* **38**: 515–550.
- Goltsman, D.S.A., Dasari, M., Thomas, B.C., Shah, M.B., VerBerkmoes, N.C., Hettich, R.L., and Banfield, J.F. (2013) New group in the *Leptospirillum* clade: Cultivation-independent community genomics, proteomics, and transcriptomics of the new species “*Leptospirillum* group IV UBA BS.” *Applied and Environmental Microbiology* **79**: 5384–5393.
- Goltsman, D.S.A., Deneff, V.J., Singer, S.W., VerBerkmoes, N.C., Lefsrud, M., Mueller, R.S., et al. (2009) Community genomic and proteomic analyses of chemoautotrophic iron-oxidizing “*Leptospirillum rubrum*” (Group II) and “*Leptospirillum ferrodiazotrophum*” (Group III) bacteria in acid mine drainage biofilms. *Applied and Environmental Microbiology* **75**: 4599–4615.
- González-Toril, E., Águilera, Á., Souza-Egipsy, V., Pamo, E.L., España, J.S., Amils, R., et al. (2011) Geomicrobiology of La Zarza-Perrunal acid mine effluent (Iberian Pyritic Belt, Spain). *Applied and Environmental Microbiology* **77**: 2685–2694.
- Gram, L., Grossart, H.-P., Schlingloff, A., and Kjørboe, T. (2002) Possible quorum sensing in marine snow bacteria: production of acylated homoserine lactones by *Roseobacter* strains isolated from marine snow. *Applied and environmental microbiology* **68**: 4111–4116.
- Grettenberger, C.L., Havig, J.R., and Hamilton, T.L. (2020) Metabolic diversity and co-occurrence of multiple *Ferrovum* species at an acid mine drainage site. *BMC Microbiology* **20**: 119.
- Grossart, H.-P. and Ploug, H. (2000) Bacterial production and growth efficiencies: Direct measurements on riverine aggregates. *Limnology and Oceanography* **45**: 436–445.
- Grossart, H.-P. and Simon, M. (1998a) Bacterial colonization and microbial decomposition of limnetic organic aggregates (lake snow). *Aquatic Microbial Ecology* **15**: 127–140.
- Grossart, H.-P. and Simon, M. (1993) Limnetic macroscopic organic aggregates (lake snow): Occurrence, characteristics, and microbial dynamics in Lake Constance. *Limnology and Oceanography* **38**: 532–546.
- Grossart, H.-P. and Simon, M. (1998b) Significance of limnetic organic aggregates (lake snow) for the sinking flux of particulate organic matter in a large lake. *Aquatic*

- Microbial Ecology* **15**: 115–125.
- Grossart, H.-P. and Ploug, H. (2001) Microbial degradation of organic carbon and nitrogen on diatom aggregates. *Limnology and Oceanography* **46**: 267–277.
- Grossart, H.P., Simon, M., and Logan, B.E. (1997) Formation of macroscopic organic aggregates (lake snow) in a large lake: The significance of transparent exopolymer particles, phytoplankton, and Zooplankton. *Limnology and Oceanography* **42**: 1651–1659.
- Gurevich, A., Saveliev, V., Vyahhi, N., and Tesler, G. (2013) QUASt: Quality assessment tool for genome assemblies. *Bioinformatics* **29**: 1072–1075.
- Hallberg, K.B., Coupland, K., Kimura, S., and Johnson, D.B. (2006) Macroscopic Streamer Growths in Acidic, Metal-Rich Mine Waters in North Wales Consist of Novel and Remarkably Simple Bacterial Communities. *Applied and Environmental Microbiology* **72**: 2022–2030.
- Hallberg, K.B. and Johnson, D.B. (2001) Biodiversity of acidophilic prokaryotes. *Advances in Applied Microbiology* **49**: 37–84.
- Hallmann, R., Friedrich, A., Koops, H., Pommerening-Röser, A., Rohde, K., Zenneck, C., and Sand, W. (1992) Physiological characteristics of *thiobacillus ferrooxidans* and *leptospirillum ferrooxidans* and physicochemical factors influence microbial metal leaching. *Geomicrobiology Journal* **10**: 193–206.
- Harrison, A.P. (1984) The acidophilic *Thiobacilli* and other acidophilic bacteria that share their habitat. *Annual Review of Microbiology* **38**: 265–292.
- Harrison, A.P., Jarvis, B.W., and Johnson, J.L. (1980) Heterotrophic bacteria from cultures of autotrophic *Thiobacillus ferrooxidans*: Relationships as studied by means of deoxyribonucleic acid homology. *Journal of Bacteriology* **143**: 448–454.
- Havig, J.R., Hamilton, T.L., McCormick, M., McClure, B., Sowers, T., Wegter, B., and Kump, L.R. (2018) Water column and sediment stable carbon isotope biogeochemistry of permanently redox-stratified Fayetteville Green Lake, New York, U.S.A. *Limnology and Oceanography* **63**: 570–587.
- Heinzel, E., Hedrich, S., Janneck, E., Glombitza, F., Seifert, J., and Schlömann, M. (2009) Bacterial Diversity in a Mine Water Treatment Plant. *Applied and Environmental Microbiology* **75**: 858–861.
- Herndl, G.J. and Reinthaler, T. (2013) Microbial control of the dark end of the biological pump. *Nature Geoscience* **6**: 718–724.
- Herrmann, M., Hädrich, A., and Küsel, K. (2012) Predominance of thaumarchaeal ammonia oxidizer abundance and transcriptional activity in an acidic fen. *Environmental Microbiology* **14**: 3013–3025.
- Hess, S., Suthaus, A., and Melkonian, M. (2016) “*Candidatus Finniella*” (*Rickettsiales*, *Alphaproteobacteria*), novel endosymbionts of viridiraptorid amoeboflagellates (Cercozoa, Rhizaria). *Applied and Environmental Microbiology* **82**: 659–670.
- Hmelo, L.R., Mincer, T.J., and Van Mooy, B.A.S. (2011) Possible influence of bacterial quorum sensing on the hydrolysis of sinking particulate organic carbon in marine environments. *Environmental Microbiology Reports* **3**: 682–688.
- Hua, Z.S., Han, Y.J., Chen, L.X., Liu, J., Hu, M., Li, S.J., et al. (2015) Ecological roles of dominant and rare prokaryotes in acid mine drainage revealed by

- metagenomics and metatranscriptomics. *ISME Journal* **9**: 1280–1294.
- Huang, Y., Niu, B., Gao, Y., Fu, L., and Li, W. (2010) CD-HIT Suite: A web server for clustering and comparing biological sequences. *Bioinformatics* **26**: 680–682.
- Huson, D.H., Beier, S., Flade, I., Górska, A., El-Hadidi, M., Mitra, S., et al. (2016) MEGAN Community Edition - Interactive Exploration and Analysis of Large-Scale Microbiome Sequencing Data. *PLoS Computational Biology* **12**: e1004957.
- Hyatt, D., Chen, G.L., LoCascio, P.F., Land, M.L., Larimer, F.W., and Hauser, L.J. (2010) Prodigal: Prokaryotic gene recognition and translation initiation site identification. *BMC Bioinformatics* **11**:119.
- Imhoff, J. F., Rahn, T., Künzel, S., & Neulinger, S. C. (2018) New insights into the metabolic potential of the phototrophic purple bacterium *Rhodospila globiformis* DSM 161T from its draft genome sequence and evidence for a vanadium-dependent nitrogenase. *Arch. Microbiol* **200**: 847–857.
- Irsfeld, M., Spadafore, M., and Prüß, B. (2013) β -Phenylethylamine, a small molecule with a large impact. *WebmedCentral* **4**: 1–15.
- Johnson, C.M., Beard, B.L., Klein, C., Beukes, N.J., and Roden, E.E. (2008) Iron isotopes constrain biologic and abiologic processes in banded iron formation genesis. *Geochimica et Cosmochimica Acta* **72**: 151–169.
- Johnson, D.B. (1998) Biodiversity and ecology of acidophilic microorganisms. *Physiology and Biochemistry of Extremophiles* **27**: 307–317.
- Johnson, D.B. (1991) Biological desulfurization of coal using mixed populations of mesophilic and moderately thermophilic acidophilic bacteria. In *Processing and Utilization of High Sulphur Coals IV*. Dugan, P.R., Quigley, D.R., and Attia, Y.A. (eds). New York: Elsevier, pp. 576–580.
- Johnson, D.B. (2009) Extremophiles: Acidic Environments. In *Encyclopedia of Microbiology*. Moselio Schaechter (ed). San Diego, CA: Elsevier, pp. 107–126.
- Johnson, D.B. (2012) Geomicrobiology of extremely acidic subsurface environments. *FEMS Microbiology Ecology* **81**: 2–12.
- Johnson, D.B. and Hallberg, K.B. (2003) The microbiology of acidic mine waters. *Research in Microbiology* **154**: 466–473.
- Johnson, D.B. and Hallberg, K.B. (2007) Techniques for Detecting and Identifying Acidophilic Mineral-Oxidizing Microorganisms. In *Bio mining*. Rawlings, D.E. and Johnson, D.B. (eds). Berlin, Heidelberg: Springer, pp. 237–261.
- Johnson, D.B., Hallberg, K.B., and Hedrich, S. (2014) Uncovering a Microbial Enigma: Isolation and Characterization of the Streamer-Generating, Iron-Oxidizing, Acidophilic Bacterium “*Ferrovum myxofaciens*.” *Applied and Environmental Microbiology* **80**: 672–680.
- Johnson, D.B., Kanao, T., and Hedrich, S. (2012) Redox Transformations of Iron at Extremely Low pH: Fundamental and Applied Aspects. *Frontiers in Microbiology* **3**: 1–13.
- Johnson, D.B. and McGinness, S. (1991) Ferric iron reduction by acidophilic heterotrophic bacteria. *Applied and Environmental Microbiology* **57**: 207–211.
- Johnson, D.B. and Rang, L. (1993) Effects of acidophilic protozoa on populations of

References

- metal-mobilizing bacteria during the leaching of pyritic coal. *Journal of General Microbiology* **139**: 1417–1423.
- Johnson, D.B. and Roberto, F.F. (1997) Heterotrophic Acidophiles and Their Roles in the Bioleaching of Sulfide Minerals. In *Bio mining*. D.E. R. (ed). Berlin, Heidelberg: Springer Berlin Heidelberg, pp. 259–279.
- Jones, R.M. and Johnson, D.B. (2015) *Acidithrix ferrooxidans* gen. nov., sp. nov.; a filamentous and obligately heterotrophic, acidophilic member of the *Actinobacteria* that catalyzes dissimilatory oxido-reduction of iron. *Research in Microbiology* **166**: 111–120.
- Juillan-Binard, C., Picciocchi, A., Andrieu, J.-P., Dupuy, J., Petit-Hartlein, I., Caux-Thang, C., et al. (2017) A two-component NADPH oxidase (NOX)-like system in bacteria is involved in the electron transfer chain to the methionine sulfoxide reductase MsrP. *Journal of Biological Chemistry* **292**: 2485–2494.
- Kaltenbock, E. and Herndl, G.J. (1992) Ecology of amorphous aggregations (marine snow) in the northern Adriatic Sea. IV. Dissolved nutrients and the autotrophic community associated with marine snow. *Marine Ecology Progress Series* **87**: 147–159.
- Kamjunke, N., Tittel, J., Krumbeck, H., Beulker, C., and Poerschmann, J. (2005) High heterotrophic bacterial production in acidic, iron-rich mining lakes. *Microbial Ecology* **49**: 425–433.
- Kanehisa, M., Sato, Y., and Morishima, K. (2016) BlastKOALA and GhostKOALA: KEGG tools for functional characterization of genome and metagenome sequences. *Journal of Molecular Biology* **428**: 726–731.
- Kappler, A. and Straub, K.L. (2005) Geomicrobiological Cycling of Iron. *Reviews in Mineralogy and Geochemistry* **59**: 85–108.
- Kay, C.M., Rowe, O.F., Rocchetti, L., Coupland, K., Hallberg, K.B., and Johnson, D.B. (2013) Evolution of microbial “Streamer” growths in an acidic, metal-contaminated stream draining an abandoned underground copper mine. *Life* **3**: 189–210.
- Kermer, R., Hedrich, S., Taubert, M., Baumann, S., Schlömann, M., Johnson, D.B., and Seifert, J. (2012) Elucidation of carbon transfer in a mixed culture of *Acidiphilium cryptum* and *Acidithiobacillus ferrooxidans* using protein-based stable isotope probing. *Journal of Integrated OMICS* **2**: 37–45.
- Klawonn, I., Bonaglia, S., Brüchert, V., and Ploug, H. (2015) Aerobic and anaerobic nitrogen transformation processes in N₂-fixing cyanobacterial aggregates. *ISME Journal*, **9**: 1456–1466.
- Klindworth, A., Pruesse, E., Schweer, T., Peplies, J., Quast, C., Horn, M., and Glöckner, F. O. (2013) Evaluation of general 16S ribosomal RNA gene PCR primers for classical and next-generation sequencing-based diversity studies. *Nucleic Acids Res*, **41**: 1–11
- Kjørboe, T. and Hansen, J.L.S. (1993) Phytoplankton aggregate formation: Observations of patterns and mechanisms of cell sticking and the significance of exopolymeric material. *Journal of Plankton Research* **15**: 993–1018.
- Kjørboe, T. and Jackson, G.A. (2001) Marine snow, organic solute plumes, and

References

- optimal chemosensory behavior of bacteria. *Limnology and Oceanography* **46**: 1309–1318.
- Kipry, J., Jwair, R.J., Gelhaar, N., Wiacek, C., Janneck, E., and Schlömann, M. (2013) Enrichment of “*Ferrovum*” spp. and *Gallionella* relatives using artificial mine water. *Advanced Materials Research* **825**: 54–57.
- Koeksoy, E., Halama, M., Konhauser, K.O., and Kappler, A. (2016) Using modern ferruginous habitats to interpret Precambrian banded iron formation deposition. *International Journal of Astrobiology* **15**: 205–217.
- Konings, W.N., Poolman, B., and van Veen, H.W. (1994) Solute transport and energy transduction in bacteria. *Antonie van Leeuwenhoek* **65**: 369–380.
- Kopylova, E., Noé, L., and Touzet, H. (2012) SortMeRNA: Fast and accurate filtering of ribosomal RNAs in metatranscriptomic data. *Bioinformatics* **28**: 3211–3217.
- Koschorreck, M. (2008) Microbial sulphate reduction at a low pH. *FEMS Microbiology Ecology* **64**: 329–342.
- Kucera, S. and Wolfe, R.S. (1957) A Selective Enrichment Method for *Gallionella Ferruginea*. *Journal of Bacteriology* **74**: 344–349.
- Kumar, S., Stecher, G., Li, M., Knyaz, C., and Tamura, K. (2018) MEGA X: Molecular evolutionary genetics analysis across computing platforms. *Molecular Biology and Evolution* **35**: 1547–1549.
- Kuntz, L.B., Laakso, T.A., Schrag, D.P., and Crowe, S.A. (2015) Modeling the carbon cycle in Lake Matano. *Geobiology* **13**: 454–461.
- Küsel, K. (2003) Microbial cycling of iron and sulfur in acidic coal mining lake sediments. *Water, Air, and Soil Pollution: Focus* **3**: 67–90.
- Küsel, K., Dorsch, T., Acker, G., and Stackebrandt, E. (1999) Microbial reduction of Fe(III) in acidic sediments: Isolation of *Acidiphilium cryptum* JF-5 capable of coupling the reduction of Fe(III) to the oxidation of glucose. *Applied and Environmental Microbiology* **65**: 3633–3640.
- Küsel, K., Roth, U., and Drake, H.L. (2002) Microbial reduction of Fe(III) in the presence of oxygen under low pH conditions. *Environmental Microbiology* **4**: 414–421.
- Laganenka, L., Colin, R., and Sourjik, V. (2016) Chemotaxis towards autoinducer 2 mediates autoaggregation in *Escherichia coli*. *Nature Communications* **7**: 1–10.
- Lambrecht, N., Wittkop, C., Katsev, S., Fakhraee, M., and Swanner, E.D. (2018) Geochemical Characterization of Two Ferruginous Meromictic Lakes in the Upper Midwest, USA. *Journal of Geophysical Research: Biogeosciences* **123**: 3403–3422.
- Langmead, B. and Salzberg, S.L. (2012) Fast gapped-read alignment with Bowtie 2. *Nature Methods* **9**: 357–359.
- Larkin, M.A., Blackshields, G., Brown, N.P., Chenna, R., Mcgettigan, P.A., McWilliam, H., et al. (2007) Clustal W and Clustal X version 2.0. *Bioinformatics* **23**: 2947–2948.
- Lehours, A.C., Evans, P., Bardot, C., Joblin, K., and Gérard, F. (2007) Phylogenetic diversity of archaea and bacteria in the anoxic zone of a meromictic lake (Lake

- Pavin, France). *Applied and Environmental Microbiology* **73**: 2016–2019.
- Lehours, A.C., Rabiet, M., Morel-Desrosiers, N., Morel, J.P., Jouve, L., Arbeille, B., et al. (2010) Ferric iron reduction by fermentative strain BS2 isolated from an iron-rich anoxic environment (Lake Pavin, France). *Geomicrobiology Journal* **27**: 714–722.
- Lepère, C., Domaizon, I., Hugoni, M., Vellet, A., and Debroas, D. (2016) Diversity and dynamics of active small microbial eukaryotes in the anoxic zone of a freshwater meromictic lake (Pavin, France). *Frontiers in Microbiology* **7**: 1–11.
- Leschine, S., Paster, B.J., and Canale-Parola, E. (2006) Free-Living Saccharolytic Spirochetes: The Genus *Spirochaeta*. In *The Prokaryotes: Volume 7: Proteobacteria: Delta, Epsilon Subclass*. Dworkin, M., Falkow, S., Rosenberg, E., Schleifer, K.-H., and Stackebrandt, E. (eds). New York, NY: Springer New York, pp. 195–210.
- Li, H., Handsaker, B., Wysoker, A., Fennell, T., Ruan, J., Homer, N., et al. (2009) The sequence alignment/map format and SAMtools. *Bioinformatics* **25**: 2078–2079.
- Li, Q., Cooper, R.E., Wegner, C.-E., and Küsel, K. (2020) Molecular Mechanisms Underpinning Aggregation in *Acidiphilium* sp. C61 Isolated from Iron-Rich Pelagic Aggregates. *Microorganisms* **8**: 314.
- Liao, Y., Smyth, G.K., and Shi, W. (2014) FeatureCounts: An efficient general purpose program for assigning sequence reads to genomic features. *Bioinformatics* **30**: 923–930.
- Liu, H., Yin, H., Dai, Y., Dai, Z., Liu, Y., Li, Q., et al. (2011) The co-culture of *Acidithiobacillus ferrooxidans* and *Acidiphilium acidophilum* enhances the growth, iron oxidation, and CO₂ fixation. *Archives of Microbiology* **193**: 857–866.
- Llirós, M., Garcíá-Armisen, T., Darchambeau, F., Morana, C., Triadó-Margarit, X., Inceoğlu, Ö., et al. (2015) Pelagic photoferrotrophy and iron cycling in a modern ferruginous basin. *Scientific Reports* **5**: 1–8.
- Lolkema, J.S., Poolman, B., and Konings, W.N. (1996) Secondary transporters and metabolic energy generation in bacteria. In *Handbook of Biological Physics*. W.N. Konings, H.R.K. and J.S.L. (ed). Haren: Elsevier Science B. V, pp. 229–260.
- Long, R.A. and Azam, F. (2001) Antagonistic Interactions among Marine Pelagic Bacteria. *Applied and Environmental Microbiology* **67**: 4975–4983.
- Lovley, D.R., Holmes, D.E., and Nevin, K.P. (2004) Dissimilatory Fe(III) and Mn(IV) reduction. In *Advances in Microbial Physiology*. pp. 219–286.
- Loy, A., Schleifer, K.-H., Lee, N., Lehner, A., Adamczyk, J., Wagner, M., et al. (2002) Oligonucleotide microarray for 16S rRNA gene-based detection of all recognized lineages of sulfate-reducing prokaryotes in the environment. *Applied and Environmental Microbiology* **68**: 5064–5081.
- Lu, S. (2012) Microbial Iron Cycling in Pelagic Aggregates (iron Snow) and Sediments of an Acidic Mine Lake.
- Lu, S., Chourey, K., Reiche, M., Nietzsche, S., Shah, M.B., Neu, T.R., et al. (2013) Insights into the structure and metabolic function of microbes that shape pelagic iron-rich aggregates (“Iron snow”). *Applied and Environmental Microbiology* **79**: 4272–4281.

References

- Lu, S., Gischkat, S., Reiche, M., Akob, D.M., Hallberg, K.B., and Küsel, K. (2010) Ecophysiology of Fe-cycling bacteria in acidic sediments. *Applied and Environmental Microbiology* **76**: 8174–8183.
- Lu, S., Peiffer, S., Lazar, C.S., Oldham, C., Neu, T.R., Ciobota, V., et al. (2016) Extremophile microbiomes in acidic and hypersaline river sediments of Western Australia. *Environmental Microbiology Reports* **8**: 58–67.
- Lueders, T., Manefield, M., and Friedrich, M.W. (2004) Enhanced sensitivity of DNA- and rRNA-based stable isotope probing by fractionation and quantitative analysis of isopycnic centrifugation gradients. *Environmental Microbiology* **6**: 73–78.
- Lundgreen, R.B.C., Jaspers, C., Traving, S.J., Ayala, D.J., Lombard, F., Grossart, H.P., et al. (2019) Eukaryotic and cyanobacterial communities associated with marine snow particles in the oligotrophic Sargasso Sea. *Scientific Reports* **9**: 1–12.
- Lynnes, T., Horne, S.M., and Prüß, B.M. (2014) β -phenylethylamine as a novel nutrient treatment to reduce bacterial contamination due to *Escherichia coli* O157: H7 on beef meat. *Meat Science* **96**: 165–171.
- Magnuson, T.S., Swenson, M.W., Paszczynski, A.J., Deobald, L.A., Kerk, D., and Cummings, D.E. (2010) Proteogenomic and functional analysis of chromate reduction in *Acidiphilium cryptum* JF-5, an Fe(III)-respiring acidophile. *BioMetals* **23**: 1129–1138.
- Mamani, S., Moinier, D., Denis, Y., Soulère, L., Queneau, Y., Talla, E., et al. (2016) Insights into the Quorum Sensing Regulon of the Acidophilic *Acidithiobacillus ferrooxidans* Revealed by Transcriptomic in the Presence of an Acyl Homoserine Lactone Superagonist Analog. *Frontiers in Microbiology* **7**:1365.
- Marcobal, A., de las Rivas, B., Landete, J.M., Tabera, L., and Muñoz, R. (2012) Tyramine and phenylethylamine biosynthesis by food bacteria. *Critical Reviews in Food Science and Nutrition* **52**: 448–467.
- McCave, I. (1984) Size spectra and aggregation of suspended particles in the deep ocean. *Deep-Sea Research* **31**: 329–352.
- McGinness, S. and Johnson, D.B. (1992) Grazing of acidophilic bacteria by a flagellated protozoan. *Microbial Ecology* **23**: 75–86.
- McMurdie, P.J. and Holmes, S. (2013) Phyloseq: An R Package for Reproducible Interactive Analysis and Graphics of Microbiome Census Data. *PLoS ONE* **8**: e61217.
- Meier, J., Babenzien, H.-D., and Wendt-Potthoff, K. (2004) Microbial cycling of iron and sulfur in sediments of acidic and pH-neutral mining lakes in Lusatia (Brandenburg, Germany). *Biogeochemistry* **67**: 135–156.
- Méndez-García, C., Peláez, A.I., Mesa, V., Sánchez, J., Golyshina, O. V., and Ferrer, M. (2015) Microbial diversity and metabolic networks in acid mine drainage habitats. *Frontiers in Microbiology* **6**: 1–17.
- Michiels, C.C., Darchambeau, F., Roland, F.A.E., Morana, C., Llíros, M., García-Armisen, T., et al. (2017) Iron-dependent nitrogen cycling in a ferruginous lake and the nutrient status of Proterozoic oceans. *Nature Geoscience* **10**: 217–221.
- Miot, J., Jézéquel, D., Benzerara, K., Cordier, L., Rivas-Lamelo, S., Skouri-Panet, F., et al. (2016) Mineralogical Diversity in Lake Pavin: Connections with Water

- Column Chemistry and Biomineralization Processes. *Minerals* **6**: 1–19.
- Miot, J., Li, J., Benzerara, K., Sougrati, M.T., Ona-Nguema, G., Bernard, S., et al. (2014) Formation of single domain magnetite by green rust oxidation promoted by microbial anaerobic nitrate-dependent iron oxidation. *Geochimica et Cosmochimica Acta* **139**: 327–343.
- Miracle, M.R., Vicente, E., Pedrós-Alió, C., Miraclel, M.R., Vicente, E., Miracle, M.R., et al. (1992) Biological Studies O F Spanish Meromictic and Stratified Karstic Lakes. *Limnetica* **8**: 59–77.
- Mitchell, J.G., Pearson, L., Dillon, S., and Kantalis, K. (1995) Natural assemblages of marine bacteria exhibiting high-speed motility and large accelerations. *Applied and Environmental Microbiology* **61**: 4436–4440.
- Morana, C., Roland, F.A.E., Crowe, S.A., Llorós, M., Borges, A. V., Darchambeau, F., and Bouillon, S. (2016) Chemoautotrophy and anoxygenic photosynthesis within the water column of a large meromictic tropical lake (Lake Kivu, East Africa). *Limnology and Oceanography* **61**: 1424–1437.
- Mo, H., Chen, Q., Du, J., Tang, L., Qin, F., Miao, B., et al. (2011) Ferric reductase activity of the ArsH protein from *Acidithiobacillus ferrooxidans*. *Journal of Microbiology and Biotechnology* **21**: 464–469.
- Mori, J. (2016) New insights into the life of Fe (II)-oxidizing bacteria.
- Mori, J.F., Lu, S., Händel, M., Totsche, K.U., Neu, T.R., Iancu, V.V., et al. (2016) Schwertmannite formation at cell junctions by a new filament-forming Fe(II)-oxidizing isolate affiliated with the novel genus *Acidithrix*. *Microbiology* **162**: 62–71.
- Mori, J.F., Ueberschaar, N., Lu, S., Cooper, R.E., Pohnert, G., and Küsel, K. (2017) Sticking together: Inter-species aggregation of bacteria isolated from iron snow is controlled by chemical signaling. *ISME Journal* **11**: 1075–1086.
- Mühling, M., Poehlein, A., Stuhr, A., Voitel, M., Daniel, R., and Schlömann, M. (2016) Reconstruction of the metabolic potential of acidophilic *Sideroxydans* strains from the metagenome of an microaerophilic enrichment culture of acidophilic iron-oxidizing bacteria from a pilot plant for the treatment of acid mine drainage reveals metabolic. *Frontiers in Microbiology* **7**: 1–16.
- Nerlich, A., Lapschies, A.M., Kohler, T.P., Cornax, I., Eichhorn, I., Goldmann, O., et al. (2019) Homophilic protein interactions facilitate bacterial aggregation and IgG-dependent complex formation by the *Streptococcus canis* M protein SCM. *Virulence* **10**: 194–206.
- Neu, T.R. (2000) In situ cell and glycoconjugate distribution in river snow studied by confocal laser scanning microscopy. *Aquatic Microbial Ecology* **21**: 85–95.
- Nitschke, W. and Bonnefoy, V. (2016) Energy acquisition in low pH environments. In *Acidophiles: Life in Extremely Acidic Environments*. Quatrini, R. and Johnson, D.B. (eds). Poole: Caister Academic Press, pp. 19–48.
- Nixdorf, B., Krumbeck, H., Jander, J., and Beulker, C. (2003) Comparison of bacterial and phytoplankton productivity in extremely acidic mining lakes and eutrophic hard water lakes. *Acta Oecologica* **24**: S281-S288.
- Nordstrom, D.K., Alpers, C.N., Ptacek, C.J., and Blowes, D.W. (2000) Negative pH

References

- and extremely acidic mine waters from Iron Mountain, California. *Environmental Science and Technology* **34**: 254–258.
- Norris, P.R. (1990) Acidophilic bacteria and their activity in mineral sulfide oxidation. In *Microbial mineral recovery*. HL, E. and CL, B. (eds). New York: McGraw-Hill, pp. 3–27.
- Ohmura, N., Sasaki, K., Matsumoto, N., and Saiki, H. (2002) Anaerobic Respiration Using Fe³⁺, S₀, and H₂ in the Chemolithoautotrophic Bacterium *Acidithiobacillus ferrooxidans*. *Journal of Bacteriology* **184**: 2081–2087.
- Olson, J. B., Steppe, T. F., Litaker, R. W., and Paer, H. W. (2017) N₂-Fixing Microbial Consortia Associated with the Ice Cover of Lake Bonney, Antarctica. *Journal of Chemical Information and Modeling*, **53**: 21–25.
- Osorio, H., Mangold, S., Denis, Y., Nancucheo, I., Esparza, M., Johnson, D.B., et al. (2013) Anaerobic sulfur metabolism coupled to dissimilatory iron reduction in the extremophile *Acidithiobacillus ferrooxidans*. *Applied and Environmental Microbiology* **79**: 2172–2181.
- Oswald, K., Jegge, C., Tischer, J., Berg, J., Brand, A., Miracle, M. R., Soria, X., Vicente, E., Lehmann, M. F., Zopfi, J., and Schubert, C. J. (2016) Methanotrophy under versatile conditions in the water column of the ferruginous meromictic Lake La Cruz (Spain). *Frontiers in Microbiology* **7**: 1762.
- Oswald, K., Milucka, J., Brand, A., Hach, P., Littmann, S., Wehrli, B., et al. (2016) Aerobic gammaproteobacterial methanotrophs mitigate methane emissions from oxic and anoxic lake waters. *Limnology and Oceanography* **61**: 101–118.
- Parks, D.H., Imelfort, M., Skennerton, C.T., Hugenholtz, P., and Tyson, G.W. (2015) CheckM: assessing the quality of microbial genomes recovered from isolates, single cells, and metagenomes. *Genome Research* **25**: 1043–1055.
- Parparov, A., Berman, T., Grossart, H.-P., and Simon, M. (1998) Metabolic activity associated with lacustrine seston. *Aquatic Microbial Ecology* **15**: 77–87.
- Passow, U. and Carlson, C.A. (2012) The biological pump in a high CO₂ world. *Marine Ecology Progress Series* **470**: 249–271.
- Passow, U., Ziervogel, K., Asper, V., and Diercks, A. (2012) Marine snow formation in the aftermath of the Deepwater Horizon oil spill in the Gulf of Mexico. *Environmental Research Letters* **7**: 035301.
- Paterson, I.A., Juorio, A. V., and Boulton, A.A. (1990) 2-Phenylethylamine: a modulator of catecholamine transmission in the mammalian central nervous system? *Journal of Neurochemistry* **55**: 1827–1837.
- Pedregosa, F., Varoquaux, G., Gramfort, A., Michel, V., Thirion, B., Grisel, O., et al. (2011) Scikit-learn: Machine Learning in Python Fabian. *Journal of Machine Learning Research* **12**: 2825–2530.
- Peduzzi, S. (2003) Interactions among sulfate-reducing and purple sulfur bacteria in the chemocline of meromictic Lake Cadagno, Switzerland.
- Peine, A., Tritschler, A., Küsel, K., and Peiffer, S. (2000) Electron flow in an iron-rich acidic sediment - Evidence for an acidity-driven iron cycle. *Limnology and Oceanography* **45**: 1077–1087.

References

- Petrash, D.A., Jan, J., Sirová, D., Osafo, N.O.A., and Borovec, J. (2018) Iron and nitrogen cycling, bacterioplankton community composition and mineral transformations involving phosphorus stabilisation in the ferruginous hypolimnion of a post-mining lake. *Environmental Science: Processes and Impacts* **20**: 1414–1426.
- Planavsky, N., Rouxel, O., Bekker, A., Shapiro, R., Fralick, P., and Knudsen, A. (2009) Iron-oxidizing microbial ecosystems thrived in late Paleoproterozoic redox-stratified oceans. *Earth and Planetary Science Letters* **286**: 230–242.
- Ploug, H., Grossart, H.-P., Azam, F., and Jørgensen, B.B. (1999) Photosynthesis, respiration, and carbon turnover in sinking marine snow from surface waters of Southern California Bight: Implications for the carbon cycle in the ocean. *Marine Ecology Progress Series* **179**: 1–11.
- Posth, N.R., Huelin, S., Konhauser, K.O., and Kappler, A. (2010) Size, density and composition of cell-mineral aggregates formed during anoxygenic phototrophic Fe(II) oxidation: Impact on modern and ancient environments. *Geochimica et Cosmochimica Acta* **74**: 3476–3493.
- Poux, S., Arighi, C.N., Magrane, M., Bateman, A., Wei, C.H., Lu, Z., et al. (2017) On expert curation and scalability: UniProtKB/Swiss-Prot as a case study. *Bioinformatics (Oxford, England)* **33**: 3454–3460.
- Pronk, J.T. and Johnson, D.B. (1992) Oxidation and reduction of iron by acidophilic bacteria. *Geomicrobiology Journal* **10**: 153-171.
- Pronk, J.T., Liem, K., Bos, P., and Kuenen, J.G. (1991) Energy transduction by anaerobic ferric iron respiration in *Thiobacillus ferrooxidans*. *Applied and Environmental Microbiology* **57**: 2063–2068.
- Pruitt, K.D., Tatusova, T., and Maglott, D.R. (2007) NCBI reference sequences (RefSeq): A curated non-redundant sequence database of genomes, transcripts and proteins. *Nucleic Acids Research* **35**: 61–65.
- Quast, C., Pruesse, E., Yilmaz, P., Gerken, J., Schweer, T., Yarza, P., et al. (2013) The SILVA ribosomal RNA gene database project: Improved data processing and web-based tools. *Nucleic Acids Research* **41**: 590–596.
- Radajewski, S., Ineson, P., Parekh, N.R., and Murrell, J.C. (2000) Stable-isotope probing as a tool in microbial ecology. *Nature* **403**: 646–649.
- R Core Team (2018) R: A language and environment for statistical computing.
- R Core Team (2020) R: A language and environment for statistical computing.
- Ram, R.J., VerBerkmoes, N.C., Thelen, M.P., Tyson, G.W., Baker, B.J., Blake, R.C., et al. (2005) Microbiology: Community proteomics of a natural microbial biofilm. *Science* **308**: 1915–1920.
- Reiche, M., Lu, S., Ciobotă, V., Neu, T.R., Nietzsche, S., Rösch, P., et al. (2011) Pelagic boundary conditions affect the biological formation of iron-rich particles (iron snow) and their microbial communities. *Limnology and Oceanography* **56**: 1386–1398.
- Reichenbach, H. (2006) The Order Cytophagales. In *The Prokaryotes*. New York, NY: Springer New York, pp. 549–590.
- Reinthal, T., van Aken, H.M., and Herndl, G.J. (2010) Major contribution of

- autotrophy to microbial carbon cycling in the deep North Atlantic's interior. *Deep-Sea Research Part II: Topical Studies in Oceanography* **57**: 1572–1580.
- Riebesell, U. (1992) The formation of large marine snow and its sustained residence in surface waters. *Limnology and Oceanography* **37**: 63–76.
- Rivas, M., Seeger, M., Holmes, D.S., and Jedlicki, E. (2005) A Lux-like quorum sensing system in the extreme acidophile *Acidithiobacillus ferrooxidans*. *Biological Research* **38**: 283–297.
- Robinson, M.D., McCarthy, D.J., and Smyth, G.K. (2009) edgeR: A Bioconductor package for differential expression analysis of digital gene expression data. *Bioinformatics* **26**: 139–140.
- Rodrigo, M.A., Miracle, M.R., and Vicente, E. (2001) The meromictic Lake La Cruz (Central Spain). Patterns of stratification. *Aquatic Sciences* **63**: 406–416.
- Rodrigo, M.A., Vicente, E., and Miracle, M.R. (1993) Short-term calcite precipitation in the karstic meromictic Lake La Cruz (Cuenca, Spain). *SIL Proceedings, 1922-2010* **25**: 711–719.
- Rognes, T., Flouri, T., Nichols, B., Quince, C., and Mahé, F. (2016) VSEARCH: A versatile open source tool for metagenomics. *PeerJ* **2016**: 1–22.
- Rothman, R.B. and Baumann, M.H. (2006) Balance between dopamine and serotonin release modulates behavioral effects of amphetamine-type drugs. *Annals of the New York Academy of Sciences* **1074**: 245–260.
- Saeed, H., Hartland, A., Lehto, N.J., Baalousha, M., Sikder, M., Sandwell, D., et al. (2018) Regulation of phosphorus bioavailability by iron nanoparticles in a monomictic lake. *Scientific Reports* **8**: 1–14.
- Saeidipour, B. and Bakhshi, S. (2013) Cutadapt Removes Adapter Sequences from High-throughput sequencing reads. *Advances in Environmental Biology* **7**: 2803–2809.
- Sand, W., Gerke, T., Hallmann, R., and Schippers, A. (1995) Sulfur chemistry, biofilm, and the (in)direct attack mechanism - a critical evaluation of bacterial leaching. *Applied Microbiology and Biotechnology* **43**: 961–966.
- Santofimia, E., González-Toril, E., López-Pamo, E., Gomariz, M., Amils, R., and Aguilera, Á. (2013) Microbial Diversity and Its Relationship to Physicochemical Characteristics of the Water in Two Extreme Acidic Pit Lakes from the Iberian Pyrite Belt (SW Spain). *PLoS ONE* **8**: e66746.
- Savage, K.S., Ashley, R.P., and Bird, D.K. (2009) Geochemical Evolution of a High Arsenic, Alkaline Pit-Lake in the Mother Lode Gold District, California. *Economic Geology* **104**: 1171–1211.
- Schädler, S., Burkhardt, C., Hegler, F., Straub, K.L., Miot, J., Benzerara, K., and Kappler, A. (2009) Formation of cell-iron-mineral aggregates by phototrophic and nitrate-reducing anaerobic Fe(II)-oxidizing bacteria. *Geomicrobiology Journal* **26**: 93–103.
- Schmid, G., Zeitvogel, F., Hao, L., Ingino, P., Floetenmeyer, M., Stierhof, Y.D., et al. (2014) 3-D analysis of bacterial cell-(iron)mineral aggregates formed during Fe(II) oxidation by the nitrate-reducing *Acidovorax* sp. strain BoFeN1 using complementary microscopy tomography approaches. *Geobiology* **12**: 340–361.

References

- Schrenk, M.O., Edwards, K.J., Goodman, R.M., Hamers, R.J., and Banfield, J.F. (1998) Distribution of *Thiobacillus ferrooxidans* and *Leptospirillum ferrooxidans*: Implications for generation of acid mine drainage. *Science* **279**: 1519–1522.
- Schröder, I., Johnson, E., and De Vries, S. (2003) Microbial ferric iron reductases. *FEMS Microbiology Reviews* **27**: 427–447.
- Schultze, M. (2013) Limnology of Pit Lakes. In *Acidic Pit Lakes, The Legacy of Coal and Metal Surface Mines*. Walter Geller, Martin Schultze, Robert Kleinmann, C.W. (ed). Springer Berlin Heidelberg.
- Schultze, M. and Geller, W. (1996) The acid lakes of lignite mining districts of the former German Democratic Republic. In *Geochemical Approaches to Environmental Engineering of Metals*. R. Reuther (ed). Berlin Heidelberg: Springer-Verlag, pp. 89–105.
- Schultze, M., Pokrandt, K.H., and Hille, W. (2010) Pit lakes of the Central German lignite mining district: Creation, morphometry and water quality aspects. *Limnologica* **40**: 148–155.
- Schultze, M., Scholz, E., Jolas, P., Bergbau-, L.M., and Braunkohlengesellschaft, M. (2011) Use of mine water for filling and remediation of pit lakes. 545–550.
- Schweitzer, B., Huber, I., Amann, R., Ludwig, W., and Simon, M. (2001) α - and β -Proteobacteria Control the Consumption and Release of Amino Acids on Lake Snow Aggregates. *Applied and Environmental Microbiology* **67**: 632–645.
- Secor, P.R., Michaels, L.A., Ratjen, A., Jennings, L.K., and Singh, P.K. (2018) Entropically driven aggregation of bacteria by host polymers promotes antibiotic tolerance in *Pseudomonas aeruginosa*. *Proceedings of the National Academy of Sciences of the United States of America* **115**: 10780–10785.
- Shanks, A.L. and Reeder, M.L. (1993) Reducing microzones and sulfide production in marine snow. *Marine Ecology Progress Series* **96**: 43–47.
- Shen, W., Le, S., Li, Y., and Hu, F. (2016) SeqKit: A cross-platform and ultrafast toolkit for FASTA/Q file manipulation. *PLoS ONE* **11**: e0163962.
- Shimada, K., Itoh, S., Iwaki, M., Nagashima, K. V. P., Matsuura, K., Kobayashi, M., et al. (1998) Reaction Center Complex Based on Zn-Bacteriochlorophyll from *Acidiphilium Rubrum*. In *Photosynthesis: Mechanisms and Effects* (pp. 909–912).
- Sienkiewicz, E. and Gasiorowski, M. (2016) The evolution of a mining lake - From acidity to natural neutralization. *Science of the Total Environment* **557–558**: 343–354.
- Simon, M., Alldredge, A., and Azam, F. (1990) Bacterial carbon dynamics on marine snow. *Marine Ecology Progress Series* **65**: 205–211.
- Simon, M., Grossart, H.-P., Schweitzer, B., and Ploug, H. (2002) Microbial ecology of organic aggregates in aquatic ecosystems. *Aquatic Microbial Ecology* **28**: 175–211.
- Smith, D.C., Simont, M., Alldredge, A.L., and Azam, F. (1992) Intense hydrolytic enzyme activity on marine aggregates and implications for rapid particle dissolution. *Nature* **359**: 139–142.

References

- Smith, D.C., Steward, G.F., Long, R.A., and Azam, F. (1995) Bacterial mediation of carbon fluxes during a diatom bloom in a mesocosm. *Deep Sea Research Part II: Topical Studies in Oceanography* **42**: 75–97.
- Steinberg, D.K., Van Mooy, B.A.S., Buesseler, K.O., Boyd, P.W., Kobari, T., and Karl, D.M. (2008) Bacterial vs. zooplankton control of sinking particle flux in the ocean's twilight zone. *Limnology and Oceanography* **53**: 1327–1338.
- Stevenson, L.G. and Rather, P.N. (2006) A novel gene involved in regulating the flagellar gene cascade in *Proteus mirabilis*. *Journal of Bacteriology* **188**: 7830–7839.
- Stevenson, L.G., Szostek, B.A., Clemmer, K.M., and Rather, P.N. (2013) Expression of the DisA amino acid decarboxylase from *Proteus mirabilis* inhibits motility and class 2 flagellar gene expression in *Escherichia coli*. *Research in Microbiology* **164**: 31–37.
- Stoderegger, K.E. and Herndl, G.J. (1998) Production and release of bacterial capsular material and its subsequent utilization by marine bacterioplankton. *Limnology and Oceanography* **43**: 877–884.
- Stoderegger, K.E. and Herndl, G.J. (1999) Production of exopolymer particles by marine bacterioplankton under contrasting turbulence conditions. *Marine Ecology Progress Series* **189**: 9–16.
- Stoodley, P., Sauer, K., Davies, D.G., and Costerton, J.W. (2002) Biofilms as complex differentiated communities. *Annual Review of Microbiology* **56**: 187–209.
- Straub, K.L. (2011) Fe(III)-Reducing prokaryotes. In *Encyclopedia of Earth Sciences Series*. pp. 370–373.
- Straub, K.L., Benz, M., Schink, B., and Widdel, F. (1996) Anaerobic, nitrate-dependent microbial oxidation of ferrous iron. *Applied and Environmental Microbiology* **62**: 1458–1460.
- Sturgill, G. and Rather, P.N. (2004) Evidence that putrescine acts as an extracellular signal required for swarming in *Proteus mirabilis*. *Molecular Microbiology* **51**: 437–446.
- Styp Von Rekowski, K., Hempel, M., and Philipp, B. (2008) Quorum sensing by N-acylhomoserine lactones is not required for *Aeromonas hydrophila* during growth with organic particles in lake water microcosms. *Archives of Microbiology* **189**: 475–482.
- Sugio, T., Taha, T.M., and Takeuchi, F. (2009) Ferrous iron production mediated by tetrathionate hydrolase in tetrathionate-, sulfur-, and iron-grown *Acidithiobacillus ferrooxidans* ATCC 23270 cells. *Bioscience, Biotechnology and Biochemistry* **73**: 1381–1386.
- Suzuki, K. and Kato, K. (1953) Studies on suspended marine snow in the sea. Part I. Sources of marine snow. *Bulletin of the faculty of fisheries hokkaido university* **4**: 132–137.
- Tabatabai, M.A. (1974) A Rapid Method for Determination of Sulfate in Water Samples. *Environmental Letters* **7**: 237–243.
- Tamura, H. and Goto, K. (1974) Spectrophotometric determination of iron(II) with 1,10-phenanthroline in the presence of large amounts of iron(III). *Talanta* **21**: 314–318.

References

- Tang, L., Schramm, A., Neu, T.R., Revsbech, N.P., and Meyer, R.L. (2013) Extracellular DNA in adhesion and biofilm formation of four environmental isolates: A quantitative study. *FEMS Microbiology Ecology* **86**: 394–403.
- Tang, X., Chao, J., Chen, D., Shao, K., and Gao, G. (2012) Organic-Aggregate-Attached Bacteria in Aquatic Ecosystems: Abundance, Diversity, Community Dynamics and Function. Marcelli, M. (ed). IntechOpen, pp. 205-232.
- Tanizawa, Y., Fujisawa, T., and Nakamura, Y. (2018) DFAST: A flexible prokaryotic genome annotation pipeline for faster genome publication. *Bioinformatics* **34**: 1037–1039.
- Tapia, J.M., Muñoz, J., González, F., Blázquez, M.L., Malki, M., and A, B. (2009) Extraction of extracellular polymeric substances from the acidophilic bacterium *Acidiphilium* 3.2Sup(5). *Water Science and Technology* **59**: 1959–1967.
- Tapia, J.M., Muñoz, J.A., González, F., Blázquez, M.L., and Ballester, A. (2011) Mechanism of adsorption of ferric iron by extracellular polymeric substances (EPS) from a bacterium *Acidiphilium* sp. *Water Science and Technology* **64**: 1716–1722.
- Tatusov, R.L. (2002) The COG database: new developments in phylogenetic classification of proteins from complete genomes. *Nucleic Acids Research* **29**: 22–28.
- Taubert, M. (2019) SIP-Metaproteomics: Linking Microbial Taxonomy, Function, and Activity. In *Stable Isotope Probing: Methods and Protocols, Methods in Molecular Biology*. pp. 57–69.
- Taubert, M., Baumann, S., Von Bergen, M., and Seifert, J. (2011) Exploring the limits of robust detection of incorporation of ¹³C by mass spectrometry in protein-based stable isotope probing (protein-SIP). *Analytical and Bioanalytical Chemistry* **401**: 1975–1982.
- Taubert, M., Jehmlich, N., Vogt, C., Richnow, H.H., Schmidt, F., von Bergen, M., and Seifert, J. (2011) Time resolved protein-based stable isotope probing (Protein-SIP) analysis allows quantification of induced proteins in substrate shift experiments. *Proteomics* **11**: 2265–2274.
- Taubert, M., Stöckel, S., Geesink, P., Girnus, S., Jehmlich, N., von Bergen, M., et al. (2018) Tracking active groundwater microbes with D₂O labelling to understand their ecosystem function. *Environmental Microbiology* **20**: 369–384.
- Taubert, M., Vogt, C., Wubet, T., Kleinsteuber, S., Tarkka, M.T., Harms, H., et al. (2012) Protein-SIP enables time-resolved analysis of the carbon flux in a sulfate-reducing, benzene-degrading microbial consortium. *ISME Journal* **6**: 2291–2301.
- Thompson, K.J., Kenward, P.A., Bauer, K.W., Warchola, T., Gauger, T., Martinez, R., et al. (2019) Photoferrotrophy, deposition of banded iron formations, and methane production in Archean oceans. *Science Advances* **5**: 1–10.
- Thornton, D. (2002) Diatom aggregation in the sea: mechanisms and ecological implications. *European Journal of Phycology* **37**: 149–161.
- Tischler, J.S., Jwair, R.J., Gelhaar, N., Drechsel, A., Skirl, A.M., Wiacek, C., et al. (2013) New cultivation medium for “*Ferrovum*” and *Gallionella*-related strains. *Journal of Microbiological Methods* **95**: 138–144.
- Tomi, T., Shibata, Y., Ikeda, Y., Taniguchi, S., Haik, C., Mataga, N., Shimada, et al.

- (2007) Energy and electron transfer in the photosynthetic reaction center complex of *Acidiphilium rubrum* containing Zn-bacteriochlorophyll a studied by femtosecond up-conversion spectroscopy. *Biochimica et Biophysica Acta - Bioenergetics* **1767**: 22–30.
- Tonolla, M., Demarta, A., & Peduzzi, R. (1998) The chemistry of Lake Cadagno. *Documenta Ist. Ital. Idrobiol*, **63**: 11–17.
- Tonolla, M., Peduzzi, S., Demarta, A., Peduzzi, R., & Hahn, D. (2004). Phototropic sulfur and sulfate-reducing bacteria in the chemocline of meromictic Lake Cadagno, Switzerland. *Journal of Limnology*, **63**: 161–170.
- Turner, J.T. (2015) Zooplankton fecal pellets, marine snow, phytodetritus and the ocean's biological pump. *Progress in Oceanography* **130**: 205–248.
- Tyson, G.W., Chapman, J., Hugenholtz, P., Allen, E.E., Ram, R.J., Richardson, P.M., et al. (2004) Community structure and metabolism through reconstruction of microbial genomes from the environment. *Nature* **428**: 37–43.
- Ullrich, S.R. (2016) Genomic and transcriptomic characterization of novel iron oxidizing bacteria of the genus “*Ferrovum*.”
- Ullrich, S.R., González, C., Poehlein, A., Tischler, J.S., Daniel, R., Schlömann, M., et al. (2015) Gene Loss and Horizontal Gene Transfer Contributed to the Genome Evolution of the Extreme Acidophile “*Ferrovum*.” *Frontiers in Microbiology* **7**: 1–23.
- Ullrich, S.R., Poehlein, A., Tischler, J.S., González, C., Ossandon, F.J., Daniel, R., et al. (2016) Genome analysis of the biotechnologically relevant acidophilic iron oxidising strain JA12 indicates phylogenetic and metabolic diversity within the novel genus “*Ferrovum*.” *PloS one* **11**: e0146832.
- Ullrich, S.R., Poehlein, A., Voget, S., Hoppert, M., Daniel, R., Leimbach, A., et al. (2015) Permanent draft genome sequence of *Acidiphilium* sp. JA12-A1. *Standards in Genomic Sciences* **10**: 1–10.
- Valdés, J., Pedroso, I., Quatrini, R., Dodson, R.J., Tettelin, H., Blake, R., et al. (2008) *Acidithiobacillus ferrooxidans* metabolism: from genome sequence to industrial applications. *BMC Genomics* **9**: 597.
- Vardanyan, A., Vardanyan, N., Khachatryan, A., Zhang, R., and Sand, W. (2019) Adhesion to mineral surfaces by cells of *Leptospirillum*, *Acidithiobacillus* and *Sulfobacillus* from Armenian sulfide ores. *Minerals* **9**: 69.
- de Vicente, I., Ortega-Retuerta, E., Romera, O., Morales-Baquero, R., and Reche, I. (2009) Contribution of transparent exopolymer particles to carbon sinking flux in an oligotrophic reservoir. *Biogeochemistry* **96**: 13–23.
- Walter, X.A., Picazo, A., Miracle, M.R., Vicente, E., Camacho, A., Aragno, M., and Zopfi, J. (2014) Phototrophic Fe(II)-oxidation in the chemocline of a ferruginous meromictic lake. *Frontiers in Microbiology* **5**: 1–9.
- Wang, H., Bigham, J.M., and Tuovinen, O.H. (2006) Formation of schwertmannite and its transformation to jarosite in the presence of acidophilic iron-oxidizing microorganisms. *Materials Science and Engineering C* **26**: 588–592.
- Wenderoth, D.F. and Abraham, W.R. (2005) Microbial indicator groups in acidic mining lakes. *Environmental Microbiology* **7**: 133–139.

References

- Widdel, F., Schnell, S., Heising, S., Ehrenreich, A., Assmus, B., and Schink, B. (1993) Ferrous iron oxidation by anoxygenic phototrophic bacteria. *Nature* **362**: 834–836.
- Winstanley, C. and Morgan, J.A.W. (1997) The bacterial flagellin gene as a biomarker for detection, population genetics and epidemiological analysis. *Microbiology* **143**: 3071–3084.
- Zafra, O., Lamprecht-Grandío, M., de Figueras, C.G., and González-Pastor, J.E. (2012) Extracellular DNA release by undomesticated *Bacillus subtilis* is regulated by early competence. *PLoS ONE* **7**: e48716.
- Zegeye, A., Bonneville, S., Benning, L.G., Sturm, A., Fowle, D.A., Jones, C., et al. (2012) Green rust formation controls nutrient availability in a ferruginous water column. *Geology* **40**: 599–602.
- Zegeye, A., Ruby, C., and Jorand, F. (2007) Kinetic and thermodynamic analysis during dissimilatory γ -FeOOH reduction: Formation of green rust 1 and magnetite. *Geomicrobiology Journal* **24**: 51–64.
- Zhang, J., Kobert, K., Flouri, T., and Stamatakis, A. (2014) PEAR: A fast and accurate Illumina Paired-End reAd mergeR. *Bioinformatics* **30**: 614–620.

Declaration of authorship

I hereby affirm that I composed this dissertation by myself and only with the assistance and literature cited in the text. Those who provided assistance for the experiments, data analysis and writing of the manuscript are listed as coauthors or mentioned in the acknowledgments in the respective chapters.

Furthermore, I confirm that I have read and dully understood the 'Course of Examination for Doctoral Candidates' (Promotionsordnung, September 23rd, 2019) by the Faculty of Biological Sciences of the Friedrich Schiller University Jena.

I did not obtain any assistance from a consultant for doctoral theses, and no third parties have received any indirect or direct financial rewards in relation with the contents of this dissertation.

This dissertation or parts of it have not been previously submitted for scientific survey to the Friedrich Schiller University Jena or to any other university.

Jena,

Qianqian Li

Acknowledgments

Doing PhD is a long and important journey in my life and I sincerely acknowledge all people who helped, supported, encouraged me to bring this work to completion.

Firstly, I would like to express my sincere and great thanks to my supervisor Prof. Dr. Kirsten Küsel for her support and encouragement. I am very grateful for your dedicated supervision towards my PhD project with your patience.

I also wish to thank reviewers for their interest in my doctoral research project and for reviewing this thesis.

I acknowledge all co-authors for their contributions to this dissertation, Dr. Rebecca Cooper, Dr. Carl-Eric Wegner, Dr. Martin Taubert. Thanks for your great help on scientific writing and projects supervision.

Furthermore, I would like to thank the entire Aquatic Geomicrobiology group and the former team members: Dr. Jiro Mori and Dr. Shipeng Lu. Thank you two for taking the time to discuss my project and selfless contribution to my project. I also thank our group technicians: Jens Wurlitzer, Falko Gutmann for sampling and lab assistance. Thanks also go to awesome former and present PhD students (Patricia, Racheal, Markus, Consti) for your warm-hearted support for my project.

I would sincerely thank my boyfriend Qing Li who takes good care of me and cheers me up. Thanks for your trust and encouragement. You make my life full of happiness. I would also like to say thank you (谢谢) to my family and Qing's family. Thanks for your spiritual support during the entire time of this PhD adventure.

This work was supported by the Graduate School of Excellence Jena School for Microbial Communication funded by Deutsche Forschungsgemeinschaft and Carl Zeiss Stiftung. Part of the work was supported by the Collaborative Research Centre Chemical Mediators in Complex Biosystems (SFB 1127 ChemBioSys), the German Centre for Integrative Biodiversity Research (iDiv) Halle-Jena-Leipzig, both funded by Deutsche Forschungsgemeinschaft.

Published articles and Pending manuscripts

The thesis chapters 2, 3, 4 were published in international, peer-reviewed journals. My contributions to each manuscript are documented below:

Chapter 2: Qianqian Li, Rebecca E. Cooper, Carl-Eric Wegner, Shipeng Lu, and Kirsten Küsel (2021) Draft genome sequences of *Acidithrix* sp. strain C25 and *Acidoceella* sp. strain C78, acidophiles isolated from iron-rich pelagic aggregates (iron snow). **Published** in *Microbiology Resource Announcement* (doi: 10.1128/MRA.00102-21).

I did the pre-analysis of genome data and submitted the data to the database under the supervision of C.-E. Wegner. S. Lu isolated the three strains. I prepared the first draft of the manuscript with R.E. Cooper and worked on the following versions with help of all co-authors. My contribution can be summarized as following:

Data Analysis: 90%

Manuscript Writing: 60%

Chapter 3: Qianqian Li, Rebecca E. Cooper, Carl-Eric Wegner, Martin Taubert, Nico Jehmlich, Martin von Bergen, and Kirsten Küsel (2021) Insights into autotrophic activities and carbon flow in iron-rich pelagic aggregates (iron snow). **Published** in *Microorganisms* (doi: 10.3390/microorganisms9071368)

I did the nucleotide extraction and metatranscriptome analysis under the supervision of C.-E. Wegener. K. Küsel, M. Taubert designed and guided the execution of the microcosms incubation experiments. I incubated iron snow microcosms, prepared protein samples for analysis, and analyzed metaproteome data under the supervision of M. Taubert. R.E. Cooper was involved in all of the above-mentioned processes. N.

Jehmilch and M. Bergen performed metaproteome peptides identification. I prepared the first draft of the manuscript with K. Küsel and worked on the following versions with help of all co-authors. My contribution can be summarized as following:

Experimental Work: 90%

Data Analysis: 80%

Manuscript Writing: 50%

Chapter 4: Qianqian Li, Rebecca E. Cooper, Carl-Eric Wegner, and Kirsten Küsel (2020) Molecular mechanisms underpinning aggregation in *Acidiphilium* sp. C61 isolated from iron-rich pelagic aggregates. **Published** in *Microorganisms* (doi: 10.3390/microorganisms8030314)

I did all the lab work, including bacterial cultivation, microscopic observations, RNA extraction, and library preparations. I did the data analysis under the supervision of C.-E. Wegner. I prepared the first draft of the manuscript with R.E. Cooper and C.-E. Wegner. K. Küsel designed and guided the execution of the experiments as well as finalized the manuscript. My contribution can be summarized as following:

Experimental Work: 100%

Data Analysis: 90%

Manuscript Writing: 30%

Jena,

Qianqian Li

Curriculum Vitae

Note: "The curriculum vitae has been removed for data protection reasons"